Desert Research Institute

Fate and Transport Modeling of the South Y PCE Groundwater Contamination Plume

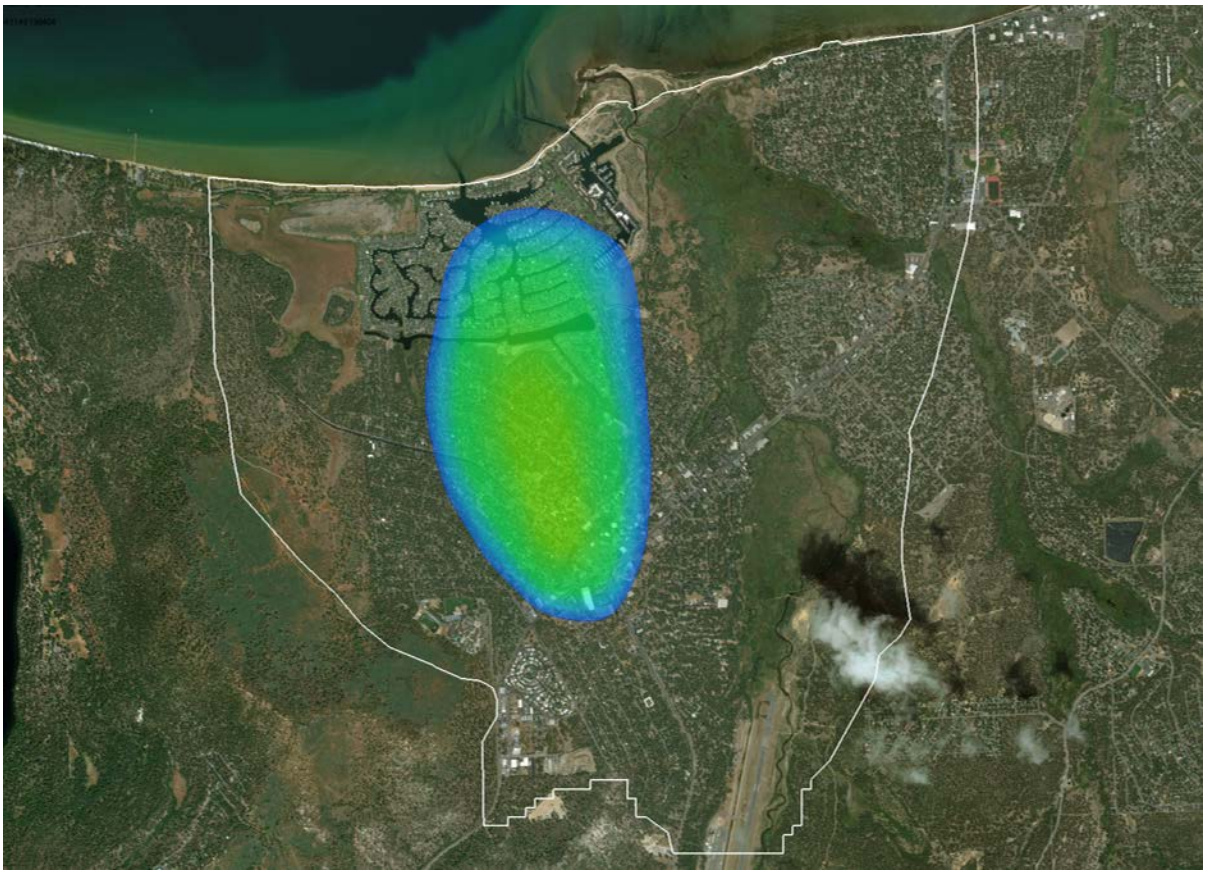

Investigators: Susie Rybarski, Rosemary Carroll, Greg Pohll and Mark Hausner

Presented to: South Tahoe Public Utility District

Date: June 28, 2019

Introduction

The South "Y" Area is named for the intersection of California State Highway 89 and U.S. Highway 50, located within the north-central part of the Tahoe Valley South Sub-basin (TVS Basin). Chlorinated hydrocarbons (tetrachloroethylene or PCE) have been detected in water supply wells north and south of the South Y Area since 1989, when these compounds were first required to be tested in regulated drinking water sources. Many of the supply wells have since ceased operating due to PCE concentrations exceeding the drinking water standard of 5 micrograms per liter (µg/L). Figure 1 shows the approximate present location of the PCE plume and nearby water supply wells.

In partnership with Lukins Brothers Water Company (LBWC) and Tahoe Keys Water Company (TKWC), South Tahoe Public Utility District (STPUD) has contracted with Kennedy Jenks Consultants (KJC) to conduct a feasibility study of remedial alternatives to continue to provide clean water supplies while removing the PCE groundwater contamination plume from the South Y Area. STPUD requested that a groundwater flow model of the Tahoe Valley South Sub-basin (TVS) (Carroll et al., 2016) be used as the basis for a PCE fate and transport model to simulate a variety of remediation activities in order to inform the design of a remediation strategy. In an effort to reduce both complexity and model run times, a small sub-section of this model was extracted for use in the transport simulations (Figure 2). This report details the changes and updates made to the TVS model for this effort, and the results of the fate and transport model for each remediation scenario.

Background

Previous studies have indicated that the likely primary source of the PCE plume is the former Lake Tahoe Laundry Works (LTLW), located at the junction of Highway 50 and Highway 89 (South Y area) (Alward and Petersen, 2016). Additional identified potential sources include Norma's Dry Cleaners, Sierra Cleaners, TCI, Redwood Oil, and Big O Tires (Figure 3). The contribution of each of these sites to the existing plume is unknown. However, these sites are all close to and generally downgradient from LTLW. For the purposes of modeling, LTLW was therefore selected as the source of PCE. LTLW was in operation from 1972 to 1979, and initial contamination would have occurred during that time period. However, PCE monitoring was not required until 1989, at which time the Lukins Brothers Water Company (LBWC) Well #4, located approximately 3,000 feet downgradient from the source, was found to exceed the MCL of 5 µg/L. This well was taken offline and was not retested until 2015. Likewise, large gaps in both the spatial and temporal record of PCE testing throughout the basin leave little available data for model calibration (Figure 4).

Though records are limited, historical sampling shows detectable PCE arriving in the Clement Well (west of the presumed point of release) in 1992 and reaching the TKWC Well #2 (over a mile downgradient) as early as 1990, though there is no record of levels there exceeding the MCL until 2002. More recent sampling has indicated that the highest PCE concentrations remain in the area of the presumed point of release near the Y, though concentrations in downgradient wells have increased in recent years (Figure 5). Furthermore, the LBWC Well #4 showed higher concentrations of PCE in 2016 and 2017 than in any previously recorded year, indicating that the PCE continues to migrate toward the Tahoe Keys. Although localized high concentrations remain in the general area of the source (147 µg/l at Rockwater Well in October 2017; 180 µg/l at a LTLW monitoring well in 2016), measurements from multiple monitoring wells at the LTLW site indicate a declining trend, suggesting that release from this source has slowed

(Figure 6). Likewise, recent samples at a monitoring well approximately 450 meters downgradient from the LTLW site have shown a decline in concentrations in recent years (Figure 7).

Model Domain

Grid Design

The model grid was inset within the existing groundwater model framework (Carroll et al., 2016). A section of the original model grid covering the area of PCE plume and extending northward to Lake Tahoe was extracted, and the grid was refined in the area of the existing plume and along the expected plume migration path, from a grid cell size of 100 meters in the original model to a refined size of 10 meters in the area of the plume. The subsection of the transport model domain relative to the existing groundwater model domain in shown in Figure 2. Vertical discretization was unchanged from the existing model, with layer thicknesses of 40 and 100 meters for the upper two layers and lower two layers, respectively.

Both a steady-state and a transient flow model were developed for this assessment. In order to recreate the calibrated head field from the Carroll et al., 2016 model and simulate lateral flow from cells not represented in the new model domain, a constant head boundary was applied to the landward boundaries of the new model grid, with heads taken from the existing model framework. Hydraulic conductivity, specific yield, and specific storage fields were also taken directly from the existing model framework. Since the development of the Carroll et al., 2016 model, one additional aquifer test had been performed. As the hydraulic conductivities in the model domain had been represented by a pilot point interpolation, this new data point was applied and the hydraulic conductivity field was re-interpolated. The hydraulic conductivity field used in this simulation is therefore slightly different than that defined in Carroll et al., 2016. Hydraulic conductivities within the newly defined model domain range from $1.7x10^{-3}$ to 22.1 m/d (Figure 9-Figure 11).

It should be noted that the Carroll et al., 2016 steady-state model was intended to represent pre-1983 conditions, while the steady-state model described here was required to represent conditions prior to 1971 in order to capture the genesis of the PCE plume in the transient model. Calibrated heads at the boundaries of the model domain were assumed to remain unchanged during this time period, as this was the best available representation of heads at the model boundary. However, active wells during this time period varied, and the pumping regime in the steady-state model described here is therefore somewhat different than in the Carroll et al., 2016 steady-state model. No additional changes were made to the steady-state model, and no attempt was made to recalibrate the flow model. Heads from the steady-state model were used as the initial condition for the transient simulation.

Clay Lens

Groundwater in the South Y area generally flows to the north, and the majority of transport is likewise to the north. However, some transport should be expected in the upgradient and lateral directions due to dispersion. The South Y and Tata 4 wells are both located within 160 meters (525 feet) upgradient of LTLW, and both began actively pumping shortly after the closure of LTLW – South Y pumped from 1983-2000, while Tata 4 pumped from 1983-1997. Despite their proximity to this source of PCE, both wells showed low or non-detectable PCE concentrations over the approximately 15 years that they were monitored. Additionally, contouring of the extent of the PCE plume in 2016 (Figure 8) (Lahontan

Regional Water Quality Control Board, 2016) indicated that plume migration had been largely horizontal for approximately 455 meters (1493 feet) north from LTLW before suddenly migrating downward.

It was therefore concluded that a low permeability clay lens was preventing the downward migration of PCE in the area of LTLW. Lithological cross sections produced by IT Corporation for a fate and transport model of the USA Gas site (IT Corporation, 2000) showed the location of a significant clay lens in this area, and these well logs were used to delineate its extent (Figure 12). Analysis of STPUD, LBWC and TKWC production well logs and domestic well logs revealed the existence of a clay lens at the same approximate elevation extending northwards towards Lake Tahoe, and the lens was extrapolated to the northern boundary. This lens was then represented in the model as an area of very low vertical conductivity (1/2000th of horizontal hydraulic conductivity) between model layers 1 and 2.

While the general direction of groundwater flow within the model domain is to the north, early detections of PCE were found at the Clement and Julie wells to the west and southwest of the LTLW site. Because these wells are generally upgradient from the presumed source, it is likely that pumping is acting as a pathway for both vertical and horizontal migration. These wells are outside of the extent of the simulated clay lens and screened only within model layer 1. LBWC 4, however, is screened in both layers 1 and 2. The layer 1 grid cell corresponding to the location of the LBWC 4 well was therefore assigned a high vertical conductivity (100x horizontal hydraulic conductivity) to represent this potential pathway for PCE migration across the aquitard.

MODFLOW-NWT

Flow simulations were run using MODFLOW-NWT. MODFLOW-NWT is the latest installment of the USGS modular program (Niswonger et al., 2011). The program relies on the Newton solution method and unstructured, asymmetric matrix solver to calculate groundwater head (Knoll and Keyes, 2004). MODFLOW-NWT is specifically designed to work with the upstream weighted (UPW) package to solve complex unconfined groundwater flow simulations while maintaining numeric stability during the wetting and drying of model cells. The UPW package replaces the traditional MODFLOW packages including the block-centered flow (BCF), the layer-property flow (LPF) and the hydrogeologic-unit flow (HUF). The UPW package differs from these previous packages by smoothing the horizontal-conductance function and storage-change function during wetting and drying to provide continuous derivatives for the solution by the Newton method, as opposed to a linear approach to their calculation. While smoothing introduces some error, the smoothing interval is defined by the user and can be made very small (e.g. 1x10-5, as is used in the simulations presented here) to limit numeric dispersion.

The model was developed within the Groundwater Modeling System (GMS) environment (version 10.3). GMS acts as a database for all of the hydrogeologic information and provides an easy to use pre- and post-processor to MODFLOW.

MT3DMS

Transport simulations were run using MT3DMS. MT3DMS is a modular three-dimensional transport model for the simulation of advection, dispersion, and chemical reactions of dissolved constituents in groundwater systems (Zheng and Wang, 1999). MT3DMS is designed to be used in conjunction with an existing flow model, where heads and cell-by-cell flux terms from the flow model results are read in by MT3DMS and utilized as the advective flow field for the transport portion of the simulation. Other

parameters affecting transport such as diffusion rates, dispersivity, porosity, sorption, and degradation rates are defined by the user.

Modeled Boundary Conditions

Recharge

Local areal recharge was applied variably over the model domain at a total rate of 1,700 afy, as spatially defined by the steady-state model described in Carroll, et al. (2016) (Figure 13). Additionally, groundwater flow into the modeled section from the larger surrounding basin was simulated with a constant head boundary, with heads defined by the same steady-state model. Net flow into the steady-state model through the constant head boundary totaled 7,200 afy, for a total simulated recharge rate of 8,900 afy. As described in Carroll, et al. (2016), evapotranspiration is accounted for in the applied recharge rates, and is therefore not explicitly modeled.

Streams

The Upper Truckee River and Trout Creek fall within the modeled section (Figure 14), and were simulated using MODFLOW's River package. Stream stages were extracted from the DEM used to define surface elevations. Minor adjustments were made to these streams during model calibration to more closely match mapped flow paths within the model domain. These streams are gaining for the entirety of the modeled section, with final outflows from the steady-state model to the streams totaling 1,100 afy.

Lake Tahoe

Groundwater flows generally northward through the model domain, discharging to Lake Tahoe. The lake is simulated as a general head boundary, with steady-state heads defined by the mean recorded lake stage over water years 1971-2018. For the transient simulation, mean annual lake stages were used to define heads along this boundary in order to more accurately simulate transport to production wells near the lake (Figure 15). Net simulated outflow to the lake for the steady-state model totaled 5,300 afy.

Wells

Few pumping records exist for wells in this area prior to 1983, and wells simulated in the steady-state model were therefore selected based on construction date, such that if the well was in existence in 1970, it was assumed to be pumping. Pumping rates at each well were determined by the first recorded pumping rate for that well. For the transient simulation, wells were assumed to pump at their steady-state rate for the period 1971-1982, and were pumped at the reported rate for the period 1983-2018 Wells constructed between 1971-1982 were allowed to pump beginning in the year of their construction. Locations of wells simulated in the steady-state model are shown in Figure 16. Locations of wells simulated in the transient model are shown in Figure 17.

PCE Source

The release of PCE into the groundwater system was simulated as a recharge concentration in the area of the LTLW. The initial concentration is therefore representative of the concentration of leaked PCE (i.e., pure PCE mixed with vadose zone/recharge water), rather than the expected concentration of PCE in the groundwater underlying the simulated source. The total volume of PCE released is unknown, and annual recharge concentrations were therefore estimated and calibrated to downgradient concentrations. Given that the LTLW was in operation from 1972-1979, recharge concentrations were

applied at a maximum of 700 mg/l during this time period, with an initial 'ramp up' concentration of 500 mg/l in 1973, assuming leaked PCE would not instantaneously reach the underlying aquifer. Following this period, decreasing concentrations were applied to the model, representing continuing infiltration through the vadose zone and capture of PCE trapped in vadose zone pore spaces during wet years where groundwater levels would be elevated (Figure 18). Wet years were identified by years of increased precipitation, and recharge concentrations were accordingly elevated during these years, though decreasing through time as the total mass trapped in pore spaces is reduced with each period of increased groundwater elevation (Figure 19). The values for these reduced concentrations were determined through model calibration.

Transport Parameters

Advective Transport

The Advection package within MT3DMS was run using the Standard Finite Difference method, implementing the Upstream weighting scheme.

Dispersivity and Diffusivity

Longitudinal dispersivity for all layers was set to 40 m (131 ft), taken from a range of possible literature values appropriate for the scale of observation (Figure 20) (Zheng and Bennett, 2002) and selected from that range through calibration to measured concentrations and arrival times. Transverse dispersivity was calibrated to 60% and 20% of this value for layers 1-2 and 3-4, respectively, while vertical dispersivity was set to 1.5% of the longitudinal dispersivity for all layers.

Calculation of the dimensionless Peclet number provides insight into the relative importance of advective and diffusive transport. The Peclet number can be defined as:

$$Pe = v_x d / D_d \quad (1)$$

where v_x is the advective velocity, d is the average grain diameter, and D_d is the coefficient of molecular diffusion. Assuming an advective velocity of 38 ft/d (0.0134 cm/s) based on the results of recent aquifer test performed at the EW-1 test well, a conservative average grain diameter of 0.01 cm representing a fine-grained sand, and a coefficient of molecular diffusion of $0.87e^{-5}$ cm^2/s for PCE in water (Hayduk and Laudie, 1974), the Peclet number is calculated to be 15.4. Where Peclet numbers are greater than 6, mechanical dispersion is considered the dominant cause of contaminant plume mixing, and the effects of diffusion can be ignored (Fetter, 1993). Because this system is dominated by advective transport, diffusion is not significant, and the diffusion rate was set to zero to increase model stability and reduce run times.

Sorption

Organic compounds, such as PCE, can be sorbed to organic carbon present in the aquifer, at varying rates largely dependent on the molecular structure of the compound and this sorbed material can then be released to water at a later time. This process causes some solutes to migrate through the aquifer at a much slower rate than the groundwater that is transporting them. Sorption was simulated in MT3DMS using a linear adsorption isotherm, such that

$$\bar{C} = K_d C \quad (2)$$

where $\bar{C}$ is the sorbed concentration, C is the dissolved concentration, and K_d is the distribution coefficient. The distribution coefficient is a function of the compound specific organic carbon/water coefficient (K_{oc}) and the fraction of organic carbon in the aquifer sediments (f_{oc}), where

$$K_d = K_{oc} f_{oc} \quad (3)$$

The retardation factor can then be calculated as a function of the distribution coefficient and aquifer structural properties, given by

$$R = 1 + \frac{\rho_b}{\theta} K_d \quad (4)$$

where ρ_b is the bulk density of the aquifer materials and θ is the porosity. K_{oc} for PCE was assigned an experimentally determined value of 152 cm^3/g (State Water Resources Control Board, 2009). As previous studies have indicated that the granitic sands and gravels in this basin likely contain very little organic carbon (Benson, 2001), the value of f_{oc} was set to a very low value of 1e-5. Assuming a bulk density of 2.65 g/cm^3, and a porosity of 10% within layer 1 and 8% within layers 2-4, retardation factors of 1.04 and 1.05 can be calculated, respectively. Thus, while sorption is simulated, its effects on the velocity of PCE migration are limited, primarily due to the believed lack of organic carbon in the aquifer.

Biogenic Degradation

PCE is a volatile organic compound, and will rapidly volatilize from surface water when exposed to air. In groundwater, however, degradation rates are linked to levels of dissolved oxygen. Many studies have shown that microorganisms under anaerobic conditions are capable of degrading PCE to trichloroehtylene (TCE), which is in turn degraded to dichloroethylene (DCE) and then vinyl chloride (Lawrence, 2006). These studies indicate that the mean half-life of anaerobic biogenic degradation of PCE is approximately 1-9 years, with field studies pointing towards the lower end of this range. Studies of PCE degradation under aerobic conditions have been limited, though these studies have indicated that degradation will be very slow or non-existent in waters with dissolved oxygen levels above 1.5 mg/l (Aronson, et al. 1999; Roberts et al., 1986).

The limited number of measurements of dissolved oxygen within the study area were highly variable, with aquifer waters ranging from poorly to well oxygenated, with levels in the upper 150 feet of the modeled domain ranging from 1.81 to 7.27 mg/l (Figure 21), a depth approximately corresponding to the 40 meter (130 feet) thickness of model layer 1. Additionally, small concentrations of both TCE and DCE have been detected at various aquifer depths, indicating the biogenic degradation is occurring to some extent (STPUD, 2017). Because concentrations of TCE and DCE have been quite low where sampled, layers 1 and 2 were assigned an estimated 17 year PCE half-life, well above the mean half-life of 1-9 years. Layers 3-4 were assigned a half-life of 2 years, as levels of dissolved oxygen are expected to decrease with depth. Both sorbed and dissolved concentrations of PCE were assumed to have the same half-life.

Transport Model Calibration

A significant data gap exists immediately downgradient of the source area over the period 1988 – 2014, which makes a detailed calibration over the historical period impossible. A more generalized calibration was therefore performed to ensure that the migration pattern is consistent with measured PCE concentrations over space and time. The purpose of the calibration simulation was to ensure that

simulated plume migration did not extend to wells where PCE has not been detected and that the timing of PCE arrival to downgradient wells is represented properly. The locations of wells used to compare simulated and observed PCE concentrations in the model are shown in Figure 20. Results of the model calibration (measured vs simulated concentrations) at these wells are displayed in Figure 23-Figure 30. The simulated position of the plume at the end of the 2018 water year is shown is Figure 31-Figure 34. These contours show the highest concentrations of PCE located in model layer 1.

For wells directly downgradient from the simulated source, simulated trends and concentrations closely match observed values. Simulated trends for wells located along the western boundary of the plume (Clement Well, LBWC 2, LBWC 5) also follow observed trends, though acute spikes in concentrations could not be simulated. Observation points along the eastern boundary of the plume are limited to the Tahoe Valley Elementary School well. While an initial observed spike in concentration in 2003 is accurately simulated, subsequent measurements indicate a rapid decline in concentrations that could not be replicated in the model – though it should be noted that this well was reported to have collapsed in 2013 (Alward and Petersen, 2016). Samples collected at this well in 2016 and 2017 indicated concentrations below detection limits, but could only be collected from the upper screened interval due to the collapse, and may not be comparable to earlier measurements.

Although simulated concentrations are somewhat too high to the east and specifically at LBWC 4, simulated trends are generally excellent, and this model is therefore deemed a viable tool for future comparative analysis of potential engineering solutions.

Particle Tracking

A particle tracking analysis was performed to more clearly illustrate plume migration pathways and to estimate average plume migration times. Particles were applied in an east-west line in model layer 1 running through the simulated source cells at the LTLW site, and the model was run forward from 1971 water year to the 2068 water year, using the pumping rates defined in the Base Treatment alternative (Alternative 1) described in the Management Scenarios section later in this report. Selected pathways terminating at LBWC 5, TKWC 2, TKWC 1, and the northern model boundary are shown in Figure 35.

Particle tracking results indicate average plume migration times to LBWC 5 and TKWC 2 to be 30-40 years, and 40-50 years at TKWC 1. The average time for plume migration to the northern model boundary is approximately 80 years. It is important to emphasize that these simulated migration times are representative of the average plume velocity, and that they more accurately represent the arrival time of the 'heart' of the plume, rather than the time to detectable concentrations at a given point. For example, PCE was first detected at TKWC 2 in 1990, suggesting a travel time of approxmately 18 years, far less than the 30-40 years shown in the particle tracking results. This more rapid arrival time is achieved in the model through the calibrated dispersivity term, which functionally represents variability in pore velocities and results in spreading of the plume.

Model Implementation

The development of the South Y fate and transport model was a lengthy and iterative process that began with the Tahoe Valley South sub-basin groundwater flow model (Carroll et al. 2016). Milestones in the development of the South Y PCE Fate and Transport model included:

- a 1971 steady state flow groundwater flow model that was used to determine initial conditions prior to the introduction of PCE into the system,
- a transient flow model to accurately simulate groundwater flows and PCE transport in response to time-varying pumping and meteorological data,
- updated model parameterization derived from changes to the regional groundwater flow model,
- incorporation of 2017 and 2018 South Y PCE data into the model calibration for improved representation PCE source and transport,
- development of a conservative modeling scenario (with a persistent source and no biogenic decay) to aid in sensitivity analysis,
- recalibration of the model to better represent local well screens and the presence of a clay lens underlying the area that affects vertical transport of PCE, and
- simulation of a variety of remedial alternatives and final management scenarios as a decision support tool for the Technical Advisory Committee to the South Y Feasibility Study of Remedial Alternatives.

The three final management scenarios simulated using this model and the results of those simulations are described in detail in the following sections.

Management Scenarios

The final management scenarios were determined after a lengthy exploratory process that involved defining and evaluating a number of preliminary simulations, public presentations of preliminary simulations and the collection of feedback from stakeholders, and consultations with both public and private agencies involved in the feasibility study. Preliminary simulations considered a baseline scenario in which pumping rates remained unchanged, the drilling of extraction wells to facilitate removal of PCE from the system, the drilling of replacement wells to allow the shutdown of existing contaminated wells, and high-rate pumping from all available wells. Each preliminary simulation was run using the calibrated model parameters (including source depletion and biogenic decay) and conservative assumptions (a persistent source with no decay). Results of preliminary simulations were presented in both technical and public meetings over the course of the modeling effort, and informed the selection of the final three management alternatives.

Three alternatives for management of the plume and distribution of pumping at the TKWC, LBWC, and STPUD production wells have been proposed:

1) Base Treatment – this alternative acts as a baseline against which to compare other remedial action alternatives, maintaining current (2018 WY) lead/lag/lag-lag status for TKWC and LBWC wells. Produced water from both LBWC 5 and TKWC 2 is treated via a

granular activated carbon (GAC) system. Simulation is run 50 years into the future (2068 WY).

2) Targeted Pumping – this alternative uses LBWC 5 and TKWC 2 as the lead wells for LBWC and TKWC, respectively, as these wells are positioned near the current simulated heart of the plume. Increased pumping at these wells is intended to remove mass from the system as well as limit potential plume migration towards TKWC 1, TKWC 3, and LBWC 1. Produced water from both LBWC 5 and TKWC 2 is treated via a GAC system. Simulation is run 50 years into the future (2068 WY).
3) Surface Water Conversion – this alternative assumes a conversion from groundwater to surface water use. This alternative uses the same pumping rates as in the 'Base Treatment' alternative, and conversion to surface water is assumed complete after 15 years. Produced water from both LBWC 5 and TKWC 2 is treated via a GAC system during the 15 year time period. LBWC 1 and TKWC 3 would be used as backup supply wells following conversion.

Development of these three alternatives was concluded following analysis of two hypothetical management scenarios, included here for completion:

4) 90% GAC Capacity – this scenario assumes pumping at both LBWC 5 and TKWC 2 ramped up to meet 90% of the GAC capacity at each well as a method of mass removal. Excess treated water beyond the needs of LBWC and TKWC would be transferred to the STPUD system, and STPUD well production rates are reduced accordingly. Simulation is run 50 years into the future (2068 WY).
5) 90% Well Capacity – this scenario assumes pumping at both LBWC 5 and TKWC 2 ramped up to meet 90% of the well capacity at each well as a method of mass removal. As in the 90% GAC Capacity scenario, excess treated water beyond the needs of LBWC and TKWC would be transferred to the STPUD system, and STPUD well production rates are reduced accordingly. Simulation is run 50 years into the future (2068 WY).

For each of the three proposed alternatives, two simulations were run – one using all calibrated model properties, and one conservative simulation. For the conservative simulations, the PCE source term is maintained at a recharge concentration of 10 mg/l for the duration of the model (as opposed to returning to zero in the calibrated simulations) and no biogenic decay is simulated (as opposed to half-lives of 17 years in layers 1 and 2, and 2 years in layers 3 and 4 in the calibrated simulations). Pumping rates, PCE source term definition, and biogenic decay rates by layer for each alternative and hypothetical scenario are listed in Table 1 and Table 2.

Results

Described here in detail, results for all alternatives are tabulated in Table 3 and Table 4 (mass removed by well and alternative, and years to PCE concentrations less than 4 µg/l, respectively).

Alternative 1A – Base Treatment

Transport model results for the 2068 WY indicate that the majority of mass will have left the system at this time. While a small area at the northern boundary of the model domain show detectable (greater than 0.5 µg/l) concentrations of PCE in layers 1 and 2 (Figure 36-Figure 37), no concentrations exceed detection limits in layers 3 and 4. Concentrations for this stress period do not exceed the MCL anywhere within the model domain.

Prior to the 2068 WY, concentrations of PCE at TKWC 1 (Figure 38), TKWC 2 (Figure 39) and LBWC 5 (Figure 42) meet or exceed the MCL of 5 µg/l for several years, while concentrations at LBWC 1 (Figure 41) and TKWC 3 (Figure 40) never exceed the detection limit of 0.5 µg/l. LBWC 5 reaches a maximum concentration of 22.6 µg/l in 2020, and declines to below 4 µg/l in 2040. TKWC 1 reaches a maximum concentration of 5.0 µg/l in 2035, and declines to below 4 µg/l in 2045. TKWC 2 reaches a maximum concentration of 13.7 µg/l in 2021, and declines to below 4 µg/l in 2040. These results indicate that given the pumping rates assigned in this scenario, concentrations are unlikely to increase substantially in the near future, though they could remain above the MCL for the next 20-25 years. At no time during this simulation did the simulated PCE concentration or prescribed pumping rate exceed the GAC capacity at LBWC5 or at TKWC2.

Alternative 1B – Base Treatment (Conservative)

Transport model results for the 2068 WY indicate that a large quantity of mass will remain in the system at this time. Simulated concentrations exceed 100 µg/l at the source in layer 1, and exceed 50 µg/l near the northern model boundary in layers 1 and 2 (Figure 43-Figure 44). Likewise, simulated concentrations exceed 10 µg/l in layers 3 and 4 (Figure 45-Figure 46) at the northern model boundary. It should be emphasized that this scenario was simulated for the purpose of creating a worst-case result, with a constant input from the source continuing for the duration of the model and with no biogenic decay, and that the results of this simulation are not consistent with observed concentrations, with the exception of LBWC 1 and TKWC 3 where simulated concentrations remain below detection limits through the present

Like Alternative 1A, simulated concentrations at LBWC 1 (Figure 50) remain below detection limits for the duration of the model. Concentrations at TKWC 3 (Figure 49) do exceed detection limits, though they remain well below the MCL, reaching a maximum concentration of 0.67 µg/l in 2042. Concentrations at TKWC 1 (Figure 47) and TKWC 2 (Figure 48) remain greater than 4 µg/l for the duration of the model, reaching maximum concentrations of 50.5 µg/l in 2039 and 108.4 µg/l in 2022, respectively. LBWC 5 (Figure 51) reaches a maximum concentration of 95.6 µg/l in 2020, declining to below 4 µg/l in 2058. At no time during this simulation did the simulated PCE concentration or prescribed pumping rate exceed the GAC capacity at LBWC5 or at TKWC2.

Alternative 2A – Targeted Pumping

As in the base scenario (Alternative 1A), transport model results for the 2068 WY indicate that the majority of mass will have left the system at this time. While a small area at the northern boundary of the model domain show concentrations of PCE exceeding detection limits in layers 1 and 2 (Figure 52-Figure 53), no concentrations exceed detection limits in layers 3 and 4. Concentrations for the 2068 WY do not exceed the MCL anywhere within the model domain.

While there is little difference in simulated concentrations between this alternative and the base scenario (Alternative 1A) for the 2068 WY, breakthrough curves at selected wells indicate a slightly more rapid return to concentrations below the MCL giving the pumping rates used for Alternative 2A. As in Alternative 1A, concentrations at LBWC 1 (Figure 57) and TKWC 3 (Figure 56) never exceed the detection limit of 0.5 µg/l. Here, LBWC 5 (Figure 58) reaches a maximum concentration of 22.3 µg/l in 2019, and declines to below 4 µg/l in 2038, 2 years earlier than in the base scenario. TKWC 1 (Figure 54) never exceeds the MCL, and reaches a maximum concentration of 4.3 µg/l in 2034, and declines to below 4 µg/l in 2040, 5 years earlier than in the base scenario. TKWC 2 (Figure 55) reaches a maximum

concentration of 13.1 µg/l in 2021, and declines to below 4 µg/l in 2039, 1 year sooner than in the base scenario. These results indicate that given the pumping rates assigned in this scenario, concentrations are unlikely to increase substantially in the near future, though they could remain above the MCL for the next 20 years. At no time during this simulation did the simulated PCE concentration or prescribed pumping rate exceed the GAC capacity at LBWC5 or at TKWC2.

Alternative 2B – Targeted Pumping (Conservative)

Transport model results for the 2068 WY indicate that a large quantity of mass will remain in the system at this time. Simulated concentrations exceed 100 µg/l at the source in layer 1, and exceed 50 µg/l near the northern model boundary in layers 1 and 2 (Figure 59-Figure 60). Likewise, simulated concentrations exceed 10 µg/l in layers 3 and 4 (Figure 61-Figure 62) at the northern model boundary. As in Alternative 1B, it should be emphasized that this scenario was simulated for the purpose of creating a worst-case result, with a constant input from the source continuing for the duration of the model and no biogenic decay, and that the results of this simulation are not consistent with observed concentrations, with the exception of LBWC 1 and TKWC 3 where simulated concentrations remain below detection limits through the present.

Like Alternative 2A, simulated concentrations at LBWC 1 (Figure 66) and TKWC 3 (Figure 65) remain below detection limits for the duration of the model. Like the conservative base scenario (Alternative 1B), concentrations at TKWC 1 (Figure 63) and TKWC 2 (Figure 64) remain greater than 4 µg/l for the duration of the model, reaching maximum concentrations of 43.8 µg/l in 2038 and 105.1 µg/l in 2022, respectively. LBWC 5 (Figure 67) reaches a maximum concentration of 93.8 µg/l in 2019, declining to below 4 µg/l in 2054, 4 years sooner than in Alternative 1B. At no time during this simulation did the simulated PCE concentration or prescribed pumping rate exceed the GAC capacity at LBWC5 or at TKWC2.

Alternative 3A – Surface Water Conversion

As this scenario was run only 15 years into the future, results are not directly comparable to Alternatives 1 and 2. Here, transport model results for the 2033 WY indicate PCE concentrations well above the MCL in layers 1 and 2 (Figure 68-Figure 69), and above detection limits (but below the MCL) in layer 3 (Figure 70). No detectable concentrations are present in layer 4 for this stress period. While concentrations at LBWC 1 (Figure 83) and TKWC 3 (Figure 82) remain well below detection limits for all stress periods in this simulation, concentrations at LBWC 5 (9.1 µg/l) (Figure 84), TKWC 1 (5.0 µg/l) (Figure 80), and TKWC 2 (7.8 µg/l) (Figure 81) all meet or exceed the MCL in the 2033 WY stress period. At no time during this simulation did the simulated PCE concentration or prescribed pumping rate exceed the GAC capacity at LBWC5 or at TKWC2.

Alternative 3B – Surface Water Conversion (Conservative)

Transport model results for the 2033 WY indicate that a large quantity of mass will remain in the system at this time. Simulated concentrations exceed 100 µg/l at the source in layer 1 and at the heart of the plume in the area of TKWC 2 in both layers 1 and 2 (Figure 76-Figure 77). Likewise, simulated concentrations exceed 50 µg/l in the area of TKWC 2 in layer 3 (Figure 78), and exceed 10 µg/l in layer 4 (Figure 79). As in Alternatives 1B and 2B, it should be emphasized that this scenario was simulated for the purpose of creating a worst-case result, with a constant input from the source continuing for the duration of the model and no biogenic decay, and that the results of this simulation are not consistent with observed concentrations.

Simulated concentrations at LBWC 1 (Figure 83) remain below detection limits for the duration of the model. While concentrations at TKWC 3 (Figure 82) remain well below the MCL for the duration of the model, the detection limit of 0.5 µg/l is reached at this well in the final stress period. Concentrations at TKWC 1 (Figure 80) and TKWC 2 (Figure 81) remain greater than 4 µg/l for the duration of the model, reaching maximum concentrations of 41.8 µg/l in 2033 and 105.1 µg/l in 2022, respectively, with TKWC 2 declining to a concentration of 66.9 µg/l at the end of the 2033 water year. LBWC 5 (Figure 84) reaches a maximum concentration of 93.8 µg/l in 2019, declining to 34.4 µg/l in at the end of the 2033 water year. At no time during this simulation did the simulated PCE concentration or prescribed pumping rate exceed the GAC capacity at LBWC5 or at TKWC2.

Alternative 4 – 90% GAC Capacity

As in the base scenario (Alternative 1A), transport model results for the 2068 WY indicate that the majority of mass will have left the system at this time. While a small area just south of the northern boundary of the model domain show concentrations of PCE exceeding detection limits in layers 1 and 2 (Figure 85-Figure 86), no concentrations exceed detection limits in layers 3 and 4. Concentrations for this stress period do not exceed the MCL anywhere within the model domain.

Breakthrough curves show a more striking difference between this alternative and the base treatment scenario (Alternative 1A). As in Alternative 1A, concentrations at TKWC 3 (Figure 89) and LBWC 1 (Figure 90) remain well below detection limits for all stress periods. Most notably for this scenario, concentrations at TKWC 1 (Figure 87) never exceed the MCL of 5 µg/l, reaching a maximum of 2.9 µg/l in 2017. Similarly, concentrations at TKWC 2 (Figure 88) decline much more rapidly than in Alternative 1A, dropping below 4 µg/l in 2030, 10 years earlier than in Alternative 1A. After an initial spike in concentrations at LBWC 5 (Figure 91) as pumping is ramped up in the 2019 water year, concentrations also decline more rapidly than in Alternative 1A, dropping below 4 µg/l in 2035 – 5 years earlier than in Alternative 1A.

Alternative 5 – 90% Well Capacity

As in the base scenario (Alternative 1A) and 90% GAC Capacity scenario (Alternative 4), transport model results for the 2068 water year indicate that the majority of mass will have left the system at this time. Concentrations in the 2068 water year do not exceed detection limits for any layer in the model domain, and contour plots are therefore not shown for this simulation.

Breakthrough curves for this scenario are similar to those seen in the 90% GAC Capacity scenario (Alternative 4), though the rates of decline in PCE concentrations are somewhat steeper at all wells, as would be expected with the increased pumping simulated in this model. As in Alternative 4, concentrations at TKWC 3 (Figure 94) and LBWC 1 (Figure 95) remain well below detection limits for all stress periods. Most notably for this scenario, concentrations at TKWC 1 (Figure 92) never exceed the MCL of 5 µg/l, reaching a maximum of 2.9 µg/l in 2017. Similarly, concentrations at TKWC 2 (Figure 93) decline much more rapidly than in Alternative 1A, dropping below 4 µg/l in 2026, 14 years earlier than in Alternative 1A and 4 years earlier than in Alternative 4. After an initial spike in concentrations at LBWC 5 (Figure 96) as pumping is ramped up in the 2019 water year, concentrations also decline more rapidly than in Alternative 1A, dropping below 4 µg/l in 2032 – 8 years earlier than in Alternative 1A and 3 years earlier than in Alternative 4. At no time during this simulation did the simulated PCE concentration exceed the GAC capacity at LBWC5 or at TKWC2. The prescribed pumping rate at TKWC2, however, was greater than the GAC capacity at that well.

Implications

Assuming the validity of the non-conservative model calibration, aquifers within the simulated area can be expected to maintain concentrations of PCE greater than 4 µg/l in localized areas for the next 20-25 years, given the pumping rates assigned in Alternatives 1-3 (Figure 97). Increased pumping rates in wells located near the heart of the existing plume, as seen in the Targeted Pumping scenario (Alternative 2A) could serve to remove mass more rapidly. Simulation results indicate concentrations at wells in this scenario drop below 4 µg/l 1-5 years sooner than in the Base Treatment scenario (Alternative 1A). In addition to the increased mass removal, this targeted pumping at LBWC 5 and TKWC 2 also appears to have a protective effect on TKWC 1, as the change in the groundwater gradient retards plume migration to the north. This effect is seen more clearly with the more greatly increased pumping using in the two hypothetical scenarios, Alternatives 4 and 5 (Figure 98). Relative to the Base Treatment scenario and the Surface Water Conversion scenarios (Alternatives 1A and 3A), concentrations at TKWC 2 are decreased in Alternative 2A, and substantially decreased in Alternatives 4 and 5 (Figure 99). This general trend is also seen at TKWC 3 (Figure 100), LBWC 1 (Figure 101), and LBWC 5 (Figure 102), though the effect is far less significant at those wells.

For all alternatives, the majority of mass removal occurs during the early years of the simulations running into the future, as the highest simulated concentrations reach the area of LBWC 5 and TKWC 2 in the near future. This can be clearly seen in a plot of mass removed by alternative and by well (Figure 103), as the mass removed at the end of Alternative 3, 15 years into the future, is approximately 2/3 of that removed by Alternative 1 after 50 years at the same pumping rates . Likewise, this figure makes clear the importance of increased pumping at LBWC 5 for the increased mass removal seen in Alternative 2, as that well is located nearest to the simulated heart of the plume.

This study serves only to assess potential future concentrations of PCE within the aquifer system, and makes no effort to analyze the costs (of operating, infrastructure, or remediation) and stakeholder input that may be associated with the management scenarios described here.

Data Sources and Gaps

Publicly available PCE, TCE, and DCE concentrations collected by STPUD, TKWC, LBWC, the Lahontan Regional Water Quality Control Board (LRWQC), and other stakeholders were used in both the pre-design investigation and in the development of the model presented in this report. In more recent years (2015-present), an effort has been made by all stakeholders to collect a continuous data set at existing production and monitoring wells in the South Y area and prevent additional temporal gaps in data.

Spatially, the dataset could be improved through additional monitoring well sites, particularly along the estimated margins of the simulated plume extent and in the large areas between TKWC 2 and TKWC 1, between TKWC 2 and TKWC 3, and between LBWC 5 and LBWC 1, as existing monitoring wells have largely been placed in an effort to locate the source(s) of the plume. Additionally, collection of samples from isolated aquifer zones within deeper production wells (LBWC 5, TKWC 2, and TKWC 1) could be used to validate the vertical extent of the plume simulated in the model.

Limitations and Disclaimer

The South Y Fate and Transport Model is intended to be used as a decision support tool for the Technical Advisory Committee for the South Y Feasibility Study of Remedial Alternatives. The goal of that program is to determine a path forward that will continue to provide clean public water supplies to all residents of South Lake Tahoe while addressing the PCE contamination in the South Y area. The intended use of the numerical model is to facilitate comparisons between remedial options (i.e., the management scenarios described above).

The available data on PCE concentrations throughout the model domain are relatively sparse in both space and time. When data are available, the uncertainties are relatively high. While the calibrated model matches the trends seen in the available data, the uncertainties in the simulated concentrations of PCE are necessarily greater than the uncertainties in observed concentrations over the last thirty years.

Although the South Y Fate and Transport Model has been verified, DRI makes no representations or warranties of any kind as to its accuracy. DRI additionally makes no warranties of merchantability or fitness for a particular use, nor are such warranties to be implied, with respect to the South Y Fate and Transport Model. Any person utilizing the South Y Fate and Transport Model is responsible for understanding its accuracy and limitations. In particular, alterations and/or manipulation of the original data may adversely affect their accuracy, meaning, and design integrity. Any person utilizing the South Y Fate and Transport Model assumes all responsibility for its correct use and for its interpretation.

In no event shall DRI be liable for any special, punitive, incidental, indirect or consequential damages of any kind, or any damages whatsoever, including, without limitation, those resulting from loss of use, data or profits, whether or not the DRI has been advised of the possibility of such damages, and on any theory of liability, arising out of or in connection with the use of the South Y Fate and Transport Model. DRI assumes no responsibility or liability for any errors or omissions in the content of the South Y Fate and Transport Model, which is provided on an “as is” basis with no guarantees of completeness, accuracy, usefulness or timeliness.

WITH RESPECT TO THE SOUTH Y FATE AND TRANSPORT MODEL, DRI MAKES NO, AND EXPRESSLY DISCLAIM ALL, COVENANTS OR WARRANTIES OF ANY KIND, ORAL OR WRITTEN, EXPRESS OR IMPLIED, ARISING FROM COURSE OF DEALING, COURSE OF PERFORMANCE OR OTHERWISE, INCLUDING, BUT NOT LIMITED TO, ANY WARRANTIES OF TITLE, MERCHANTABILITY, FITNESS FOR A PARTICULAR PURPOSE, CONFORMITY TO ANY REPRESENTATION OR DESCRIPTION, COMPLETELY SECURE OR ERROR-FREE SERVICE, NON-INTERRUPTION, NON-INTERFERENCE OR NON-INFRINGEMENT.

References

Aronson, D., Citra, M., Shuler, K., Printup, H., and Howard, P., 1999. Aerobic biodegradation of organic chemicals in environmental media – a summary of field and laboratory studies: Prepared for the U.S. Environmental Protection Agency by Environmental Science Center, Syracuse Research Corporation, North Syracuse, N.Y., SRC TR 99-002, 189 p.

Alward, R., and C. Petersen, 2016. Technical Memorandum on the Results of PCE Investigation for Tahoe Keys Property Owners Association.

Carroll, R.W.H., G. Pohll, and S. Rajagopal, 2016a. South Lake Tahoe Groundwater Model, Desert Research Institute, February 25, 2016, 28p.

Carroll, R.W.H., G. Pohll, and S. Rajagopal, 2016b. South Lake Tahoe Groundwater Model, Desert Research Institute, August 26, 2016, 12p.

Harding ESE, 2001. Groundwater Investigation, Hurzel Properties LLC, 949 Emerald Bay Road.

Hogen Lovells, 2016. Response to proposed cleanup and abatement order for former Lake Tahoe Laundry Works; 1024 Lake Tahoe Boulevard, South Lake Tahoe, California.

IT Corporation, 2000. Fate and Transport Modeling Report and Revised Drawings for the Groundwater Modeling Report.

Kipp, K.L., Jr., Hsieh, P.A., and Charlton, S.R., 2008. Guide to the revised groundwater flow and heat transport simulator: HYDROTHERM — Version 3: U.S. Geological Survey Techniques and Methods 6−A25, 160 p.

Knoll, D.A., and Keyes, D.E., 2004. Jacobian-free Newton-Krylov methods: a survey of approaches and applications, Journal of Computational Physics 193 (2), pp 357-397.

Lahontan Regional Water Quality Control Board, 2016. PCE Monitoring Well Data, Tahoe South Y, Fall 2016. Memo distributed December 21, 2016.

Lawrence, S., 2006. Description, properties, and degradation of selected volatile organic compounds detected in groundwater – a review of selected literature. USGS Open-File Report 2006-1338.

Leonard, B.P., 1988. Universal Limiter for transient interpolation modeling of the advective transport equations: the ULTIMATE conservative difference scheme, NASA Technical Memorandum 100916 ICOMP-88-11.

Leonard, B.P., and Niknafs, H.S., 1990. Cost-effective accurate coarse-grid method for highly convective multidimensional unsteady flows, NASA Conference Publication 3078: Computational Fluid Dynamics Symposium on Aeropropulsion, April 1990.

Leonard, B.P., and Niknafs, H.S., 1991. Sharp monotonic resolution of discontinuities without clipping of narrow extrema, Computer and Fluids, 19(1), pp 141-154.

Niswonger, R., Panday, S., and Ibaraki, M., 2011. MODFLOW-NWT, A Newton Formulation for MODFLOW-2005. Groundwater Resources Program. Techniques and Methods 6-A37, 44p.

Roache, P.J., 1992. A flux-based modified method of characteristics. Int. J. Numerical Methods in Fluids, 15, pp 1259-1275.

Roberts, P., Goltz, M., and Mackay, D., 1986. A natural gradient experiment on solute transport in a sand aquifer-III. Retardation estimates and mass balances for organic solutes: Water Resources Research, v 22 (13), pp 2047-2058.

Saad, Y., 2003, Iterative methods for sparse linear systems (2d ed.): Philadelphia, Penn., Society for Industrial and Applied Mathematics, 528 p.

SECOR, 2008. Site Investigation Report, Former Dry Cleaning Business, 949 Emerald Bay Drive.

South Tahoe Public Utility District, 2017. South Y VOC and water quality data, unpublished.

State Water Resources Control Board, 2009. Groundwater Information Sheet: Tetrachloroethylene (PCE). Division of Water Quality, GAMA Program, Revised February 9 2009.

Zaidel, J., 2013. Discontinuous steady-state analytical solutions of the Boussinesq equation and their numerical representation by MODFLOW. Ground Water, Method Note/ doi: 10.1111/gwat.12019. pp 1-8.

Zheng, C., and P.P. Wang, 1999. MT3DMS: A Modular Three-Dimensional Multispecies Transport Model for Simulation of Advection, Dispersion, and Chemical Reactions of Contaminants in Groundwater Systems; Documentation and User's Guide, U.S. Army Corps of Engineers Contract Report SERDP-99-1, Vicksburg, Mississippi, 220 pages.

Zheng, C., and Bennett, G.D., 2002. Applied Contaminant Transport Modeling, 2nd ed. New York: John Wiley & Sons.

Tables

Table 1. Pumping rates used for the three alternatives and two hypothetical scenarios.

Alternative	Description	Pumping Rates (m^3/d)									
		LBWC 1	LBWC 5	TKWC 1	TKWC 2	TKWC 3	Sunset	Paloma	Helen 2	Bayview	Al Tahoe 2
1A	Base Treatment	872.19	199.66	532.54	1,219.49	1,316.98	1,735.79	195.74	713.22	8,997.45	1,462.21
1B	Base Treatment Conservative	872.19	199.66	532.54	1,219.49	1,316.98	1,735.79	195.74	713.22	8,997.45	1,462.21
2A	Targeted Pumping	199.66	872.19	532.54	1,316.98	1,219.49	1,735.79	195.74	713.22	8,997.45	1,462.21
2B	Targeted Pumping Conservative	199.66	872.19	532.54	1,316.98	1,219.49	1,735.79	195.74	713.22	8,997.45	1,462.21
3A	SW Conversion	872.19	199.66	532.54	1,219.49	1,316.98	1,735.79	195.74	713.22	8,997.45	1,462.21
3B	SW Conversion Conservative	872.19	199.66	532.54	1,219.49	1,316.98	1,735.79	195.74	713.22	8,997.45	1,462.21
4	90% of GAC Capacity	389.52	3,434.13	1,458.14	2,698.24	808.56	1,165.41	131.57	478.85	6,039.43	981.75
5	90% of Well Capacity	389.52	3,434.13	1,458.14	8,830.61	808.56	353.01	39.85	145.05	1,829.36	297.38

Table 2. PCE recharge concentration for predictive simulations and biodegradation half-lives by layer.

Alternative	Description	Source Term – Future Recharge PCE	Source Term – Future Recharge PCE	Biodegradation Half-life (years)			
		(mg/l)	(kg/yr)	Layer 1	Layer 2	Layer 3	Layer 4
1A	Base Treatment	0	0	17	17	2	2
1B	Base Treatment Conservative	10	4.45	0	0	0	0
2A	Targeted Pumping	0	0	17	17	2	2
2B	Targeted Pumping Conservative	10	4.45	0	0	0	0
3A	SW Conversion	0	0	17	17	2	2
3B	SW Conversion Conservative	10	4.45	0	0	0	0
4	90% of GAC Capacity	0	0	17	17	2	2
5	90% of Well Capacity	0	0	17	17	2	2

*Table 3. Mass removed and removal rate by well for all alternatives. **Alternatives 3A and 3B simulated for WY 2019-2033.*

Alternative	Description	PCE Mass Removed (0.4536 kg) or (lbs); WY 2019-2068**				Total Extracted Groundwater Volume; WY 2019-2068	Average PCE Mass Removal Rate
		LBWC 5	TKWC 1	TKWC 2	Total	(3785 m^3) or (MG)	(lb/MG)
Alternative 1A	Baseline	54.1	68.8	224.1	347.0	9416.1	0.04
Alternative 1B	Conservative Baseline	260.4	763.8	1548.3	2572.5	9416.1	0.27
Alternative 2A	Targeted	204.7	60.5	232.0	497.2	13131.1	0.04
Alternative 2B	Conservative Targeted	971.2	678.4	1615.0	3264.6	13131.1	0.25
Alternative 3A**	SW Conversion	43.0	26.8	162.4	232.2	2824.9	0.08
Alternative 3B**	Conservative SW Conversion	189.2	224.0	1004.9	1418.1	2824.9	0.50
Alternative 4	90% of GAC capacity	697.6	48.1	249.6	995.3	36621.0	0.03
Alternative 5	90% of well capacity	626.5	16.2	506.5	1149.2	66207.1	0.02

Table 4. Simulated year PCE concentrations drop below 4 ug/l, by well, and the number of years after 2018 each well drops below 4 ug/l for all alternatives. N.E. = Never Exceeds.

Alternative	Description	Year PCE < 4 µg/l					Years after 2018 (PCE < 4 µg/l)				
		LBWC 1	LBWC 5	TKWC 1	TKWC 2	TKWC 3	LBWC 1	LBWC 5	TKWC 1	TKWC 2	TKWC 3
Alternative 1A	Baseline	N.E.	2040	2045	2040	N.E.	N.E.	22	27	22	N.E.
Alternative 1B	Conservative Baseline	N.E.	2058	>2068	>2068	N.E.	N.E.	40	> 50	> 50	N.E.
Alternative 2A	Targeted	N.E.	2038	2040	2039	N.E.	N.E.	20	22	21	N.E.
Alternative 2B	Conservative Targeted	N.E.	2054	>2068	>2068	N.E.	N.E.	36	> 50	> 50	N.E.
Alternative 3A	SW Conversion	N/A	N/A	N/A	N/A	N/A	N/A	N/A	N/A	N/A	N/A
Alternative 3B	Conservative SW Conversion	N/A	N/A	N/A	N/A	N/A	N/A	N/A	N/A	N/A	N/A
Alternative 4	90% of GAC capacity	N.E.	2035	N.E.	2030	N.E.	N.E.	17	N.E.	12	N.E.
Alternative 5	90% of well capacity	N.E.	2032	N.E.	2026	N.E.	N.E.	14	N.E.	8	N.E.

Figures

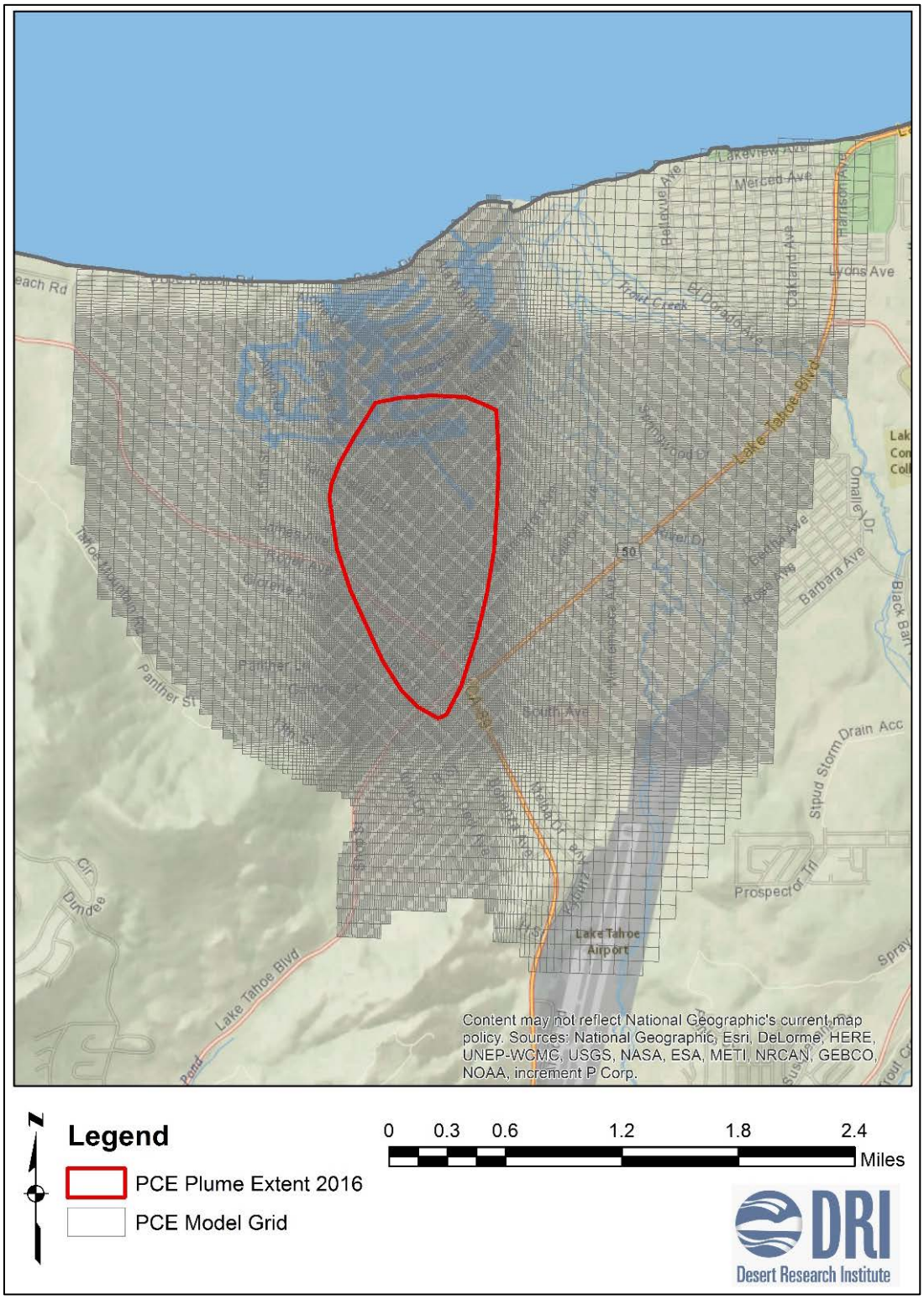

Figure 1. Estimated extent of PCE plume as of 2016.

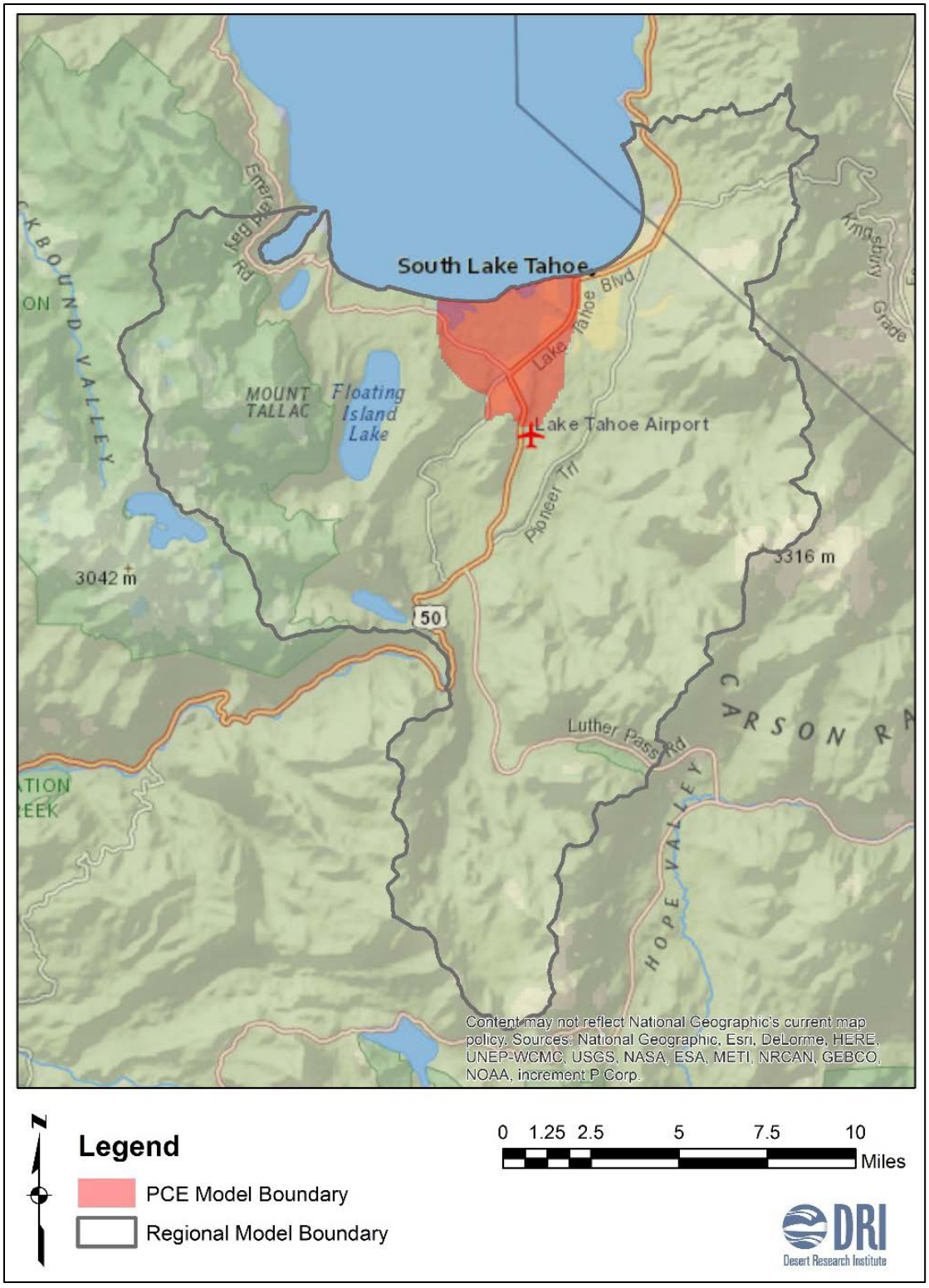

Figure 2. Section of Carroll, 2016 model domain used for PCE model.

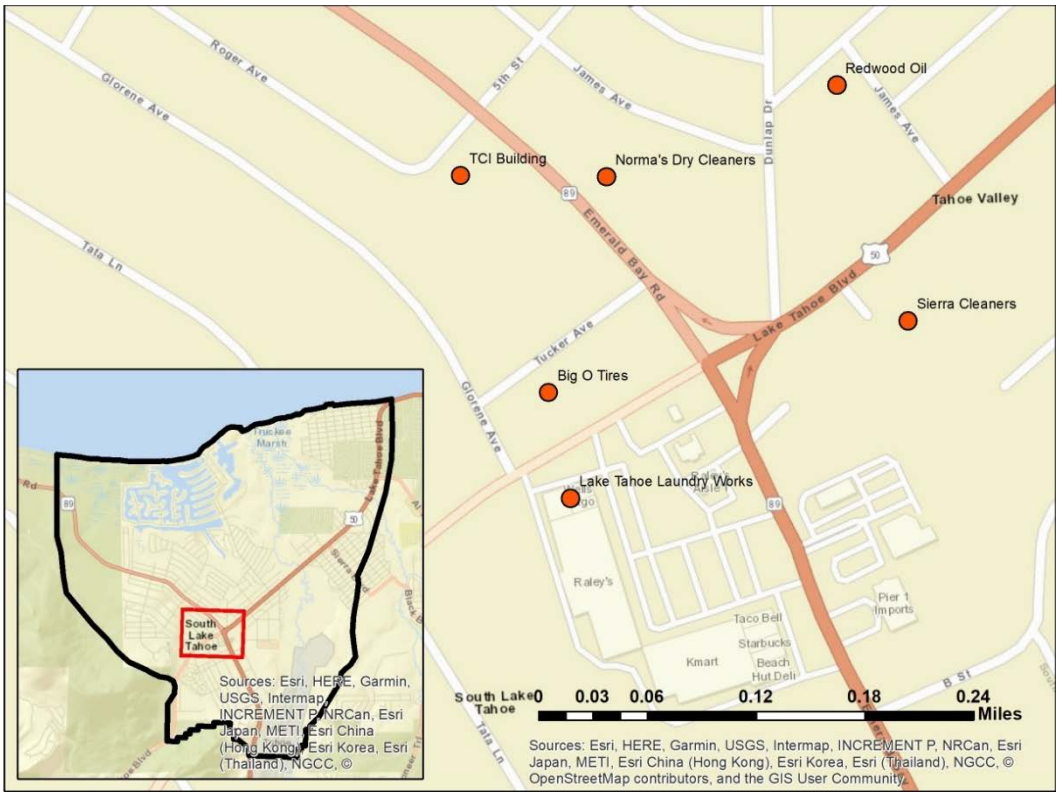

Figure 3. Identified potential sources of PCE contamination in the South Y area (Harding ESE, 2001; SECOR, 2008; Hogen Lovells, 2016)

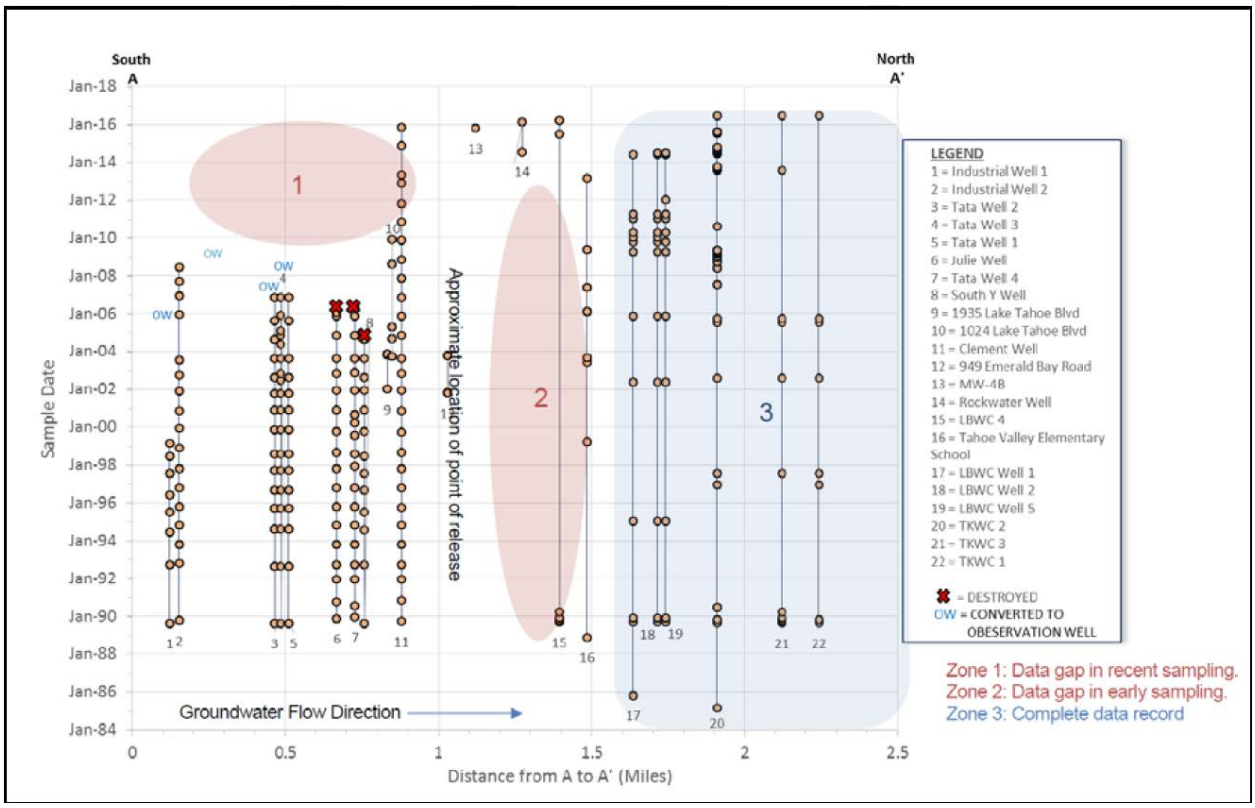

Figure 4. Spatial and temporal gaps in PCE concentration data (from Alward and Petersen, 2016).

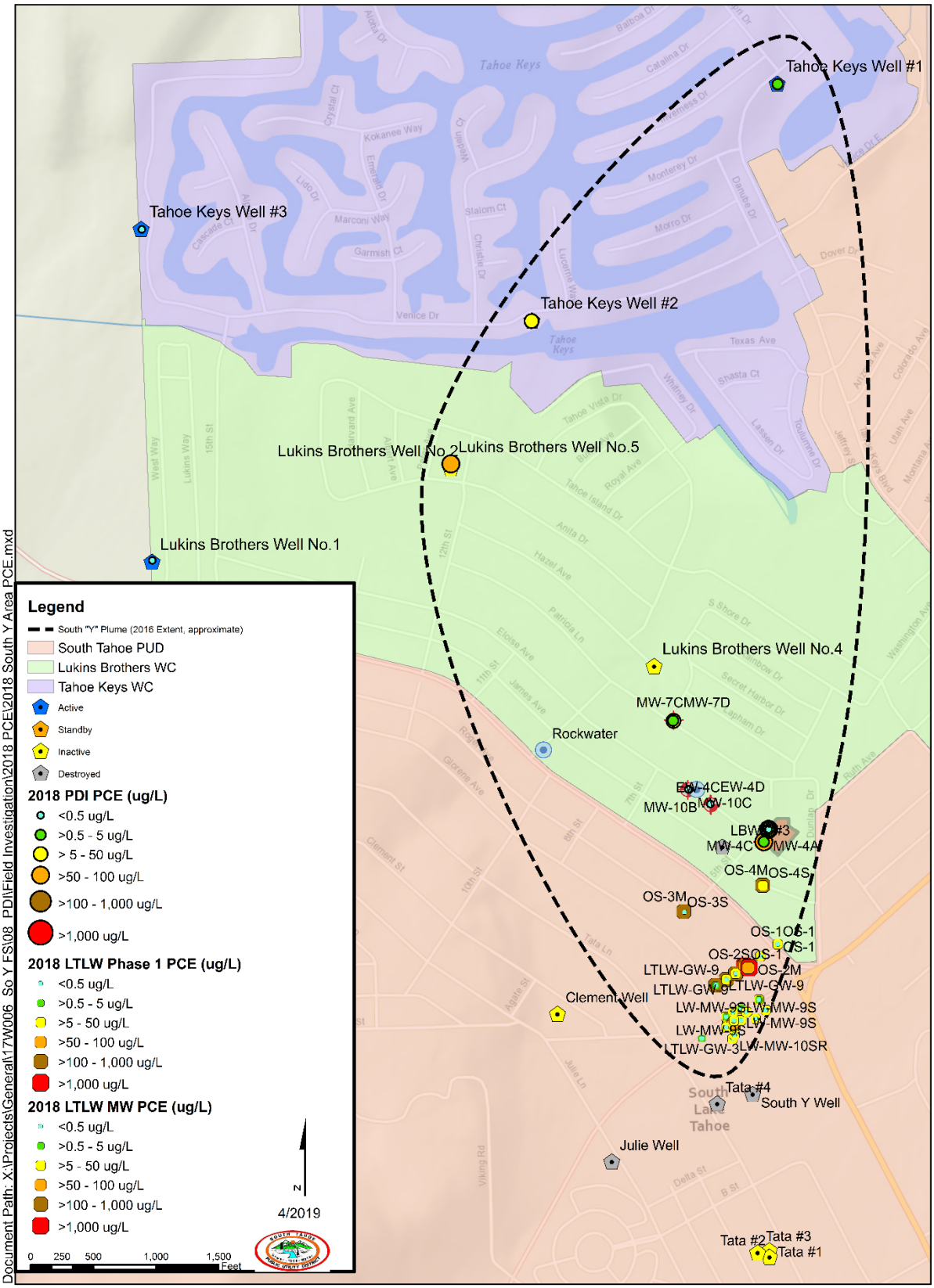

Figure 5. 2018 PCE concentrations (STPUD, 2018).

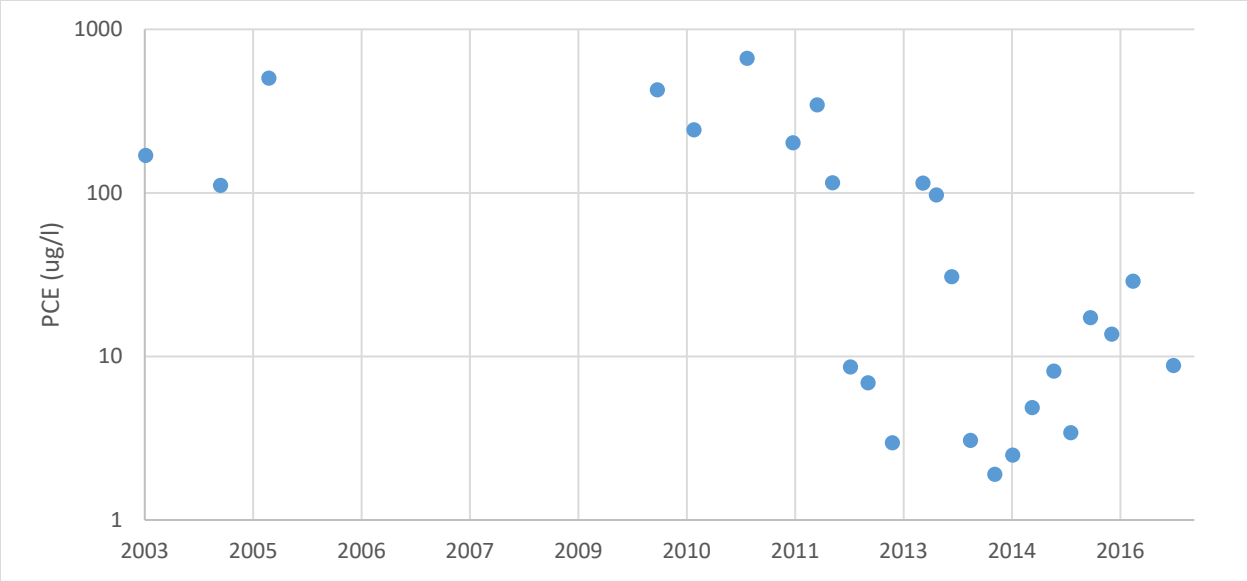

Figure 6. Mean PCE concentrations from all sampled monitoring wells on the LTLW site. Each point represents the mean concentration at a group of wells where samples were collected on the same day.

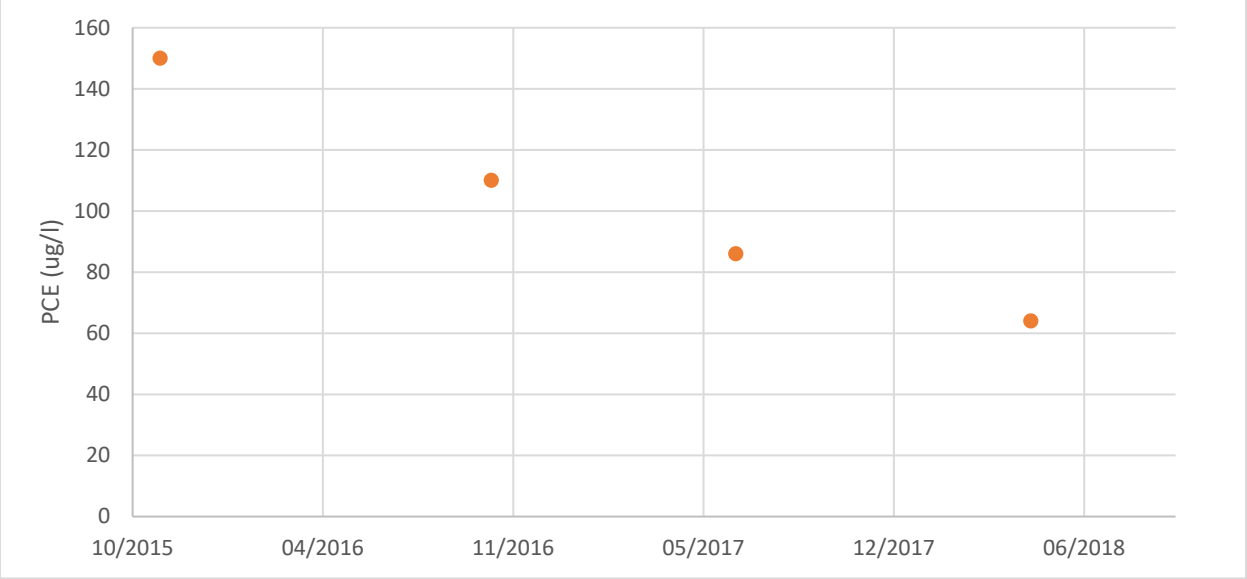

Figure 7. Observed PCE concentrations at MW-4B, approximately 450 meters downgradient of the LTLW site.

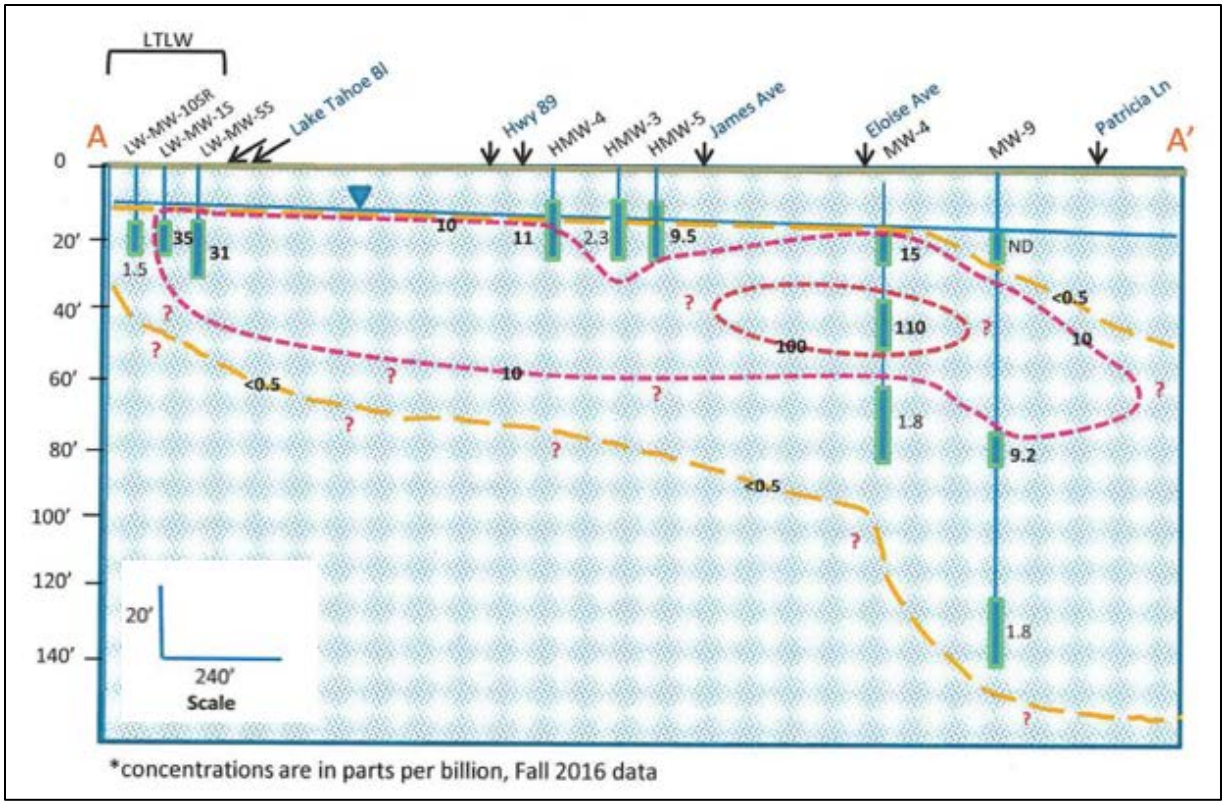

Figure 8. Vertical extent of PCE plume in Fall 2016 (from Lahontan Regional Water Quality Control Board, 2016).

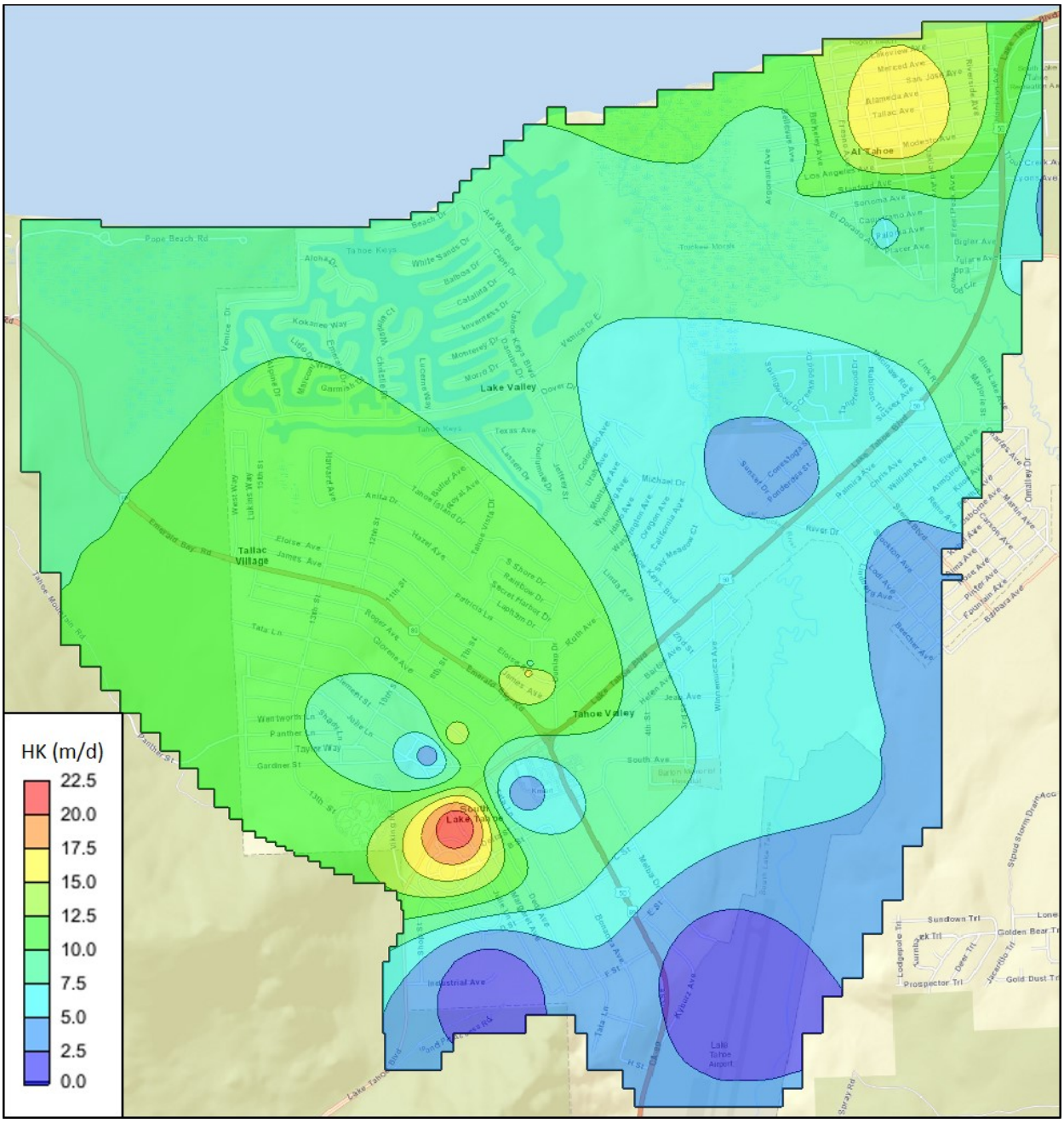

Figure 9. Simulated hydraulic conductivities for model layers 1 and 2.

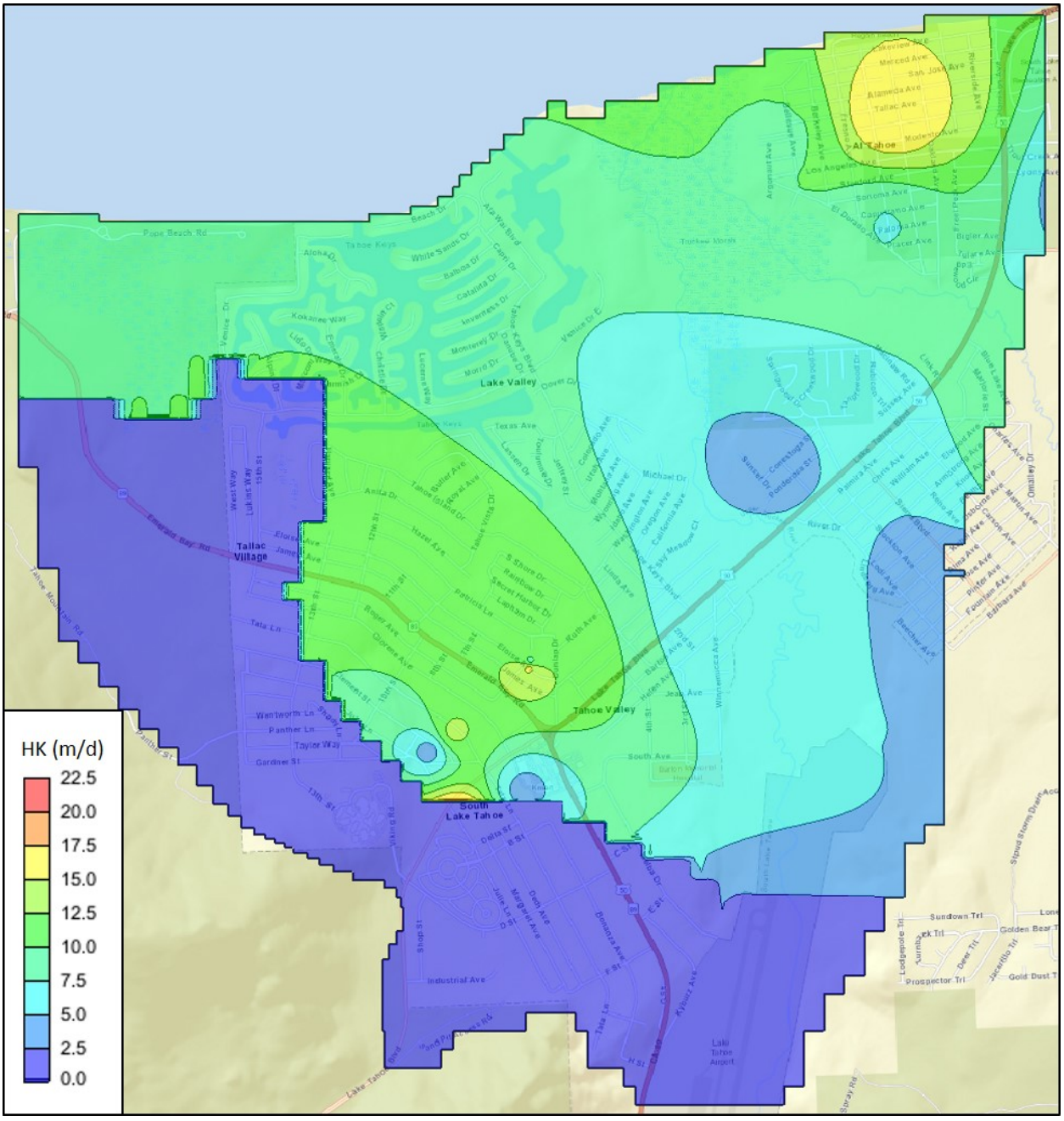

Figure 10. Simulated hydraulic conductivities for model layer 3.

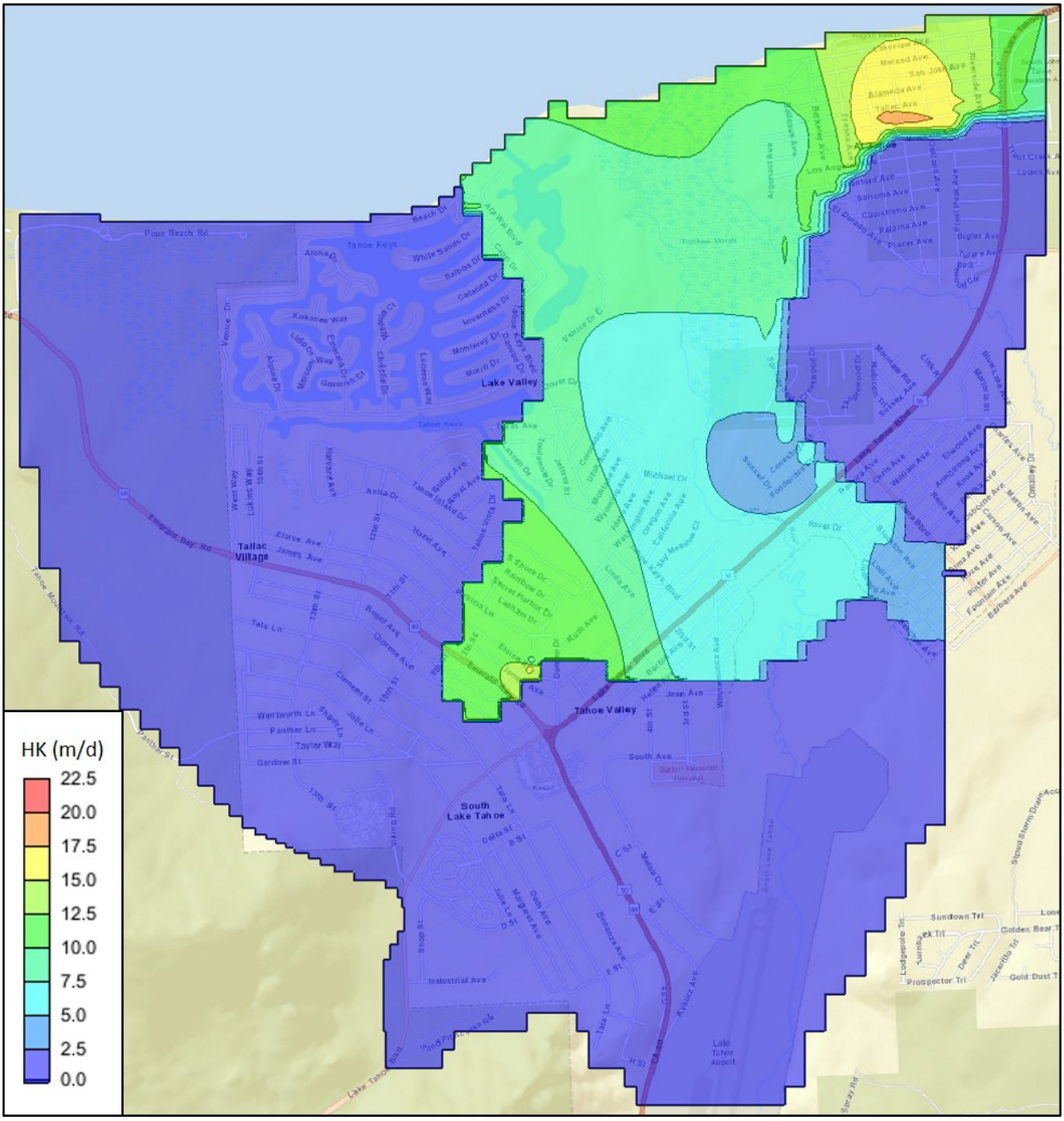

Figure 11. Simulated hydraulic conductivities for model layer 4.

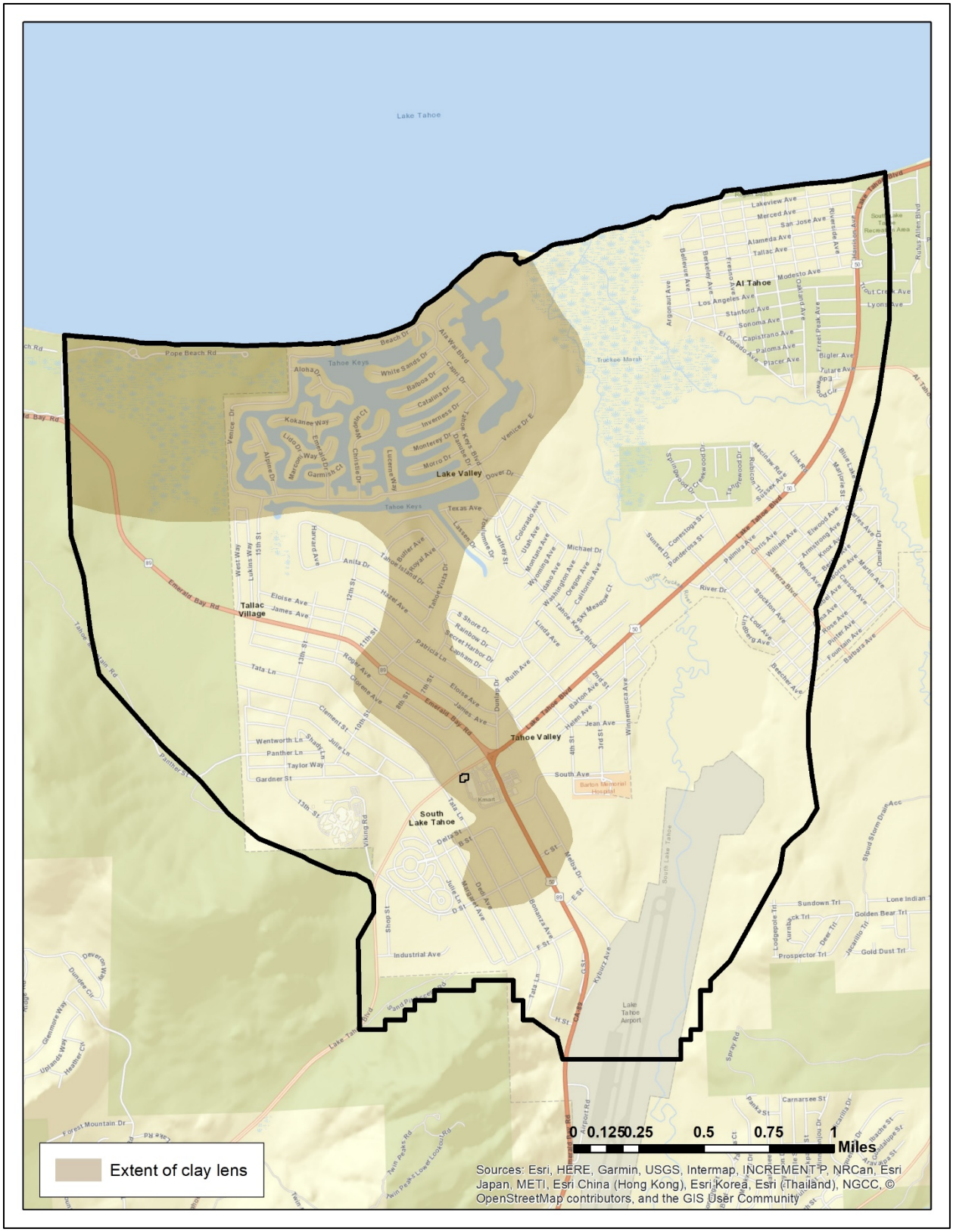

Figure 12. Extent of simulated clay lens underlying PCE source, as defined by USA Gas well logs, and local production and domestic water well logs.

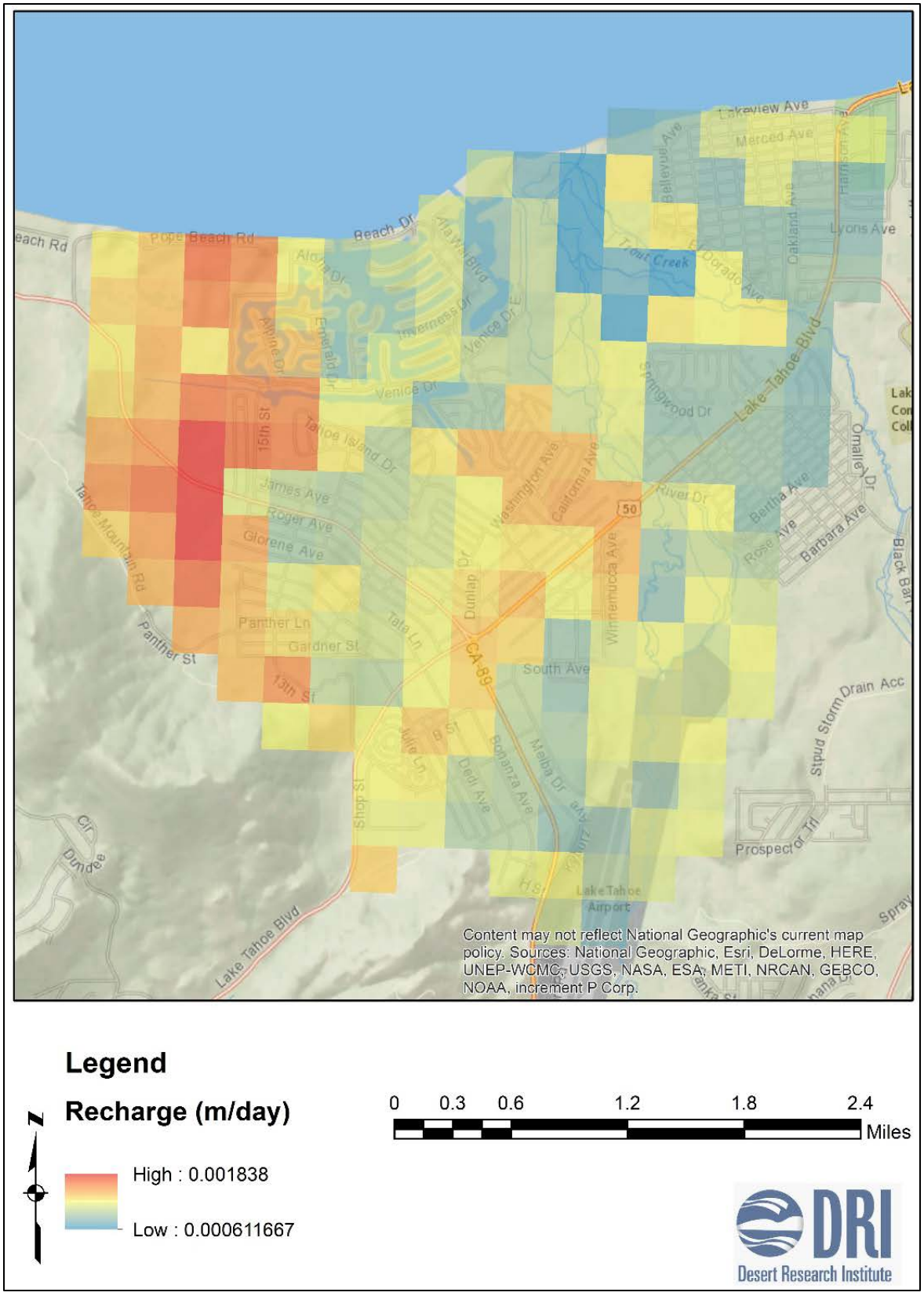

Figure 13. Areal recharge rates applied over model domain, as taken from Carroll, 2016.

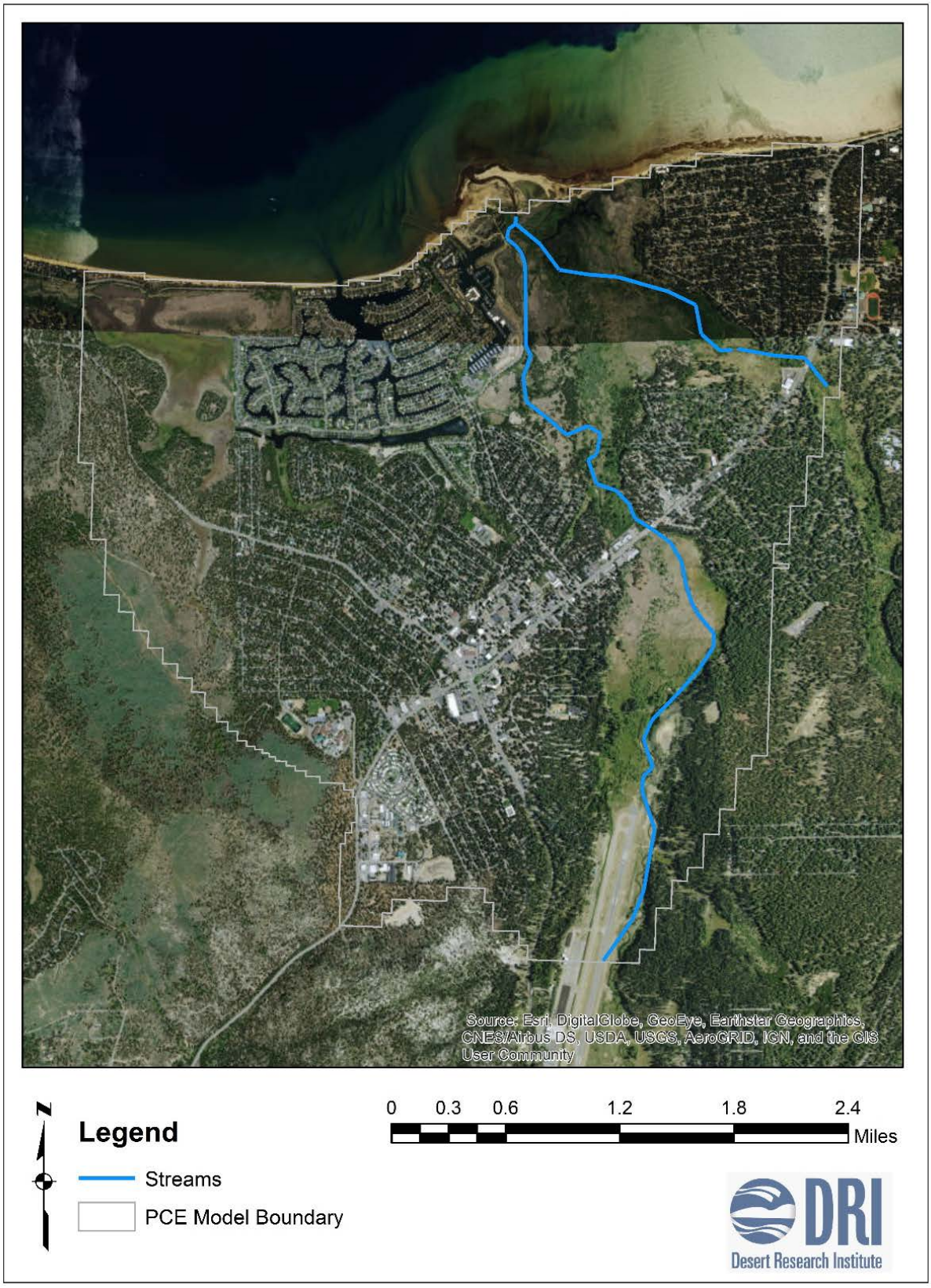

Figure 14. Locations of simulated streams.

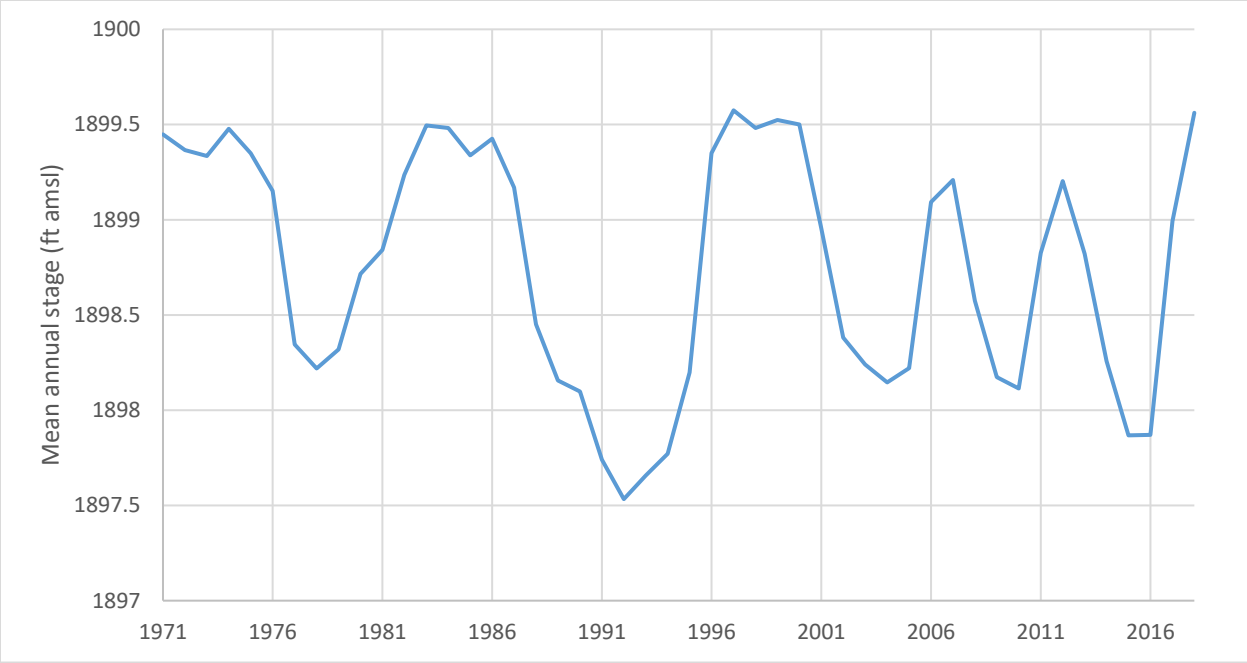

Figure 15. Mean annual stage by water year at Lake Tahoe used to define heads in the General Head Boundary along the northern boundary of the model.

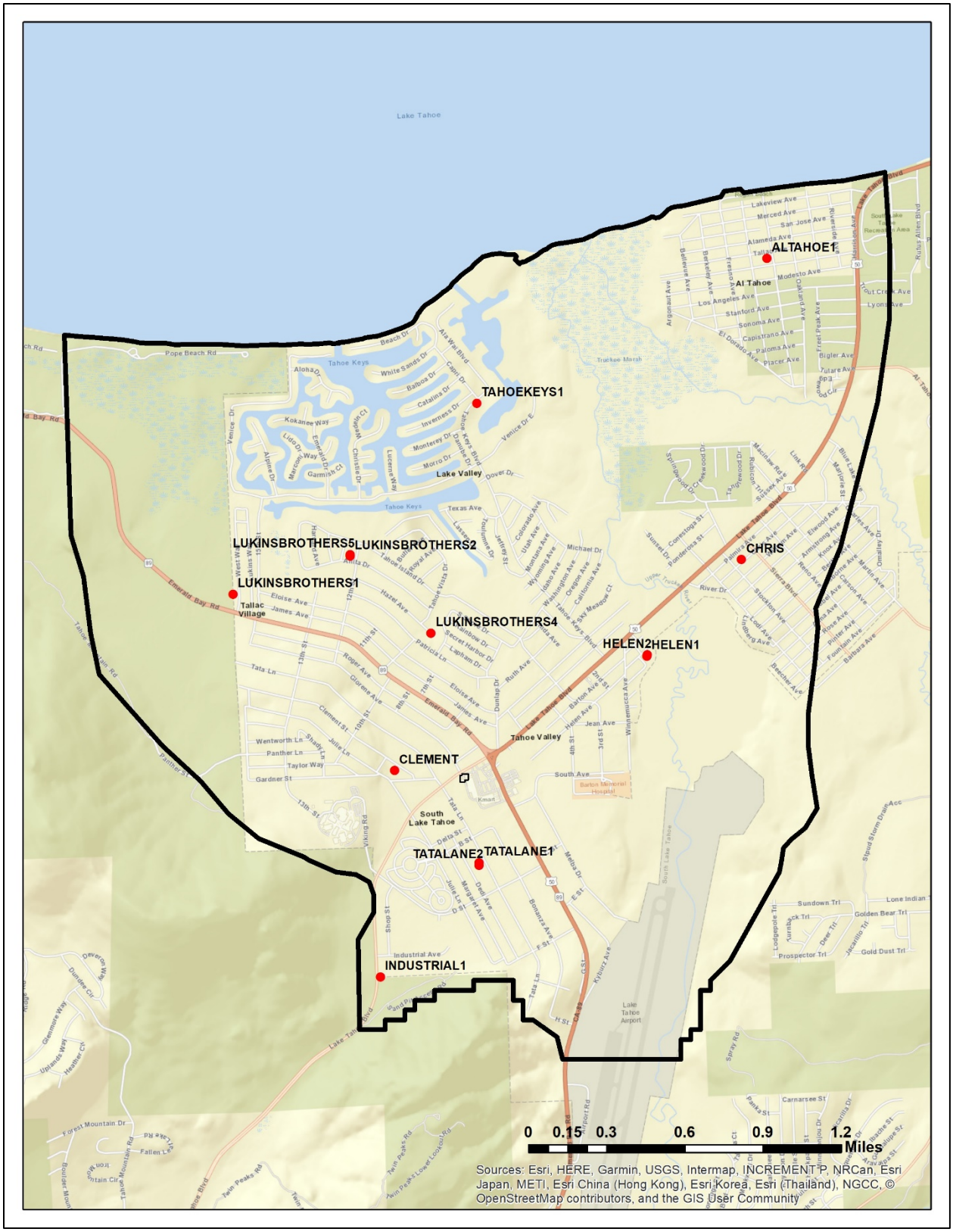

Figure 16. Locations of steady-state pumping wells.

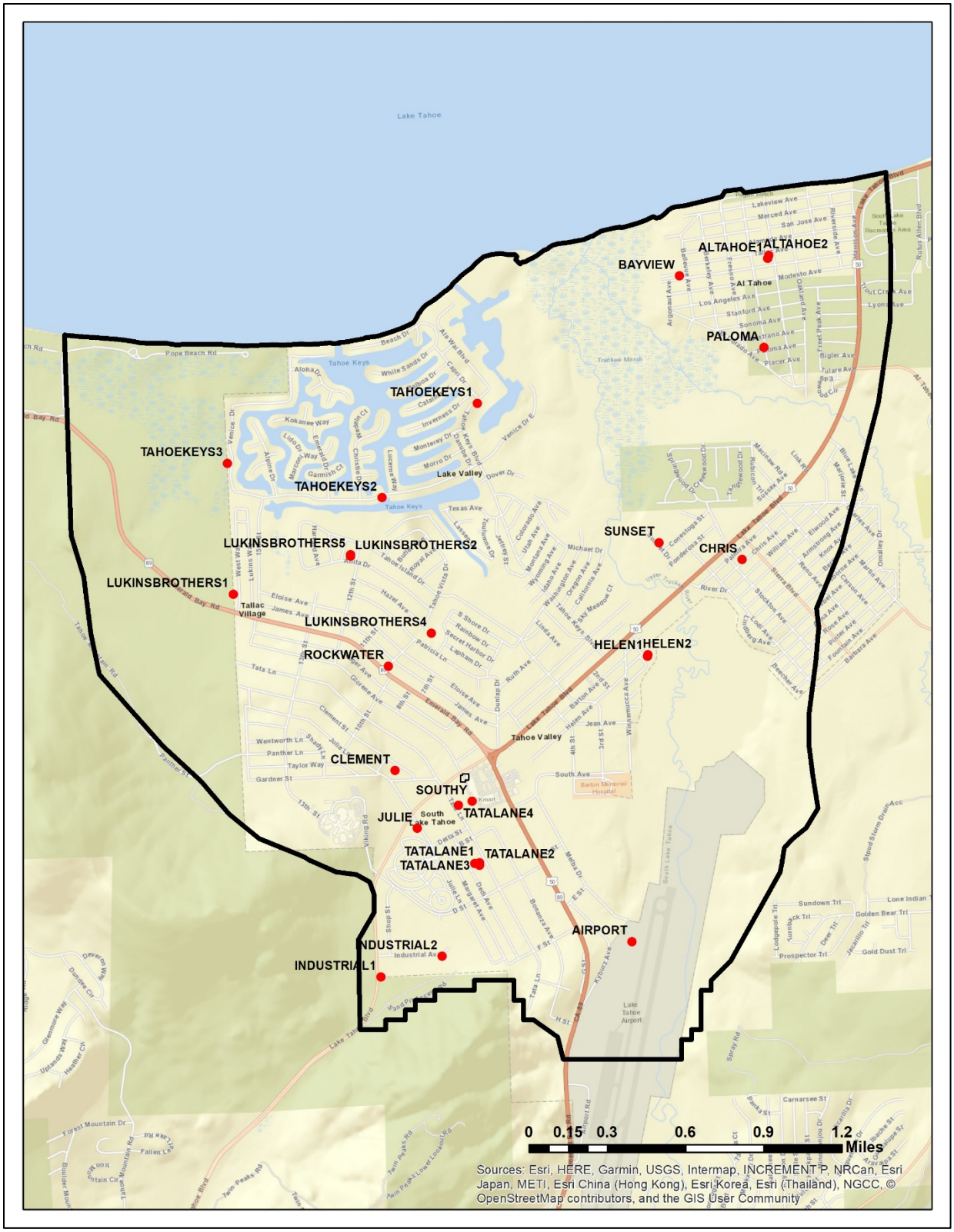

Figure 17. Locations of transient pumping wells.

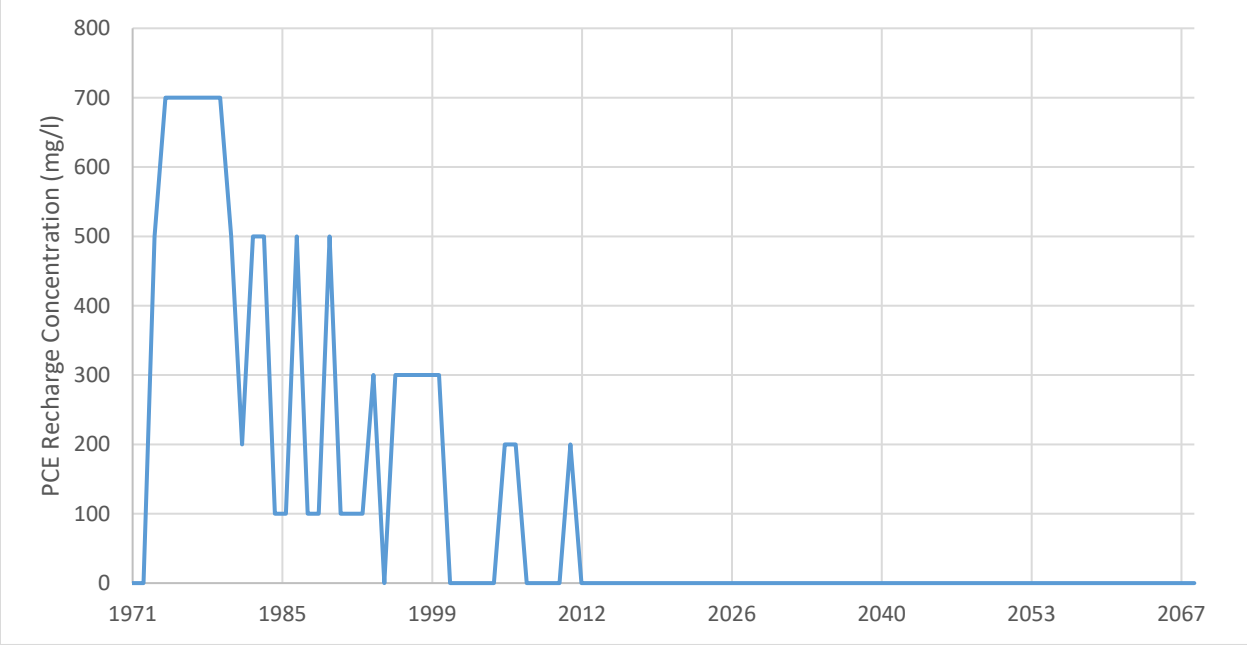

Figure 18. Simulated PCE recharge concentrations for the calibrated model.

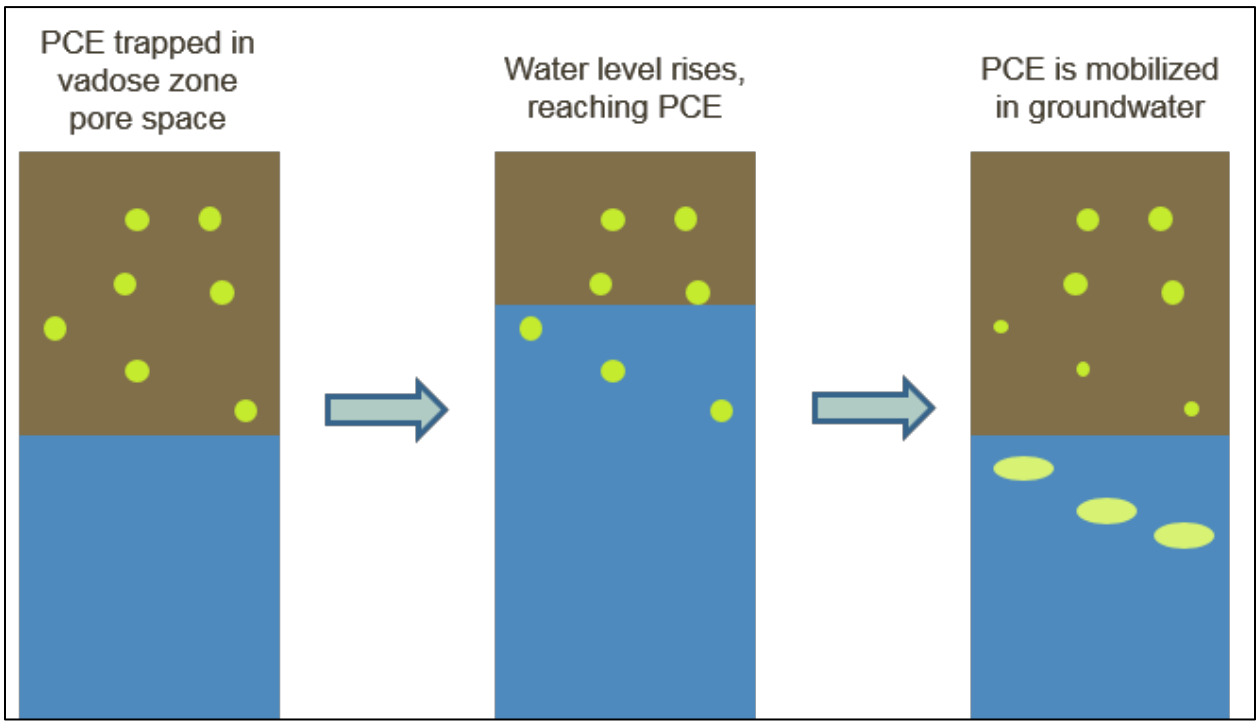

Figure 19. Conceptualized mobilization of soil-bound PCE as groundwater levels rise during 'big water' years.

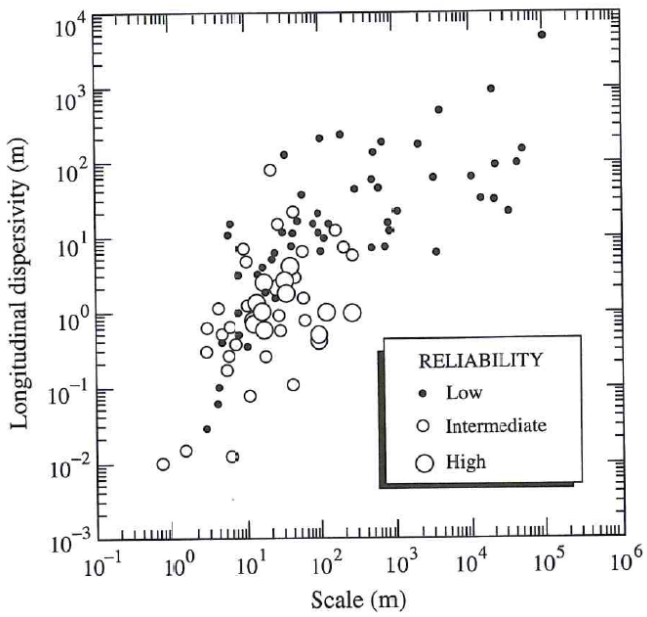

Figure 20. Range of appropriate longitudinal dispersivity relative to scale of observation (from Zheng and Bennett, 2002).

Figure 21. Observed concentrations of dissolved oxygen in groundwater.

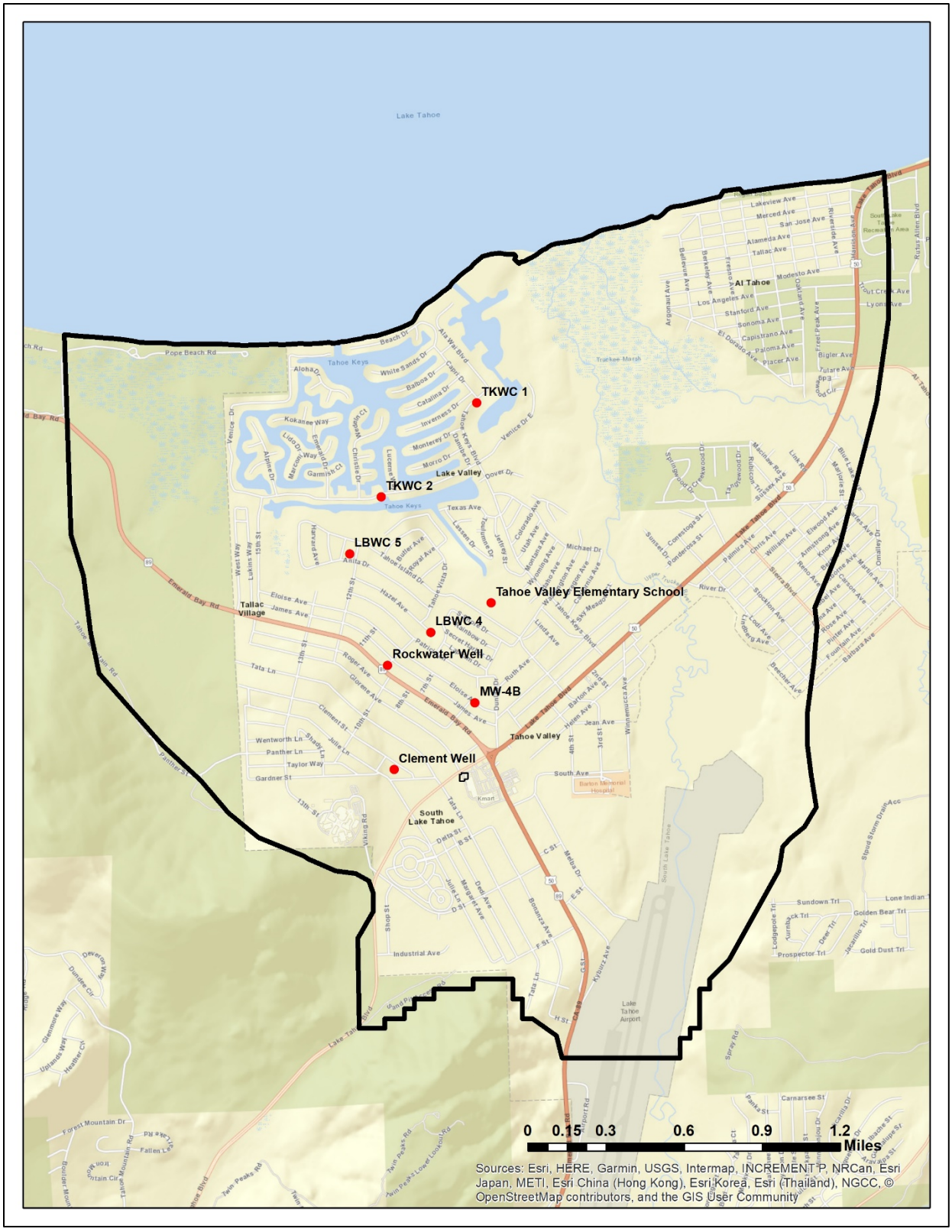

Figure 22. Locations of simulated and observed PCE concentrations detailed in this report.

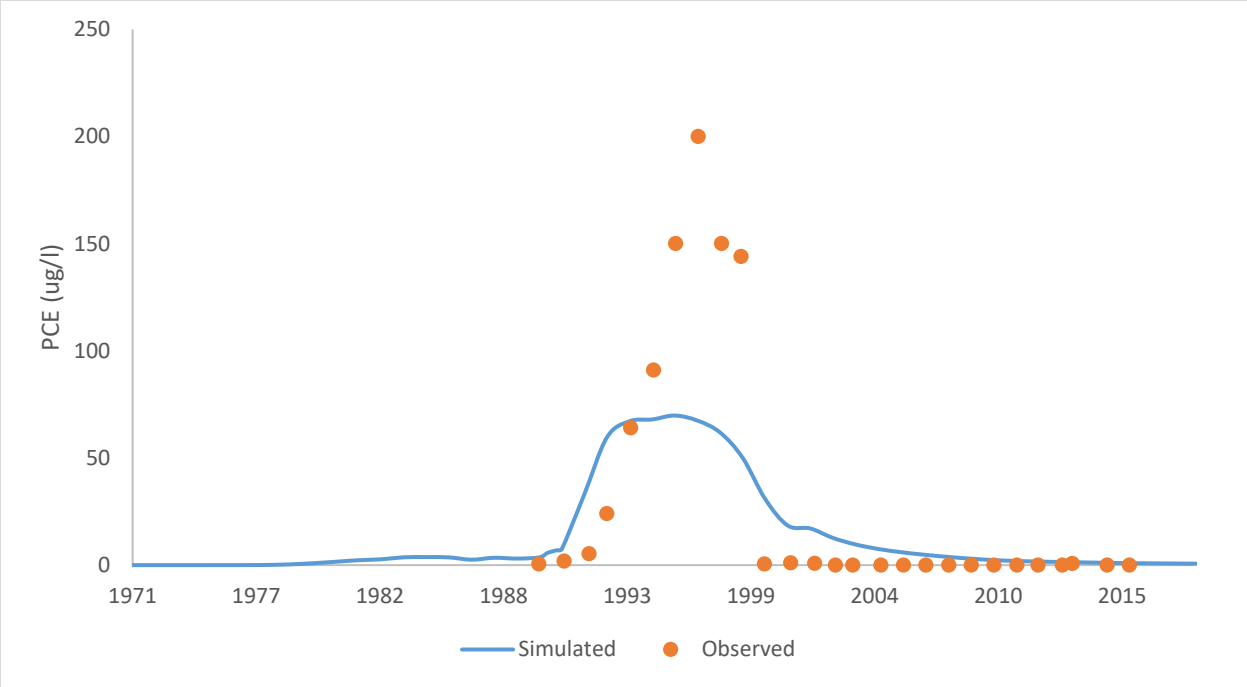

Figure 23. Simulated vs. observed concentrations of PCE at Clement Well.

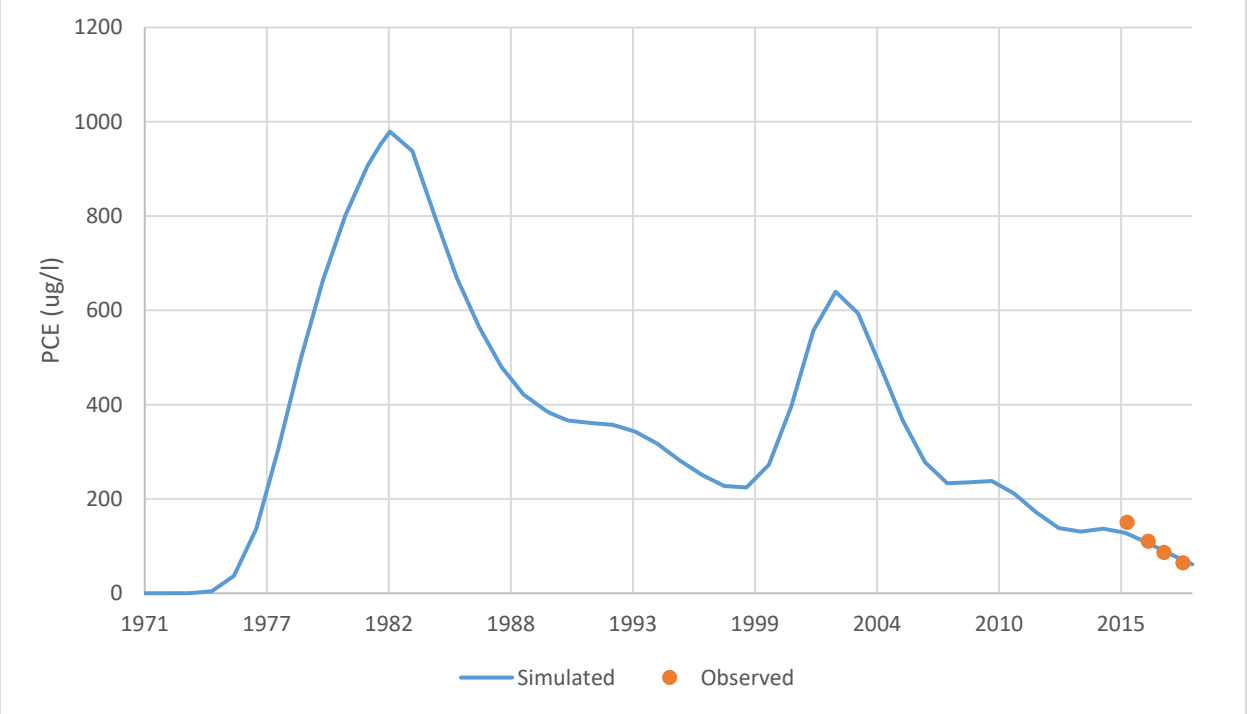

Figure 24. Simulated vs. observed concentrations of PCE at MW-4B.

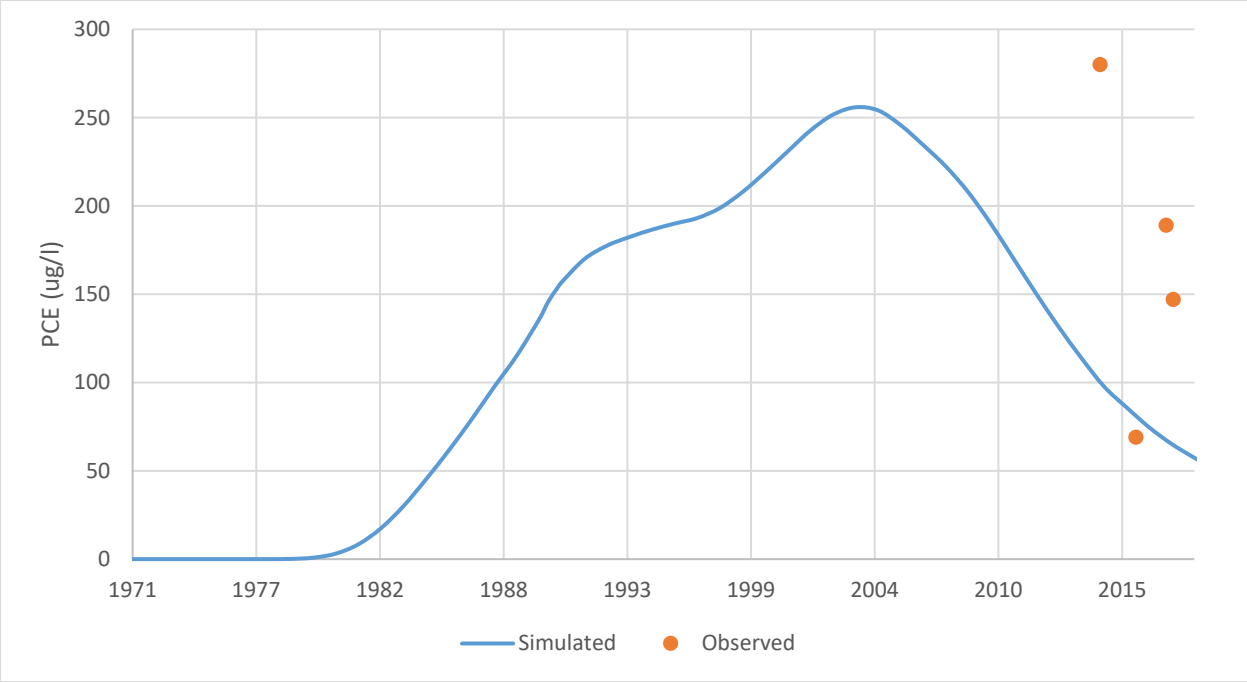

Figure 25. Simulated vs. observed concentrations of PCE at Rockwater Well.

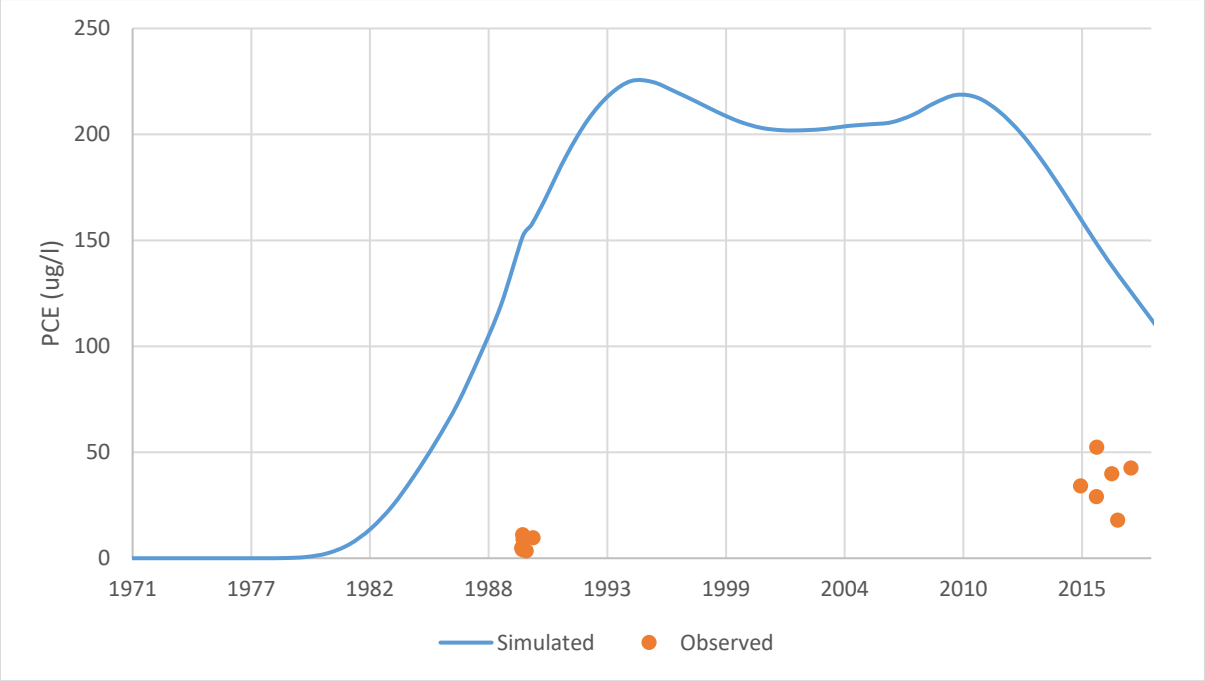

Figure 26. Simulated vs. observed concentrations of PCE at LBWC 4 Well.

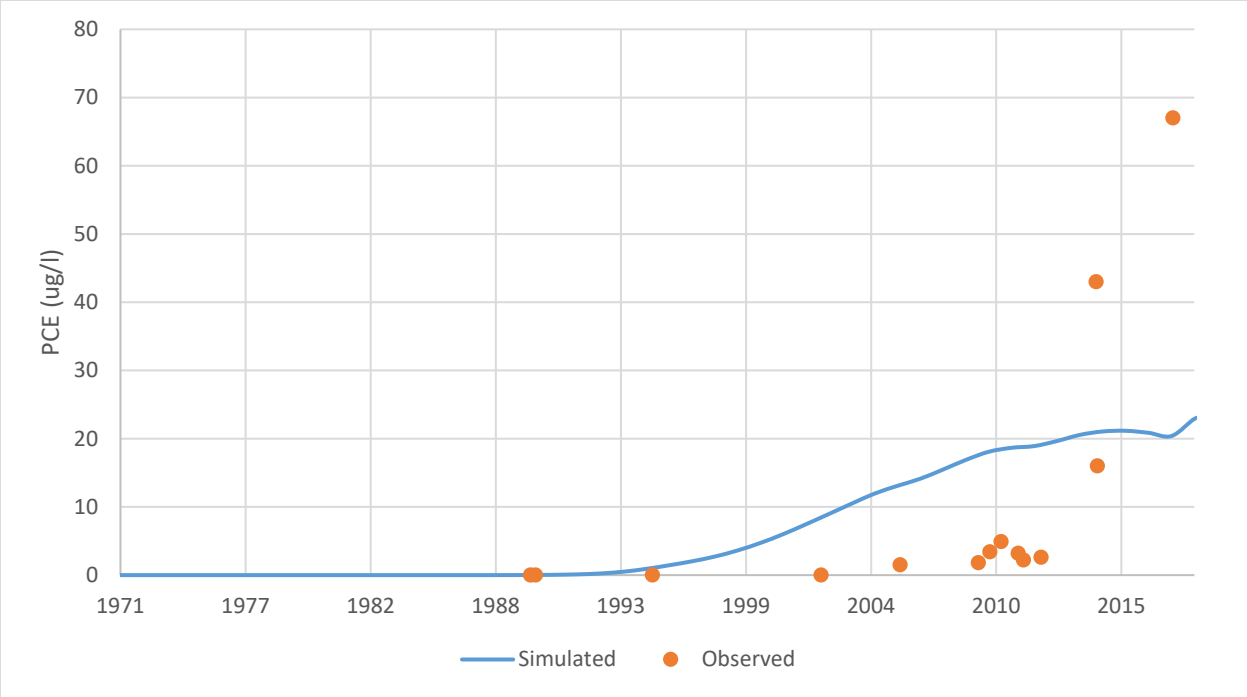

Figure 27. Simulated vs. observed concentrations of PCE at LBWC 5 Well.

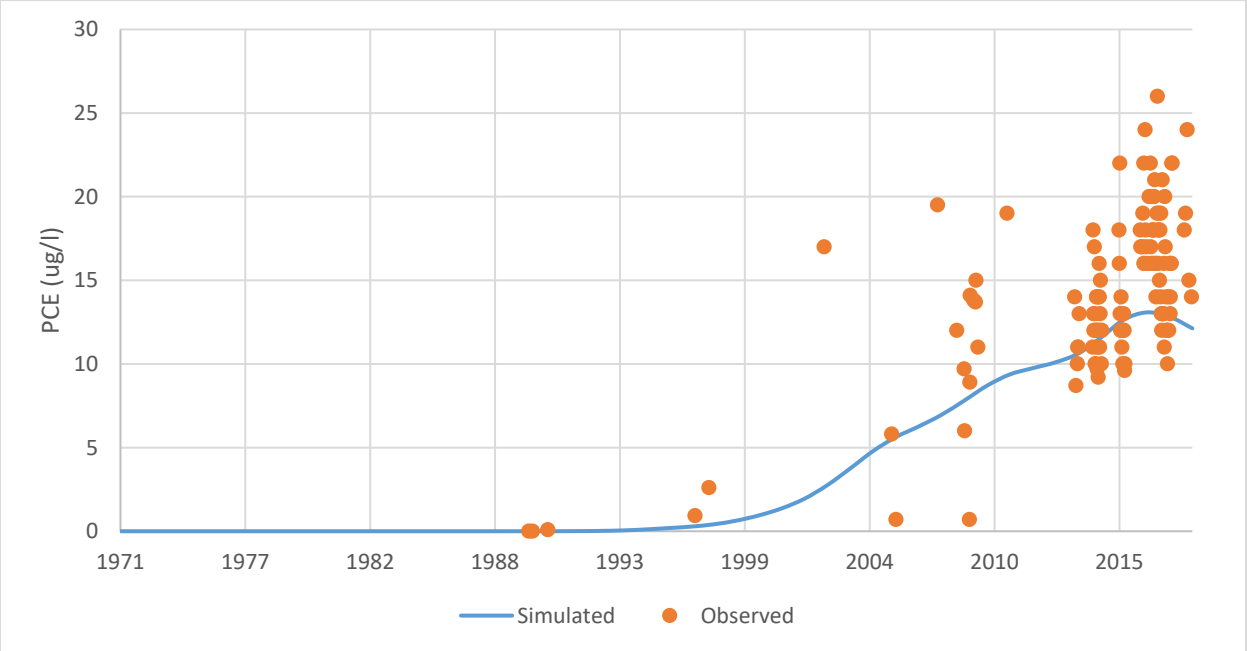

Figure 28. Simulated vs. observed concentrations of PCE at TKWC 2 Well.

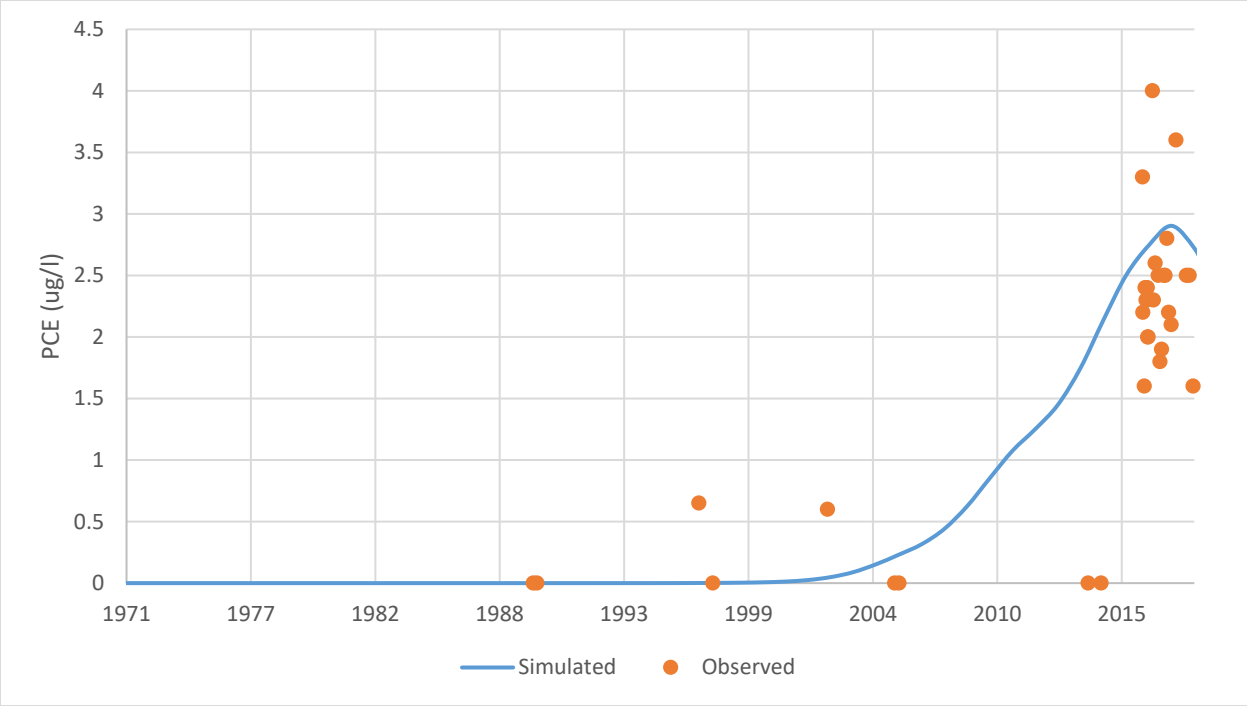

Figure 29. Simulated vs. observed concentrations of PCE at TKWC 1 Well.

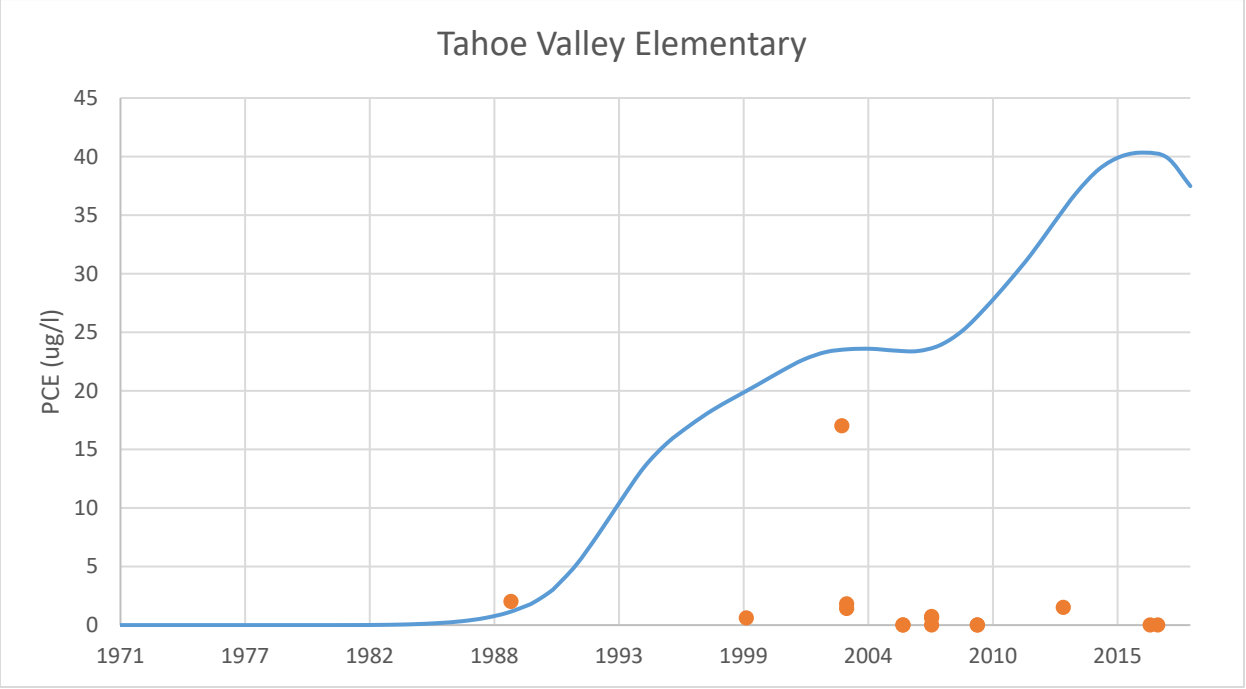

Figure 30. Simulated vs. observed concentrations of PCE at Tahoe Valley Elementary School Well.

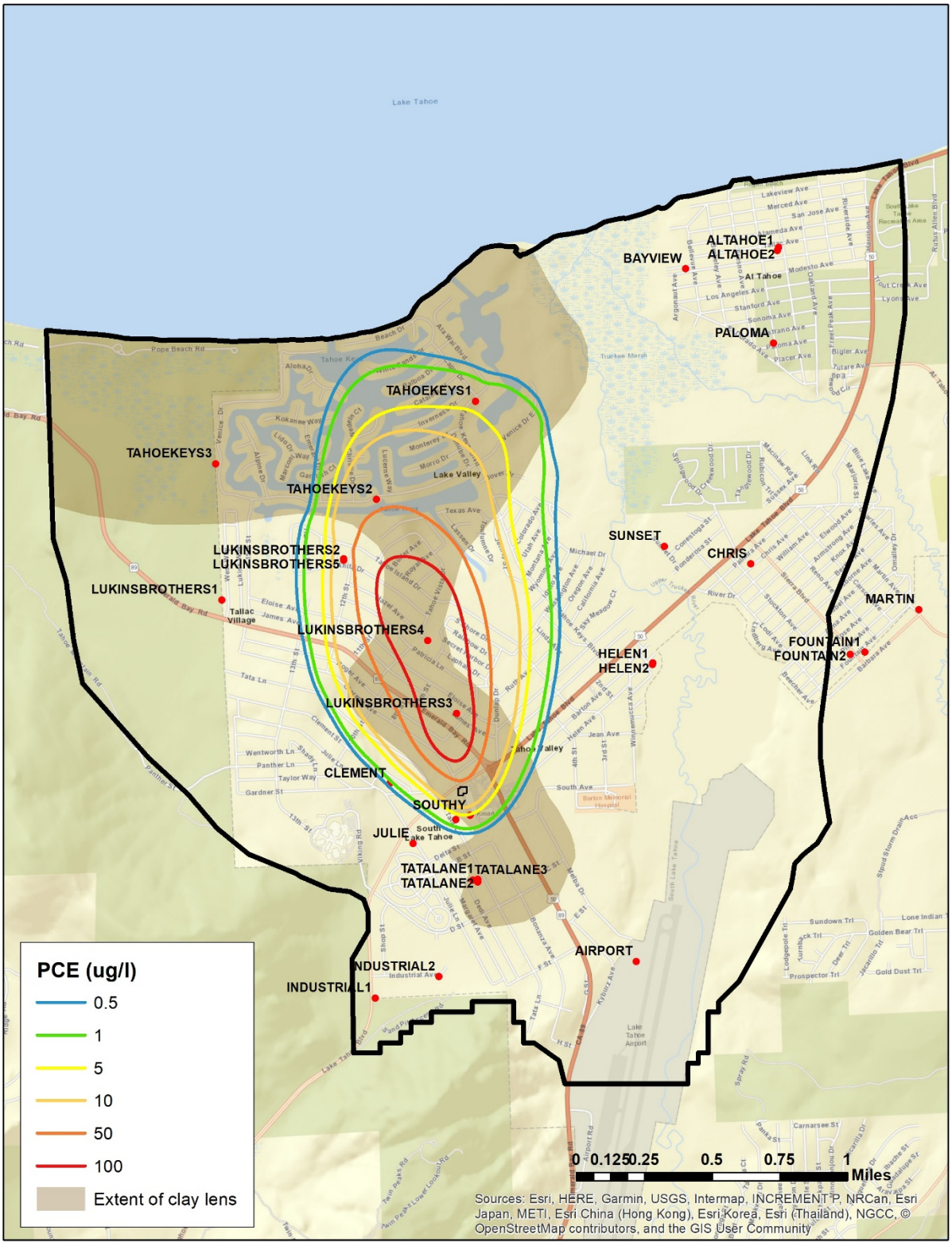

Figure 31. Simulated PCE plume in model layer 1 at the end of the 2018 water year.

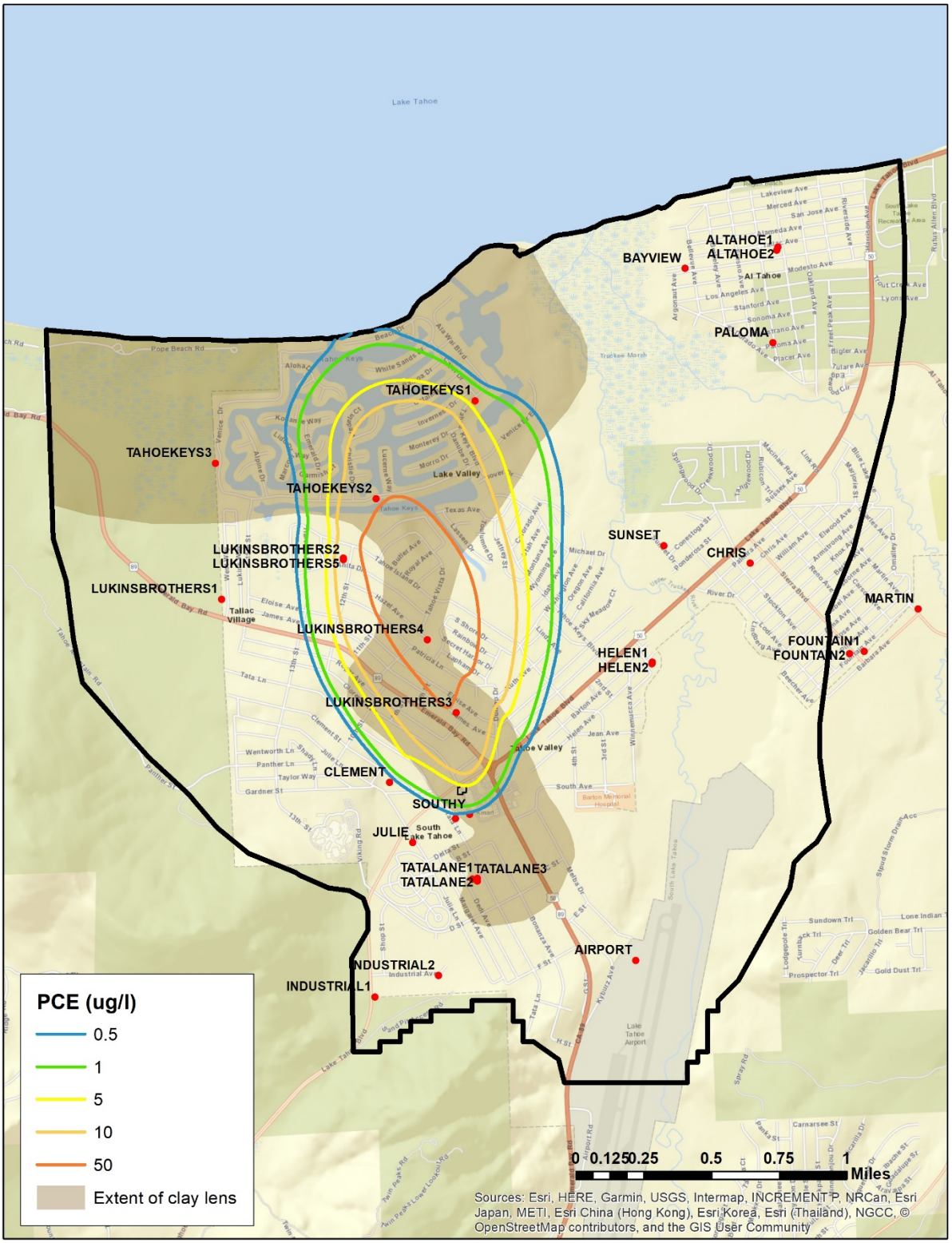

Figure 32. Simulated PCE plume in model layer 2 at the end of the 2018 water year.

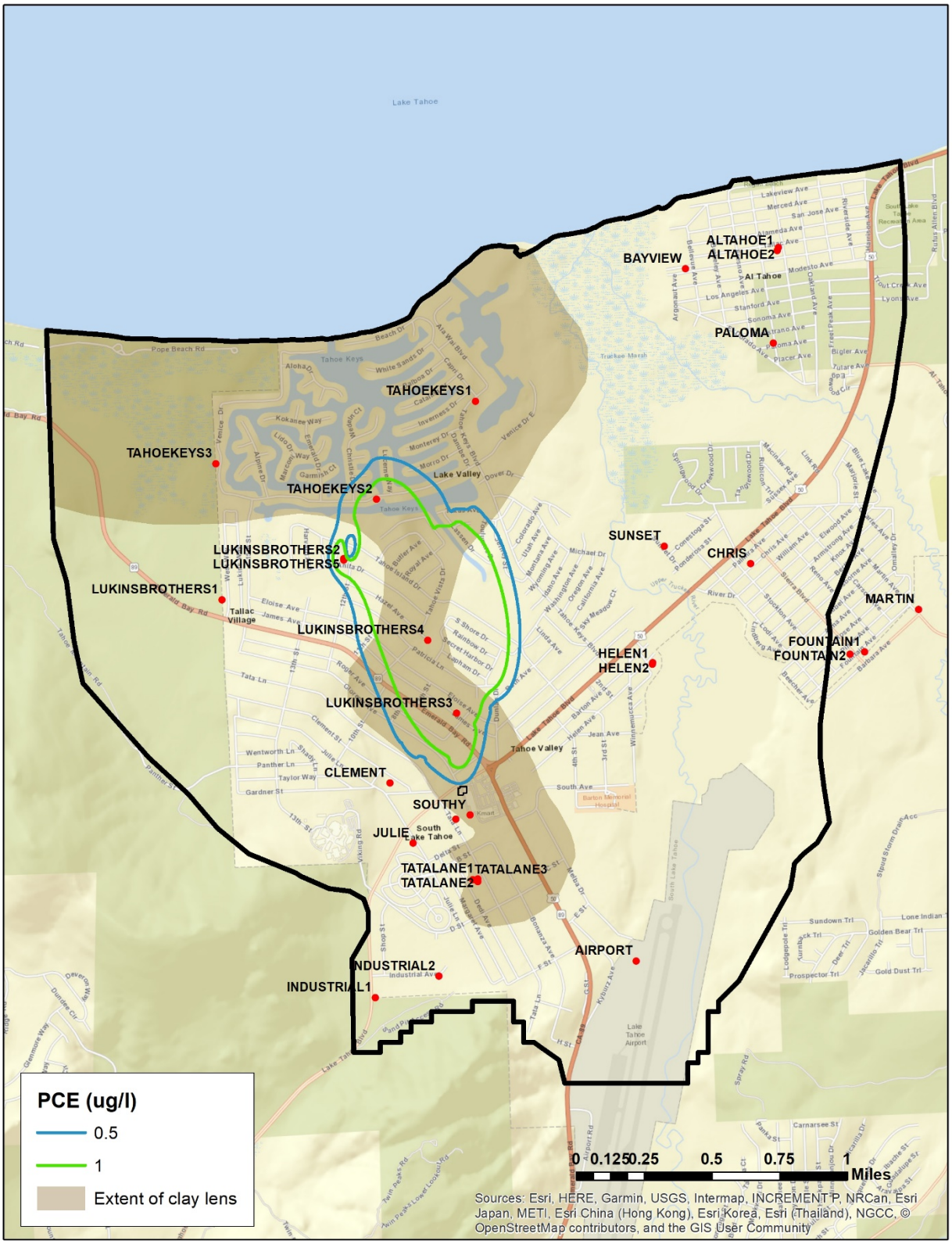

Figure 33. Simulated PCE plume in model layer 3 at the end of the 2018 water year.

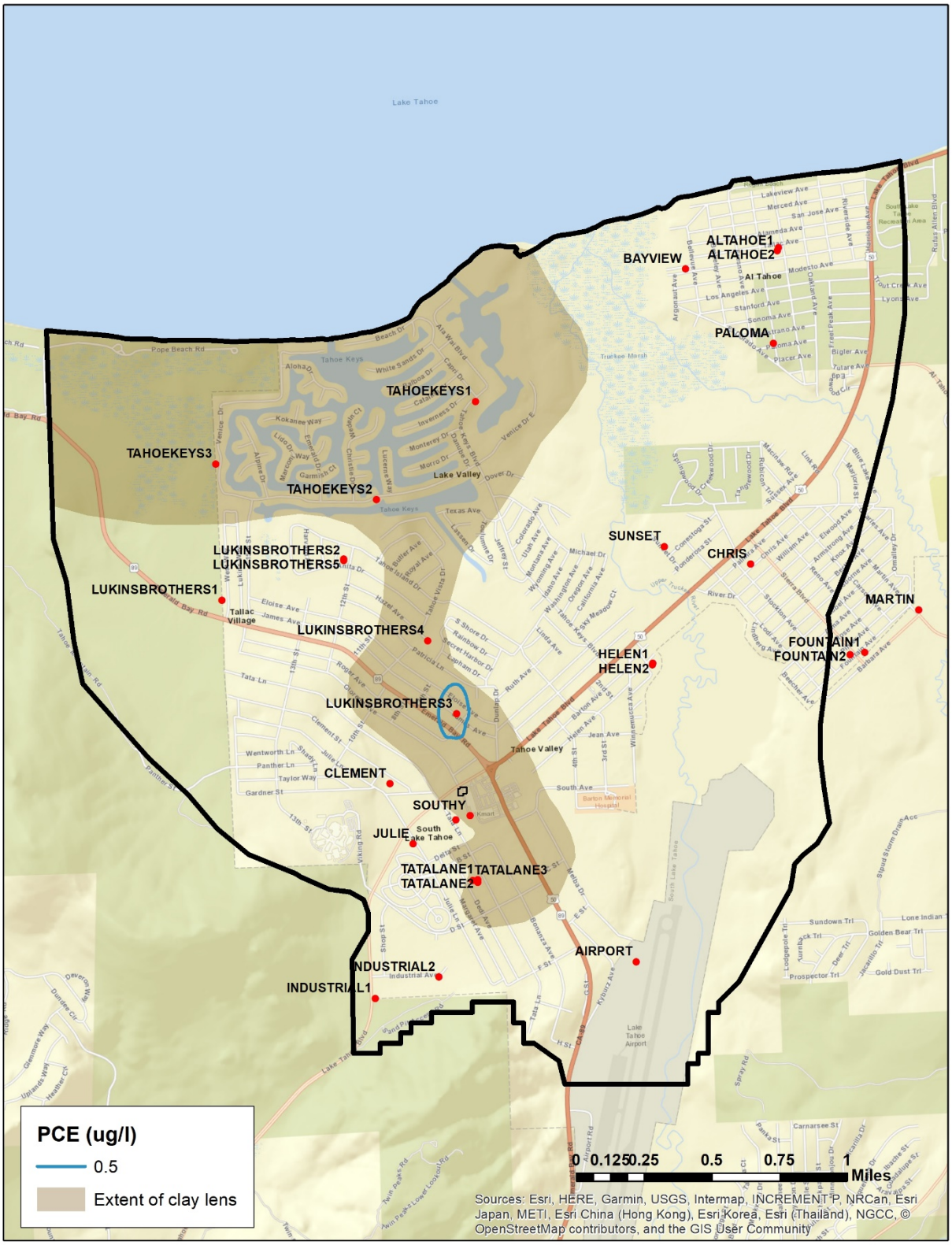

Figure 34. Simulated PCE plume in model layer 4 at the end of the 2018 water year.

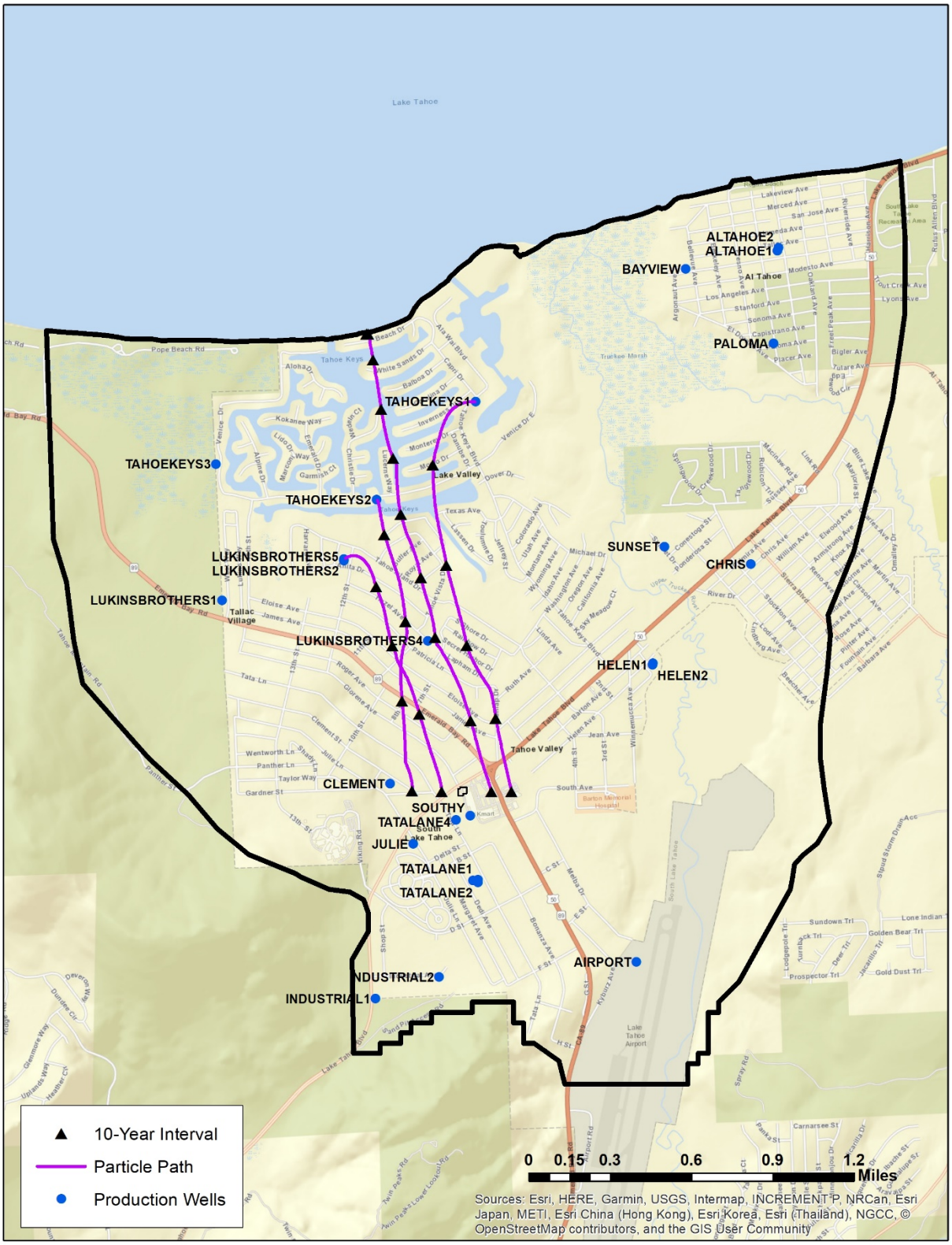

Figure 35. Selected particle tracking pathways showing average migration times to LBWC 5, TKWC 2, TKWC 1, and the northern model boundary. Purple line segments between black triangles indicate 10-year intervals.

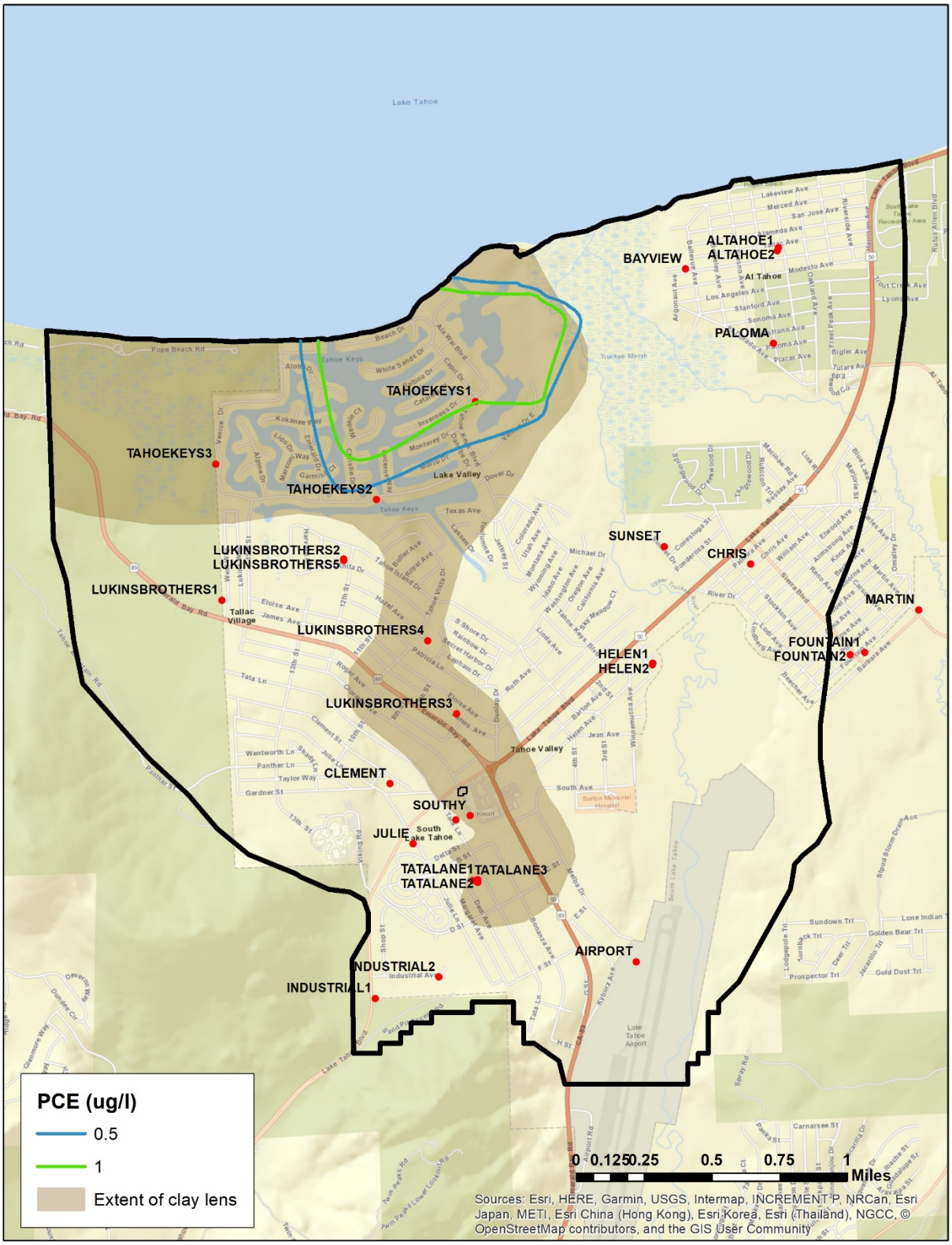

Figure 36. Alternative 1 – Base Treatment. Simulated PCE plume in model layer 1 at the end of the 2068 water year. All concentrations are below the MCL for this stress period.

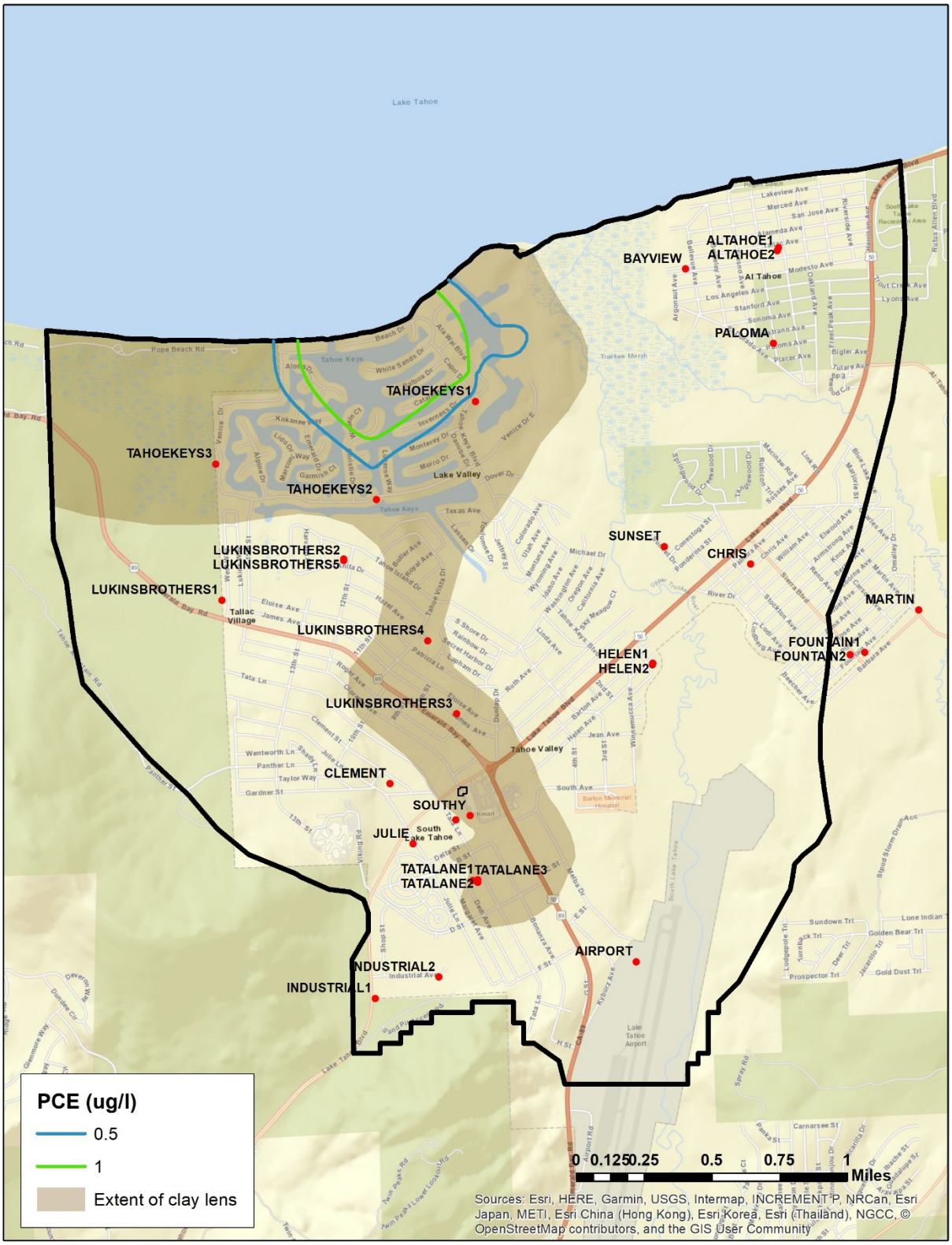

Figure 37. Alternative 1 – Base Treatment. Simulated PCE plume in model layer 2 at the end of the 2068 water year. All concentrations are below the MCL for this stress period.

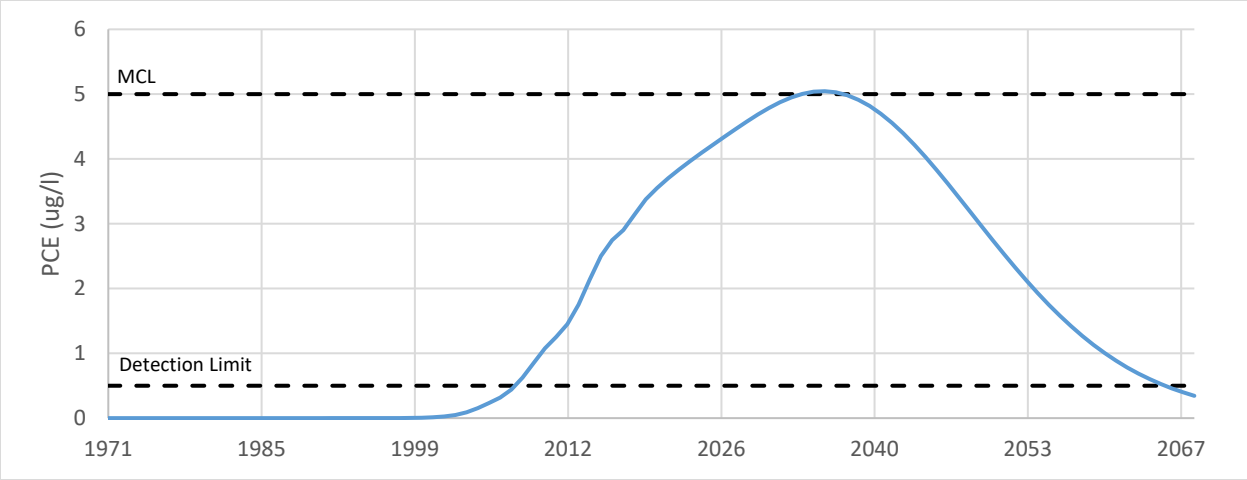

Figure 38. Breakthrough curve for TKWC 1 for Alternative 1A – Base Treatment.

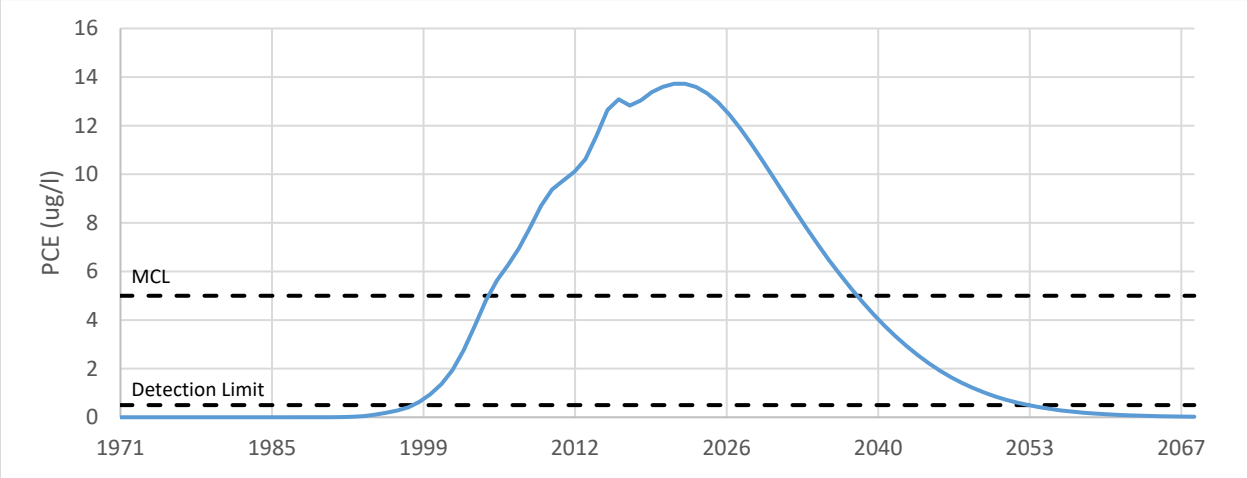

Figure 39. Breakthrough curve for TKWC 2 for Alternative 1A - Base Treatment.

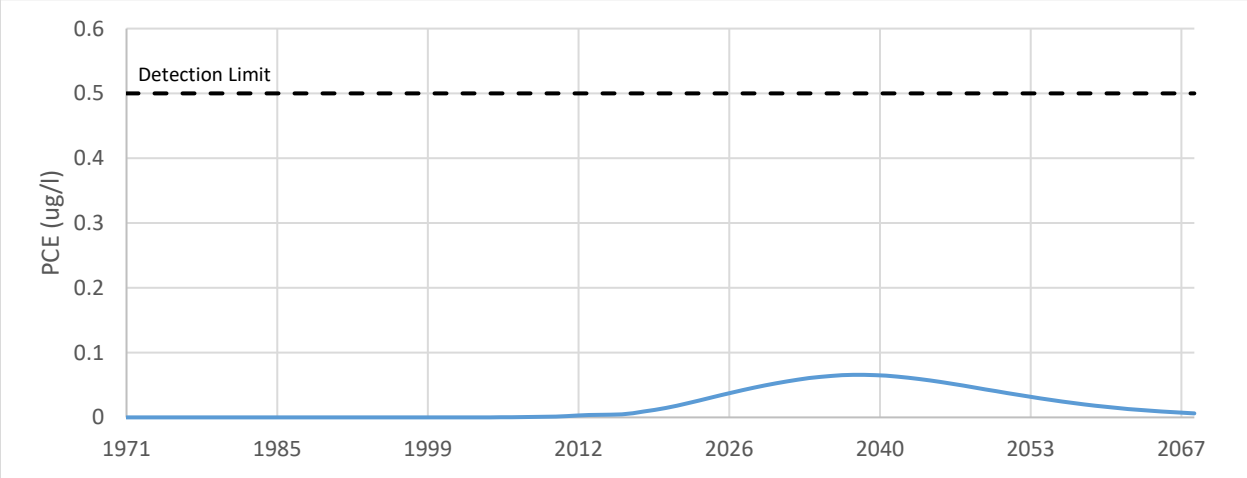

Figure 40. Breakthrough curve for TKWC 3 for Alternative 1A - Base Treatment.

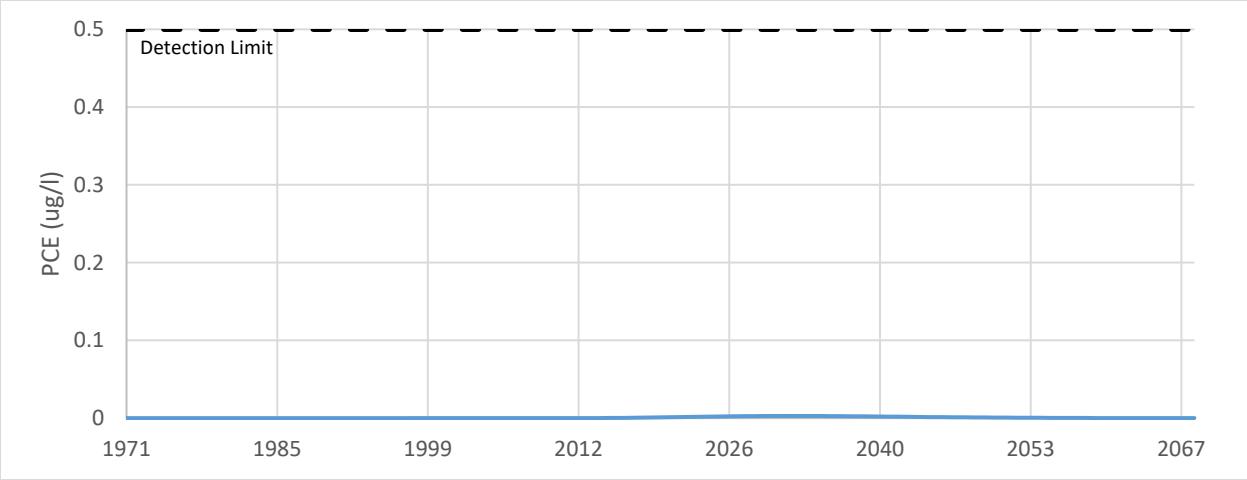

Figure 41. Breakthrough curve for LBWC 1 for Alternative 1A - Base Treatment.

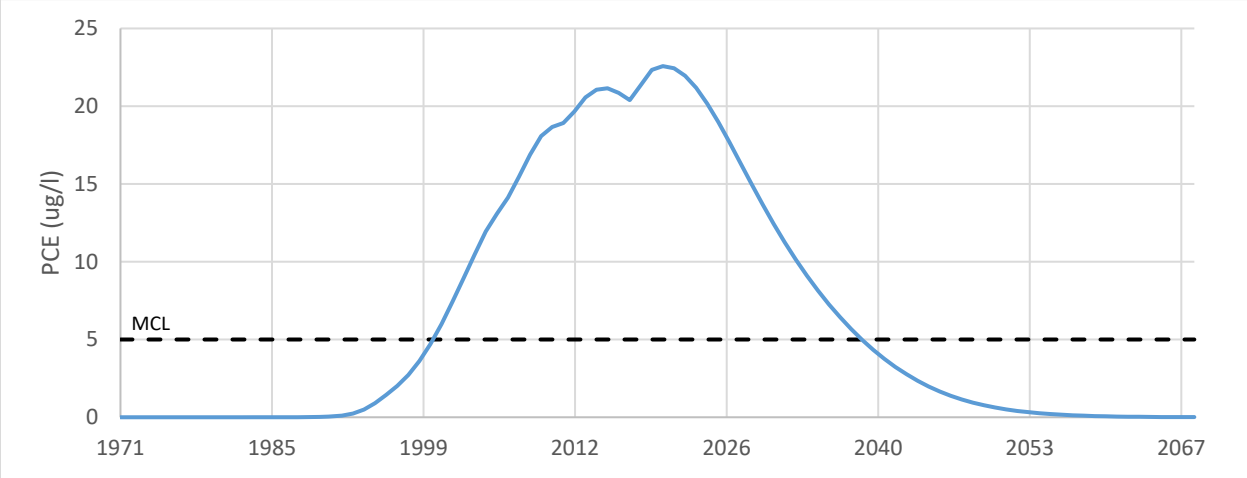

Figure 42. Breakthrough curve for LBWC 5 for Alternative 1A - Base Treatment.

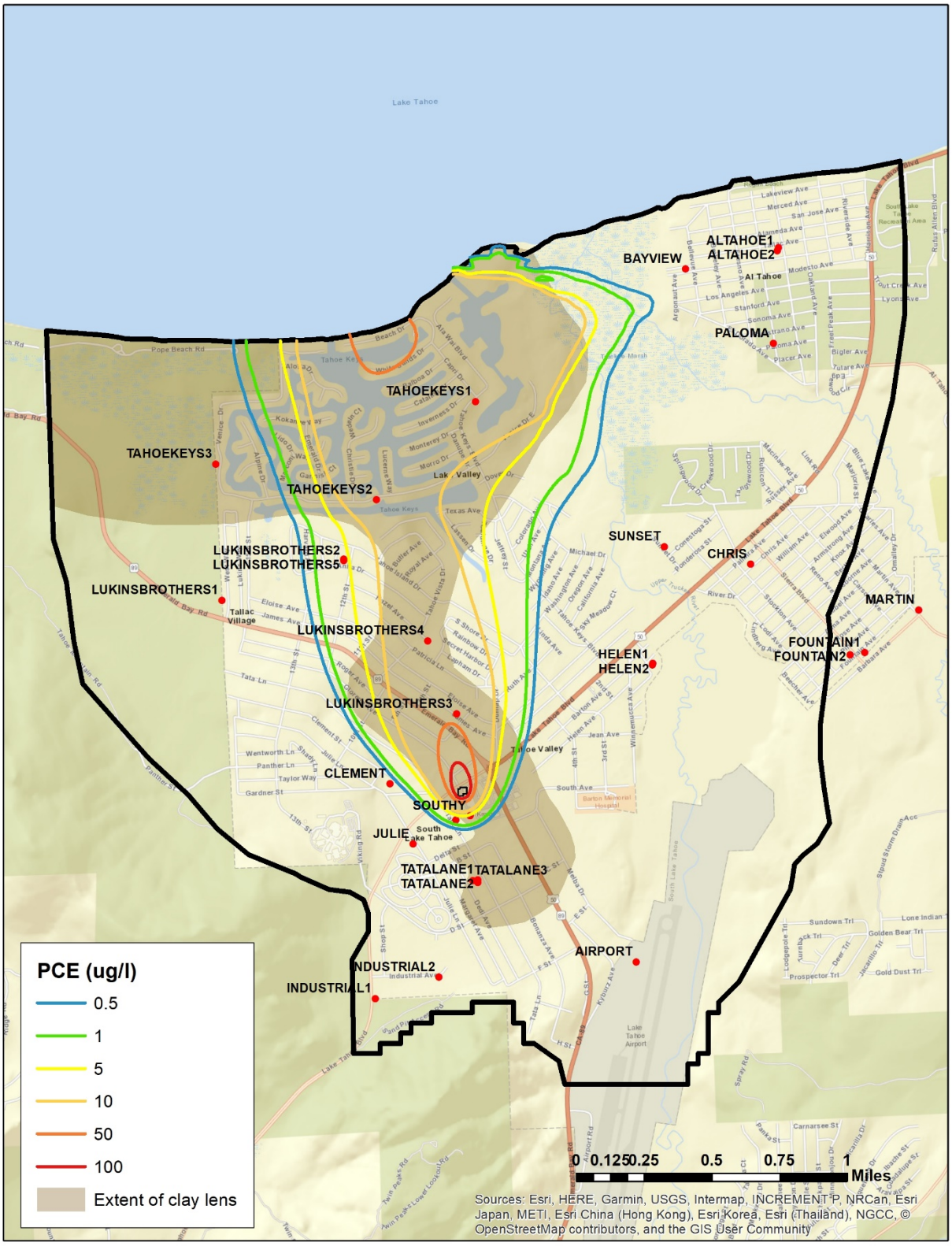

Figure 43. Alternative 1 – Base Treatment (Conservative). Simulated PCE plume in model layer 1 at the end of the 2068 water year.

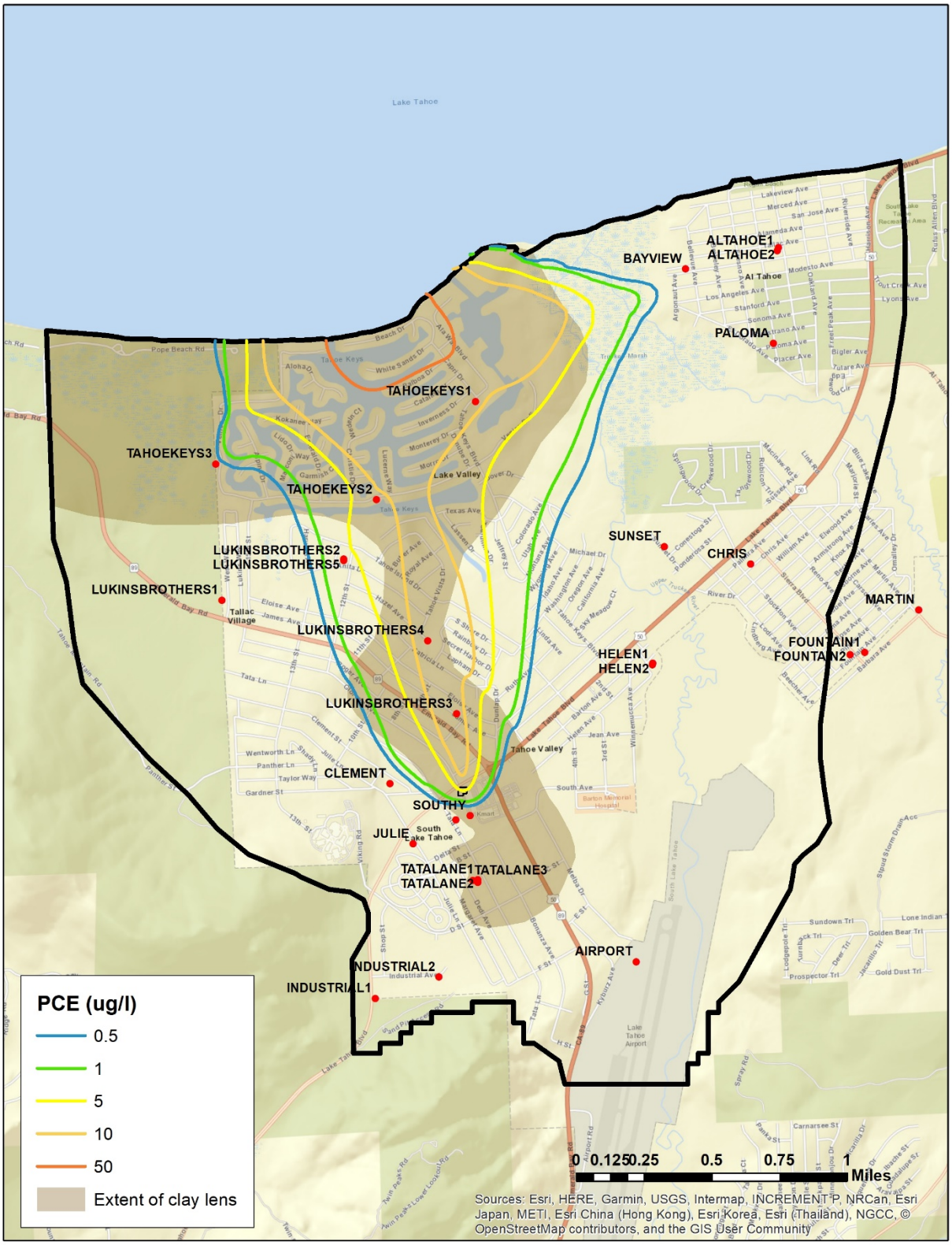

Figure 44. Alternative 1 – Base Treatment (Conservative). Simulated PCE plume in model layer 2 at the end of the 2068 water year.

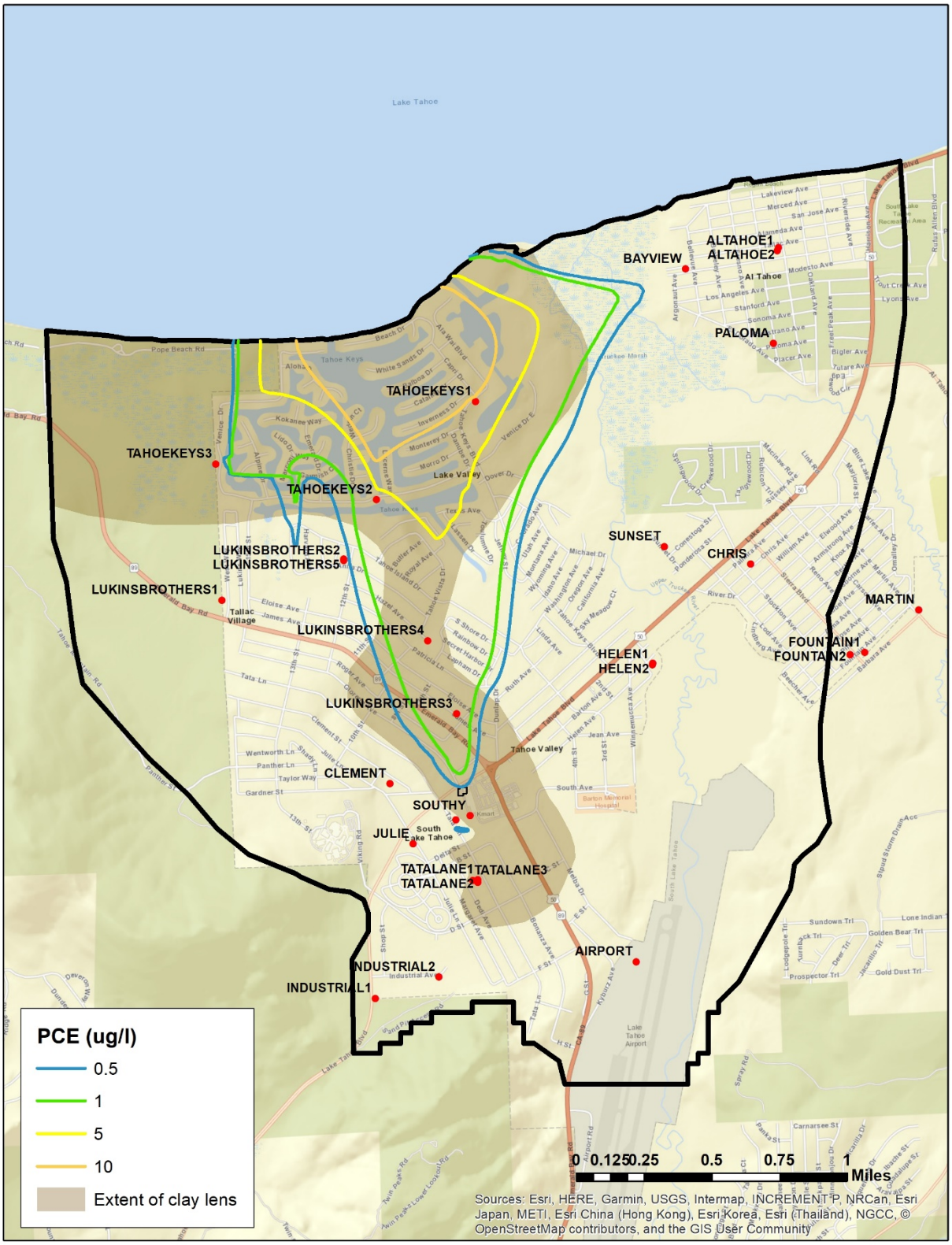

Figure 45. Alternative 1 – Base Treatment (Conservative). Simulated PCE plume in model layer 3 at the end of the 2068 water year.

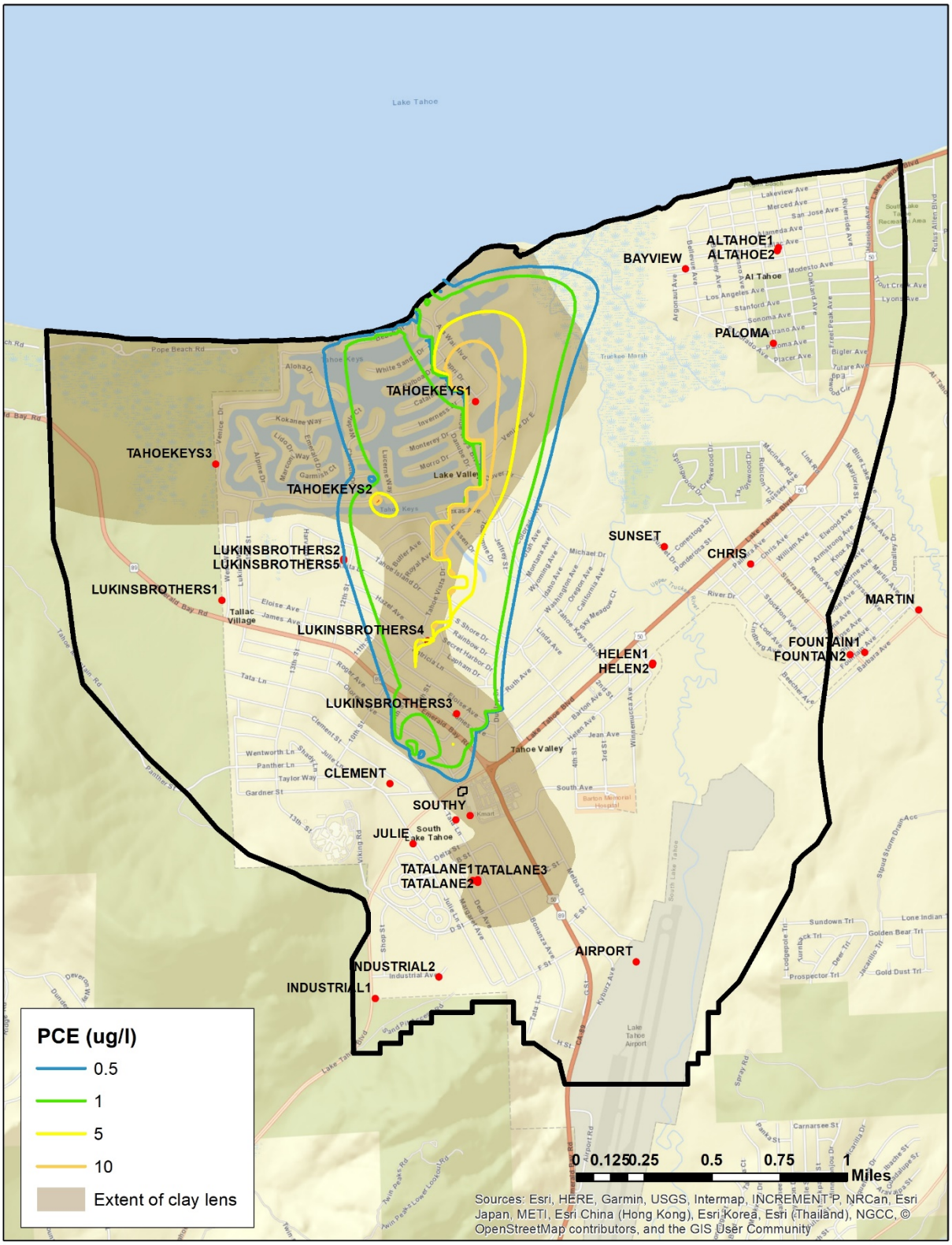

Figure 46. Alternative 1 – Base Treatment (Conservative). Simulated PCE plume in model layer 4 at the end of the 2068 water year.

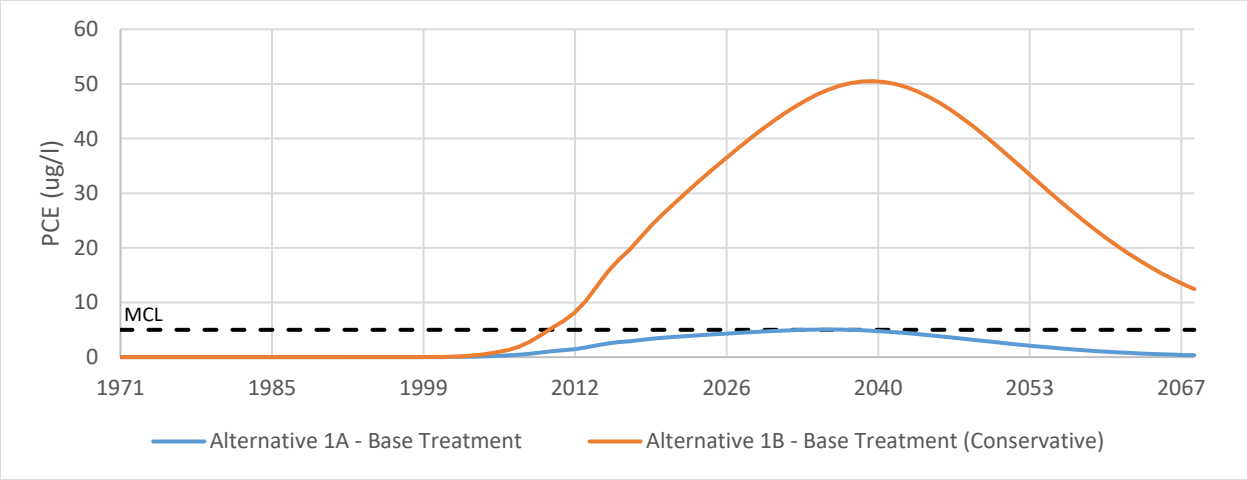

Figure 47. Breakthrough curve for TKWC 1 for Alternatives 1A (blue) and 1B (orange).

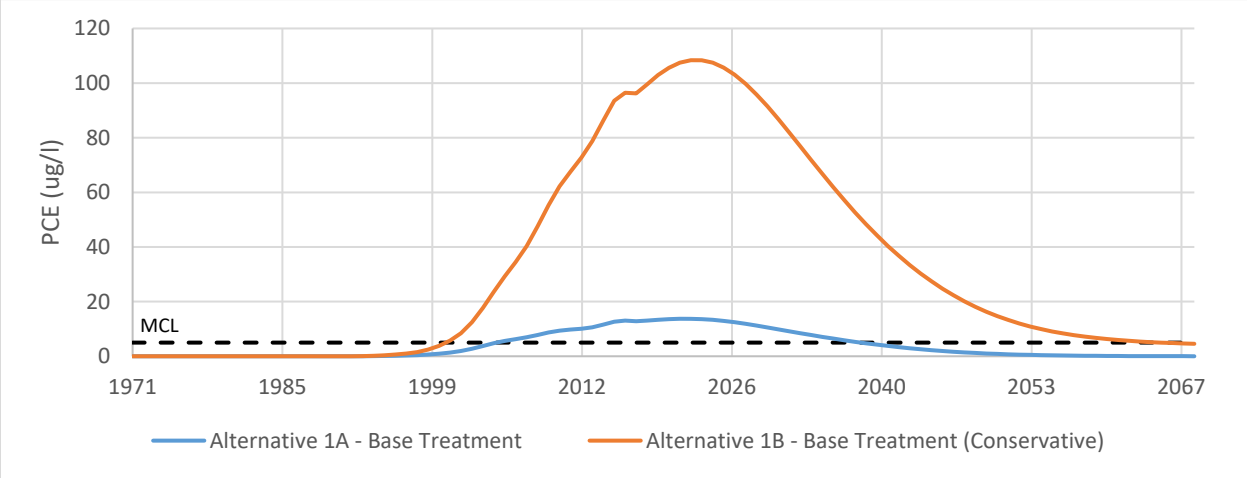

Figure 48. Breakthrough curve for TKWC 2 for Alternatives 1A (blue) and 1B (orange).

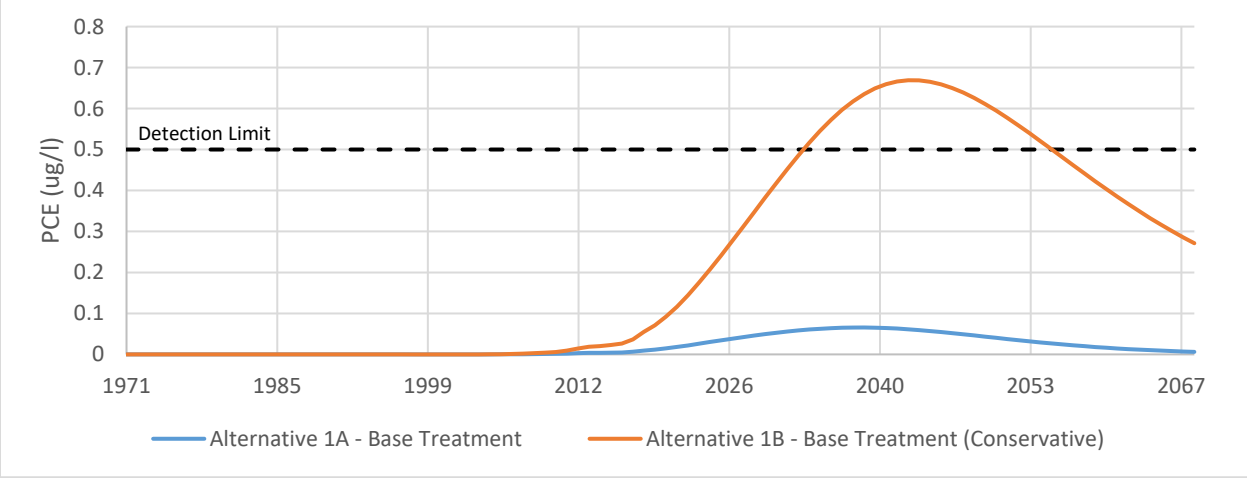

Figure 49. Breakthrough curve for TKWC 3 for Alternatives 1A (blue) and 1B (orange).

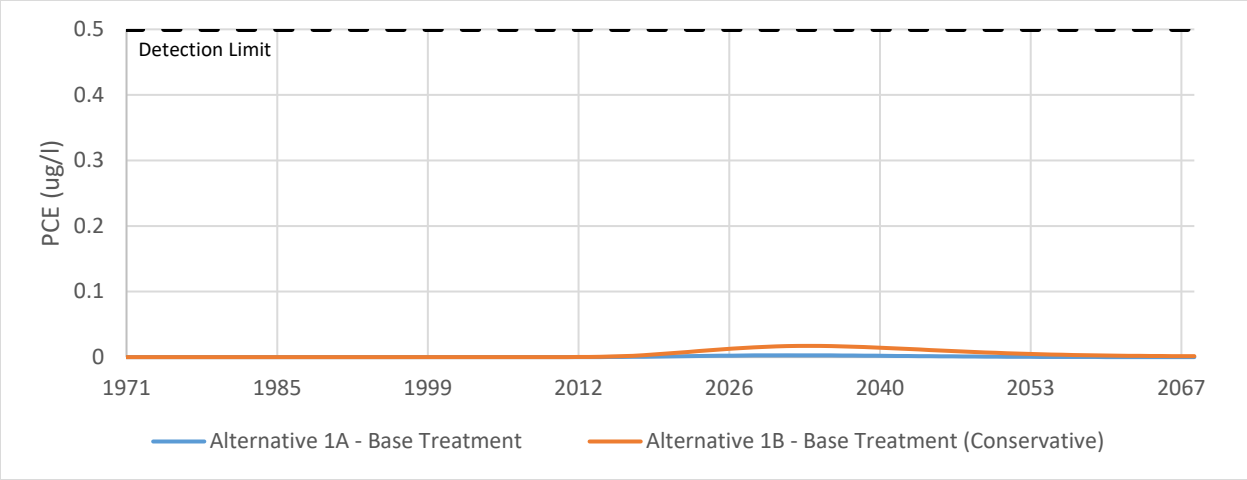

Figure 50. Breakthrough curve for LBWC 1 for Alternatives 1A (blue) and 1B (orange).

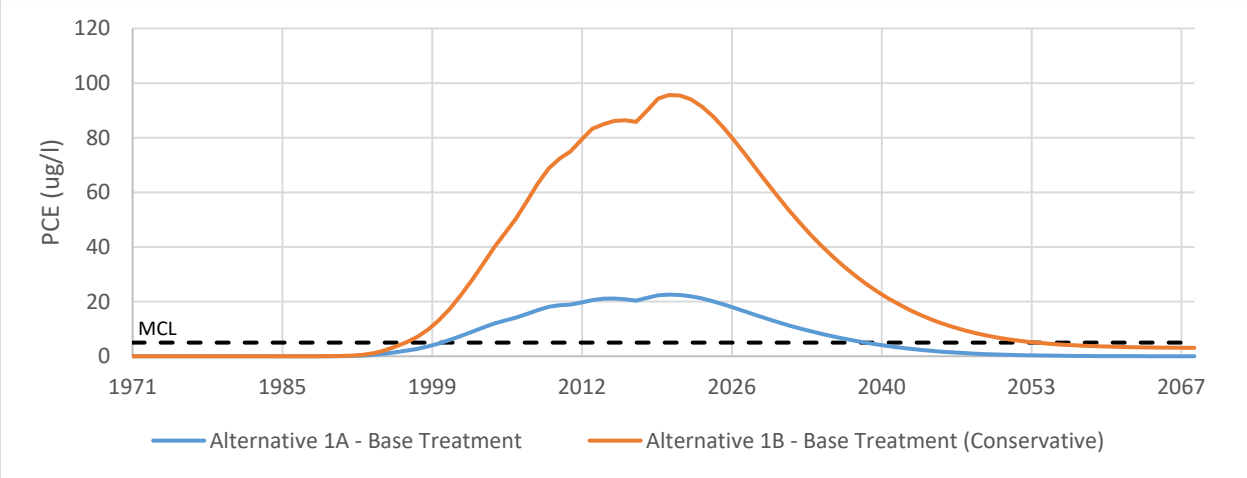

Figure 51. Breakthrough curve for LBWC 5 for Alternatives 1A (blue) and 1B (orange).

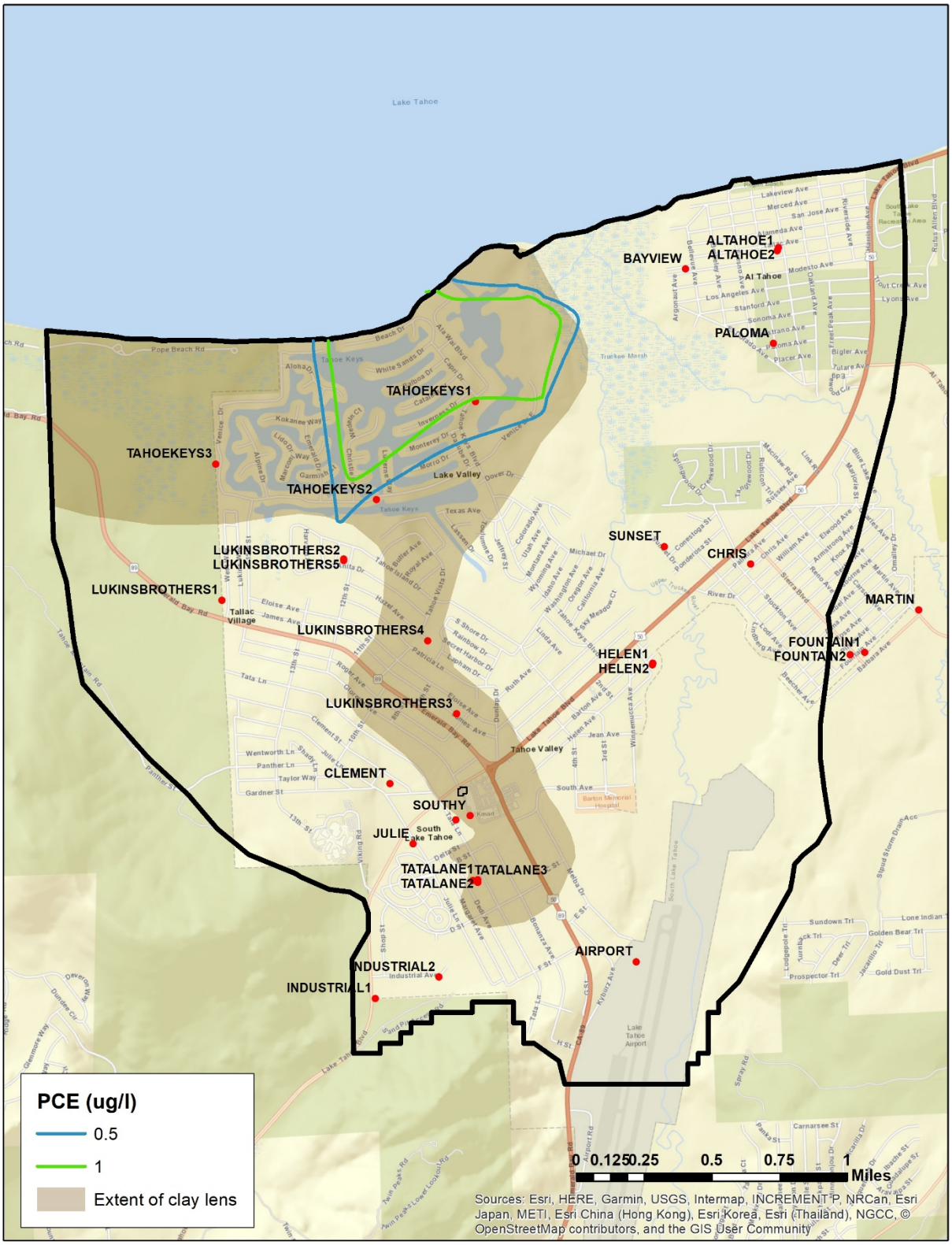

Figure 52. Alternative 2 – Targeted Pumping. Simulated PCE plume in model layer 1 at the end of the 2068 water year. All concentrations are below the MCL for this stress period.

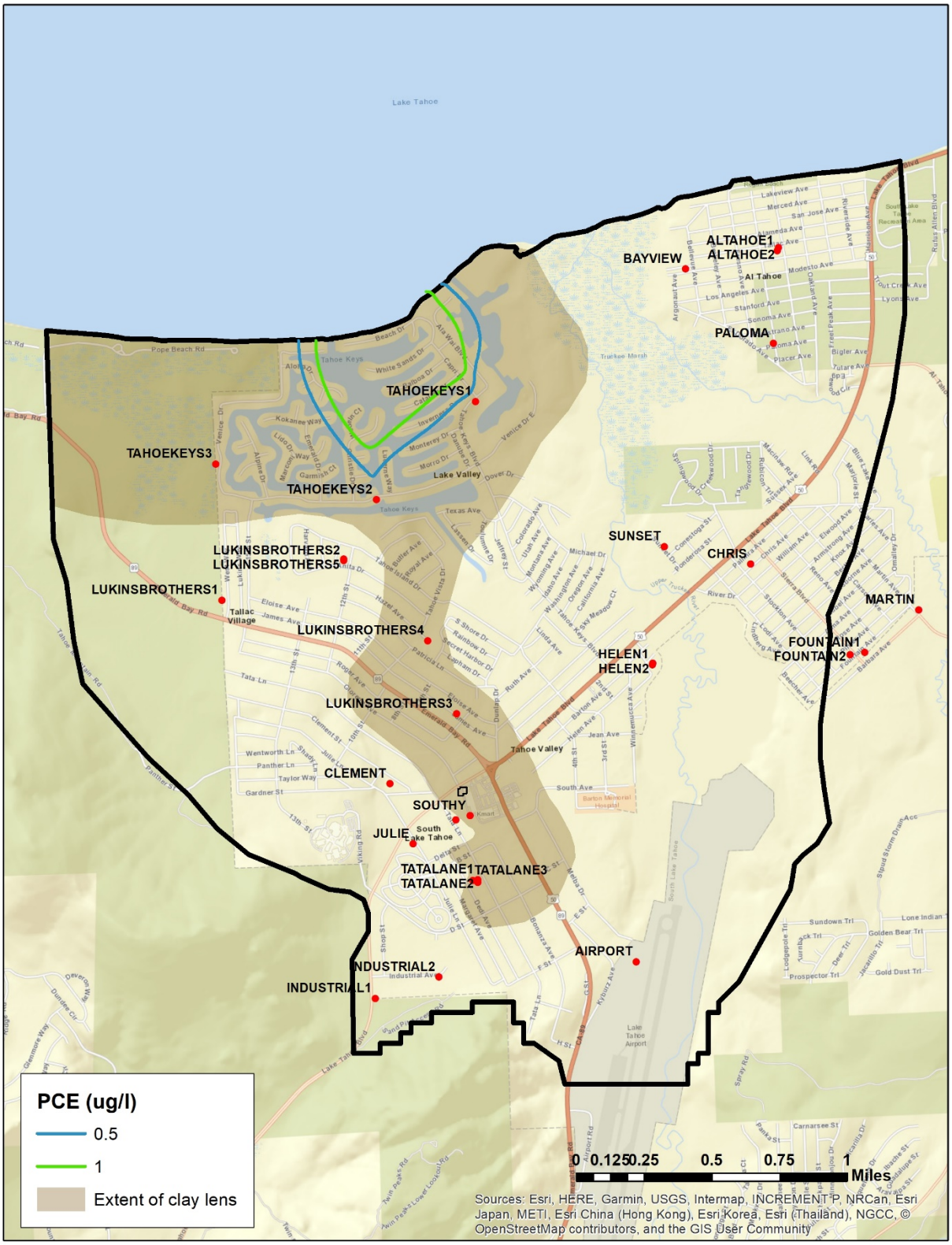

Figure 53. Alternative 2 – Targeted Pumping. Simulated PCE plume in model layer 2 at the end of the 2068 water year. All concentrations are below the MCL for this stress period.

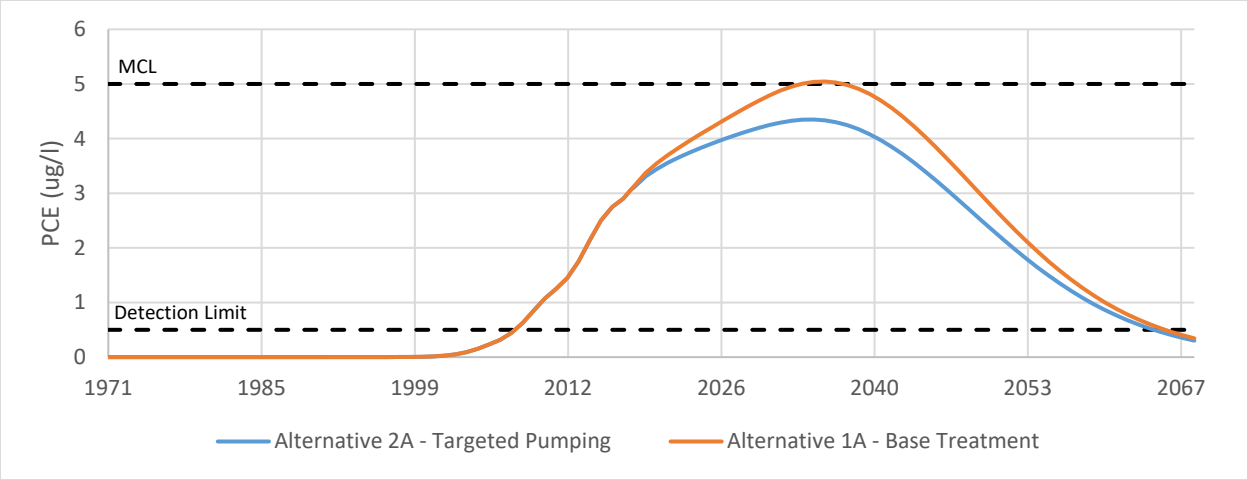

Figure 54. Breakthrough curve for TKWC 1 for Alternatives 2A (blue) and 1A (orange).

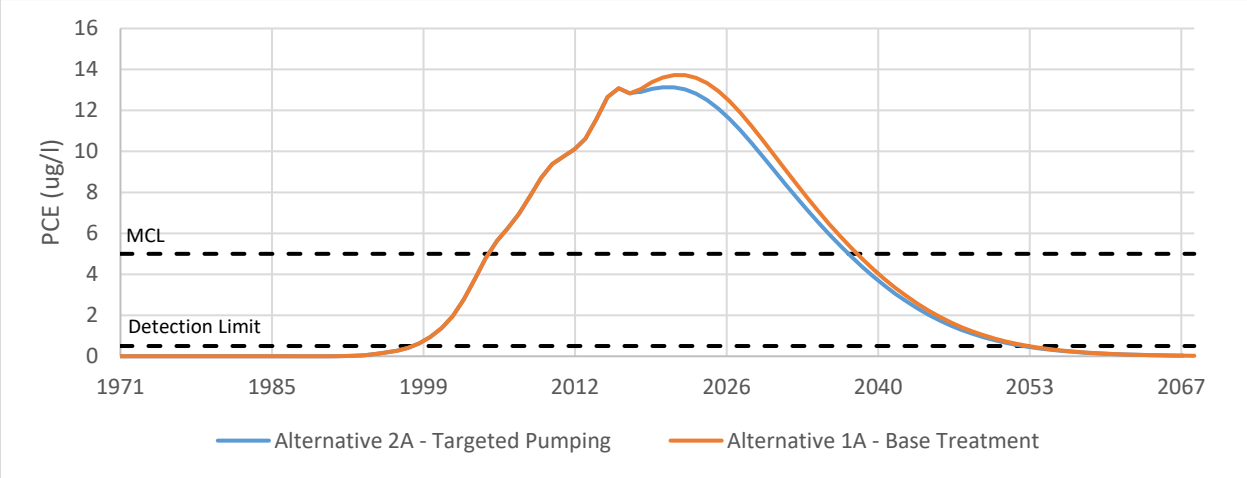

Figure 55. Breakthrough curve for TKWC 2 for Alternatives 2A (blue) and 1A (orange).

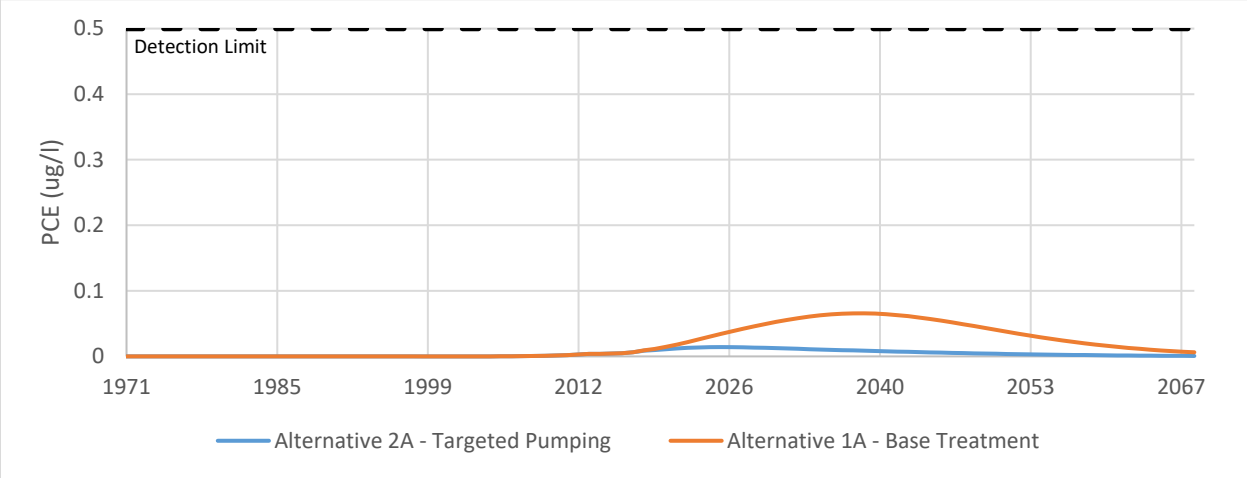

Figure 56. Breakthrough curve for TKWC 3 for Alternatives 2A (blue) and 1A (orange).

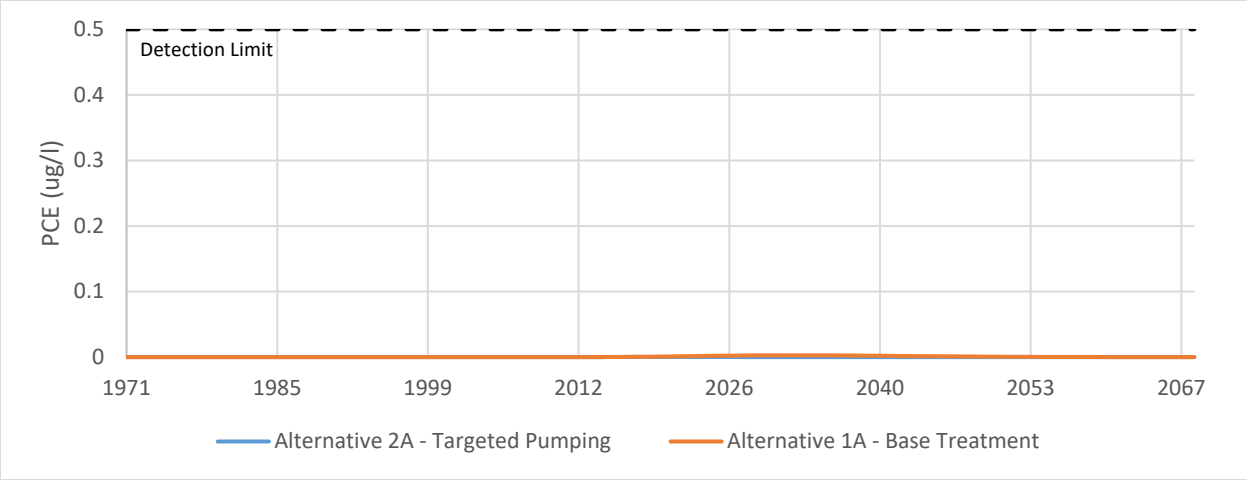

Figure 57. Breakthrough curve for LBWC 1 for Alternatives 2A (blue) and 1A (orange).

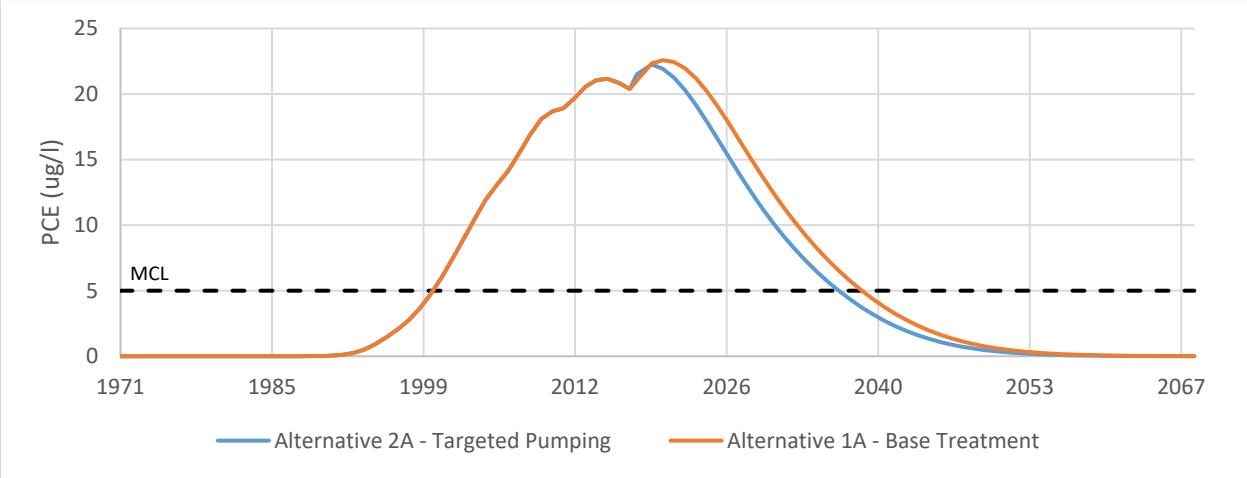

Figure 58. Breakthrough curve for LBWC 5 for Alternatives 2A (blue) and 1A (orange).

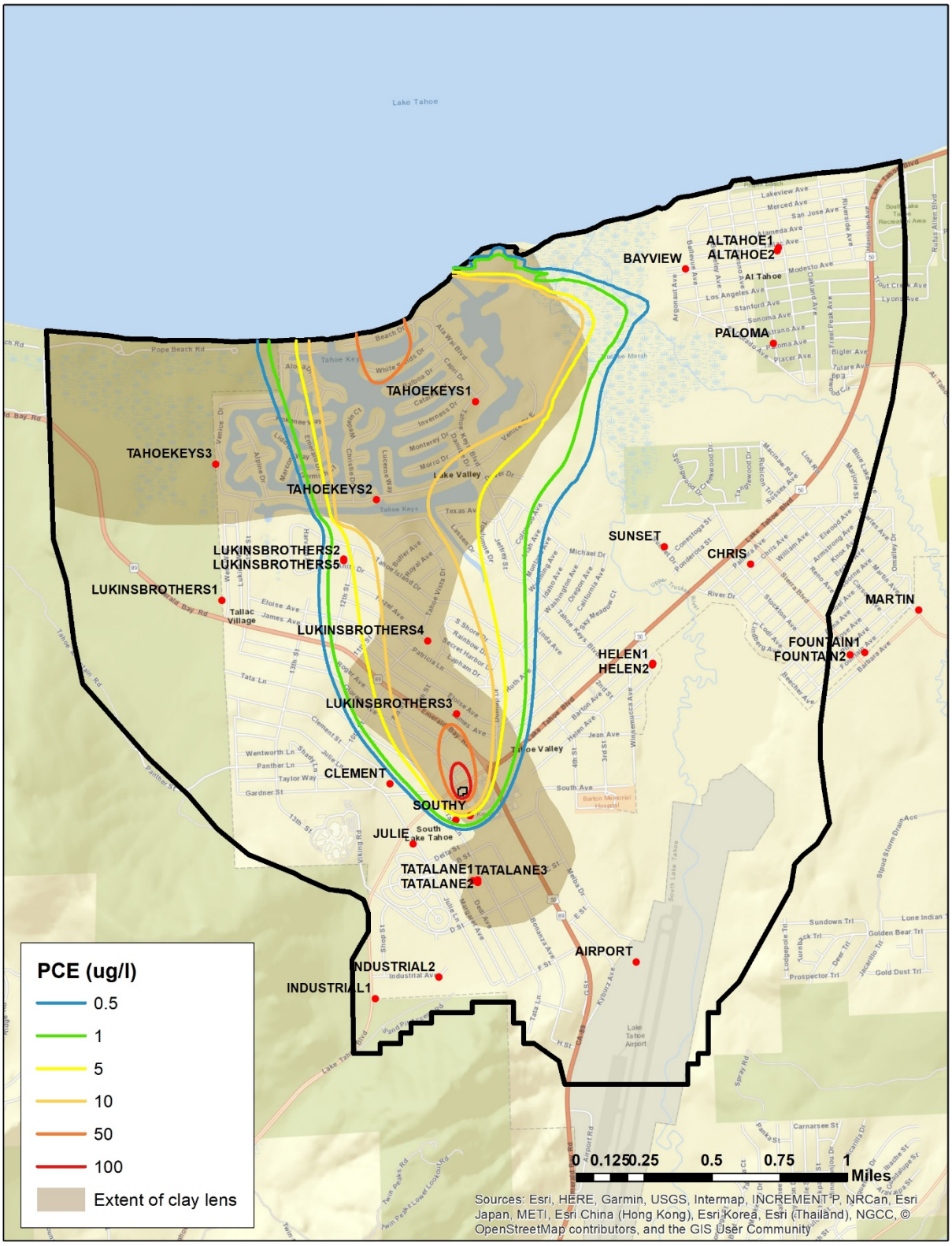

Figure 59. Alternative 2 – Targeted Pumping (Conservative). Simulated PCE plume in model layer 1 at the end of the 2068 water year.

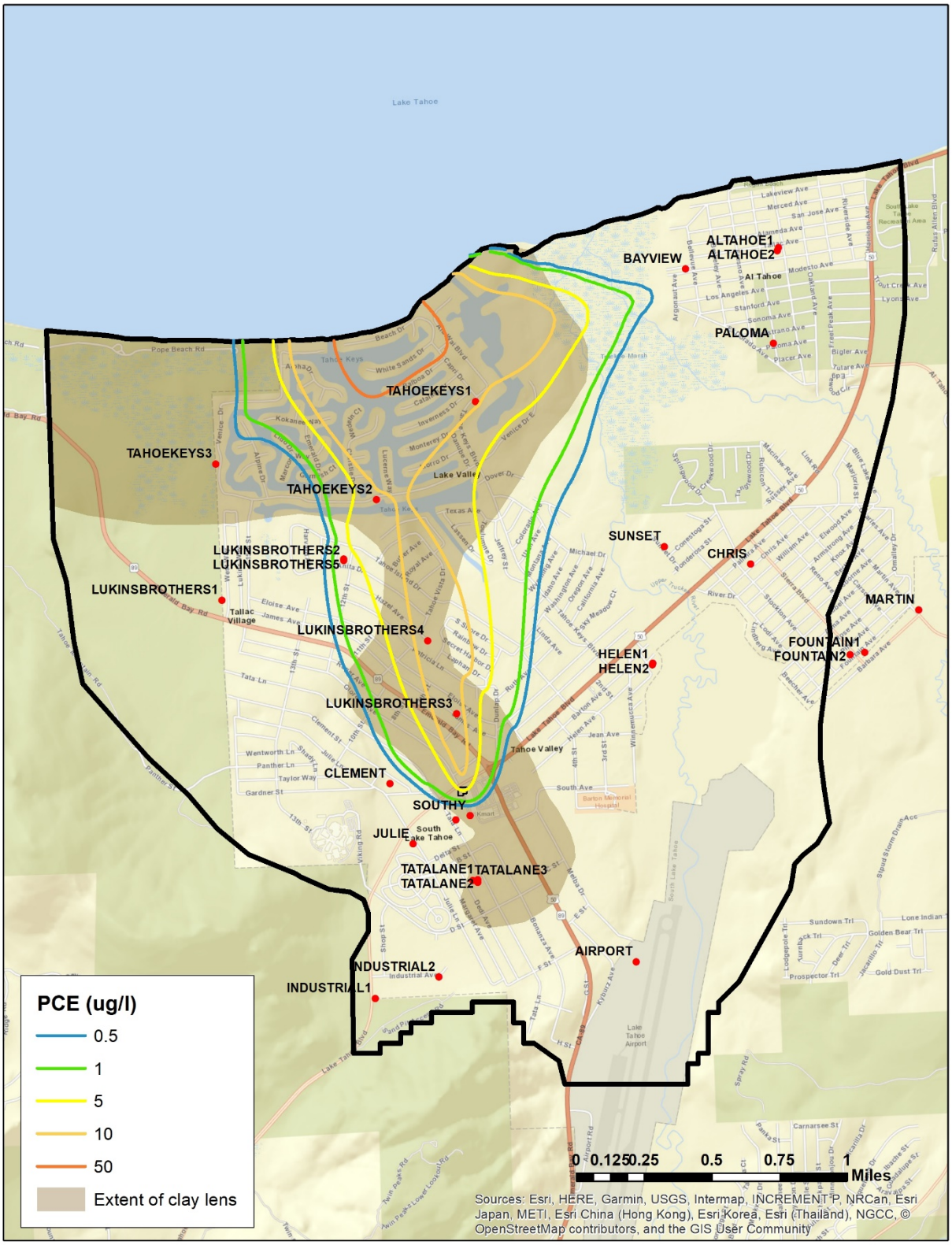

Figure 60. Alternative 2 – Targeted Pumping (Conservative). Simulated PCE plume in model layer 2 at the end of the 2068 water year.

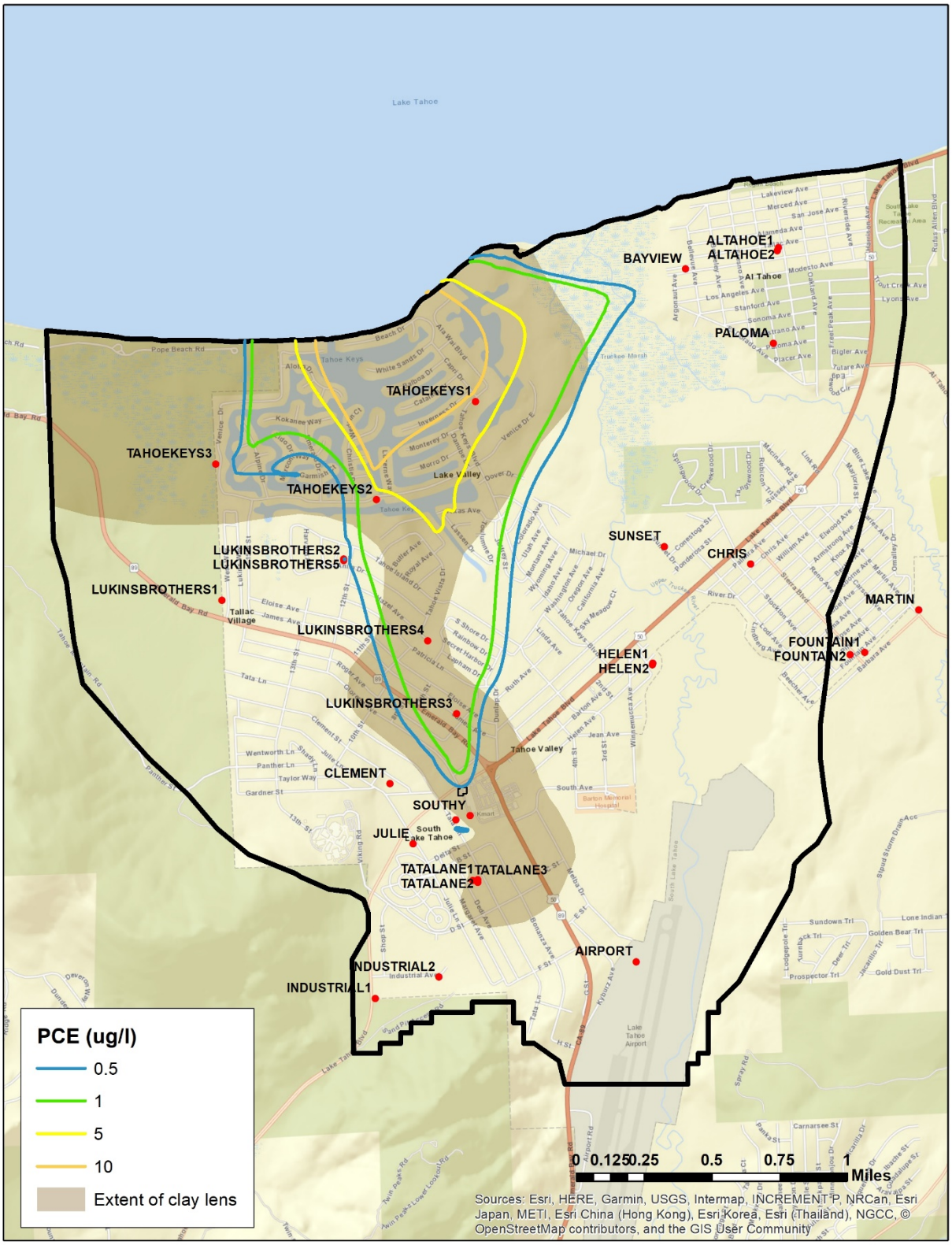

Figure 61. Alternative 2 – Targeted Pumping (Conservative). Simulated PCE plume in model layer 3 at the end of the 2068 water year.

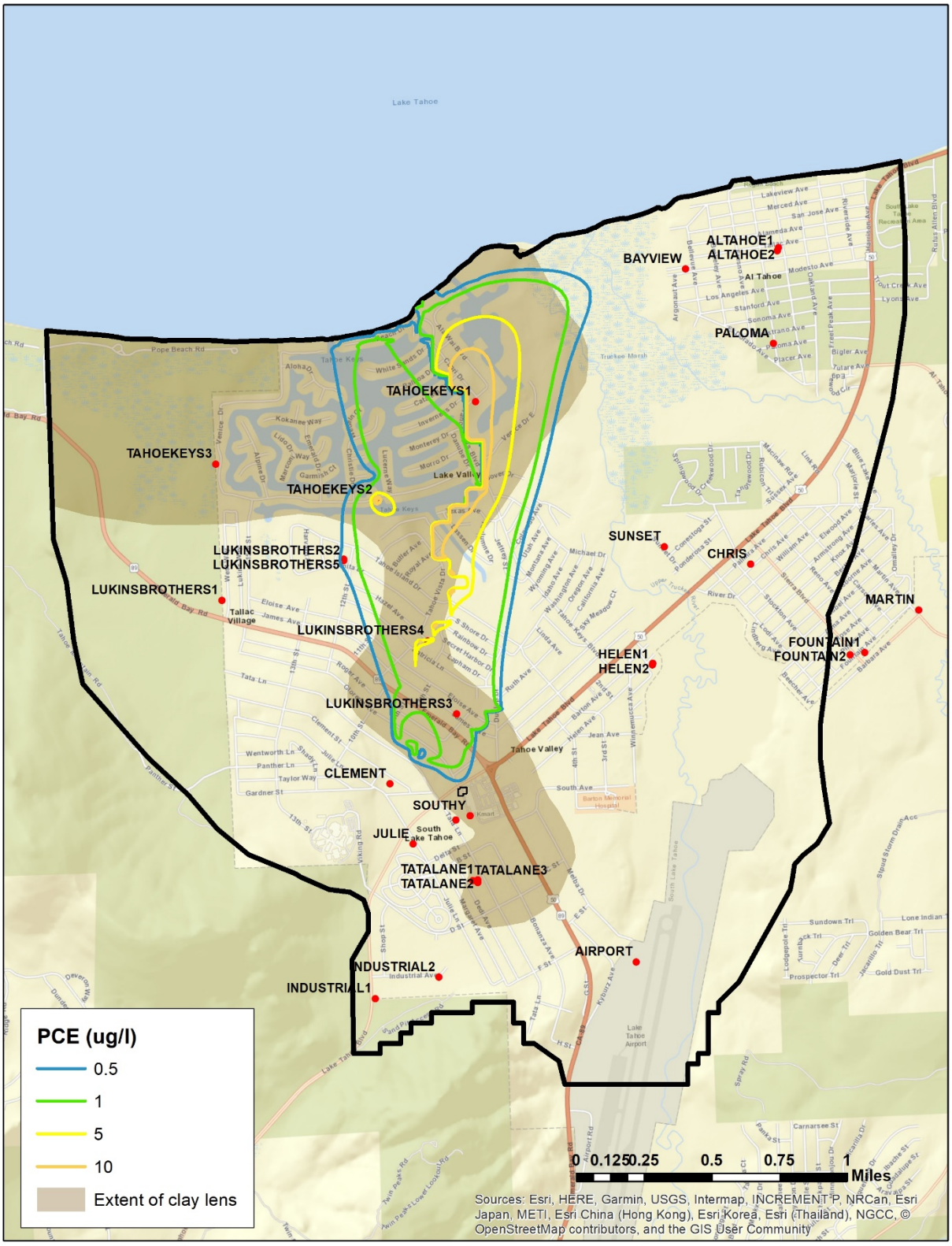

Figure 62. Alternative 2 – Targeted Pumping (Conservative). Simulated PCE plume in model layer 4 at the end of the 2068 water year.

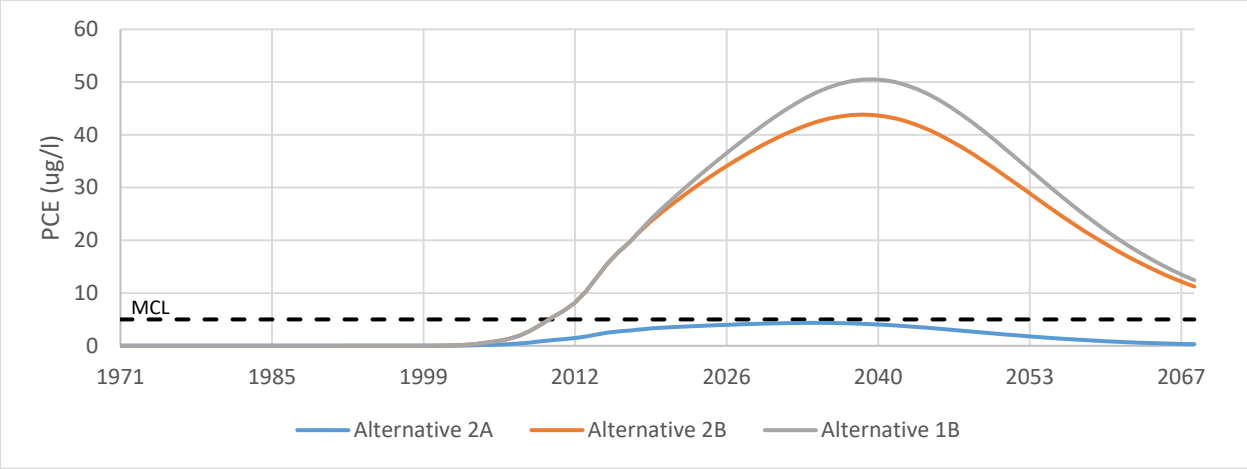

Figure 63. Breakthrough curve for TKWC 1 for Alternatives 2A – Targeted Pumping (blue), 2B – Targeted Pumping (Conservative) (orange), and 1B – Base Treatment (Conservative) (grey).

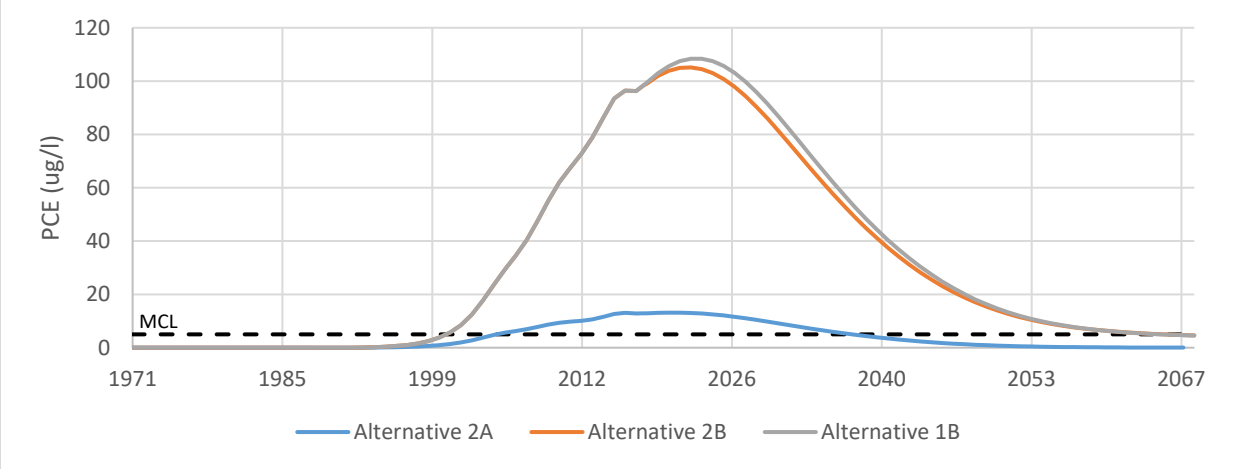

Figure 64. Breakthrough curve for TKWC 2 for Alternatives 2A – Targeted Pumping (blue), 2B – Targeted Pumping (Conservative) (orange), and 1B – Base Treatment (Conservative) (grey).

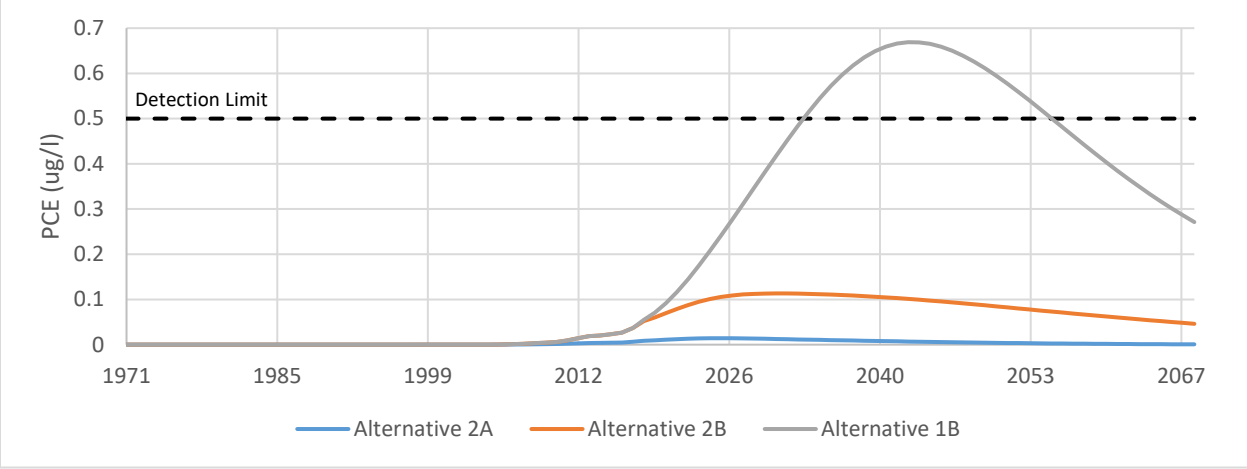

Figure 65. Breakthrough curve for TKWC 3 for Alternatives 2A – Targeted Pumping (blue), 2B – Targeted Pumping (Conservative) (orange), and 1B – Base Treatment (Conservative) (grey).

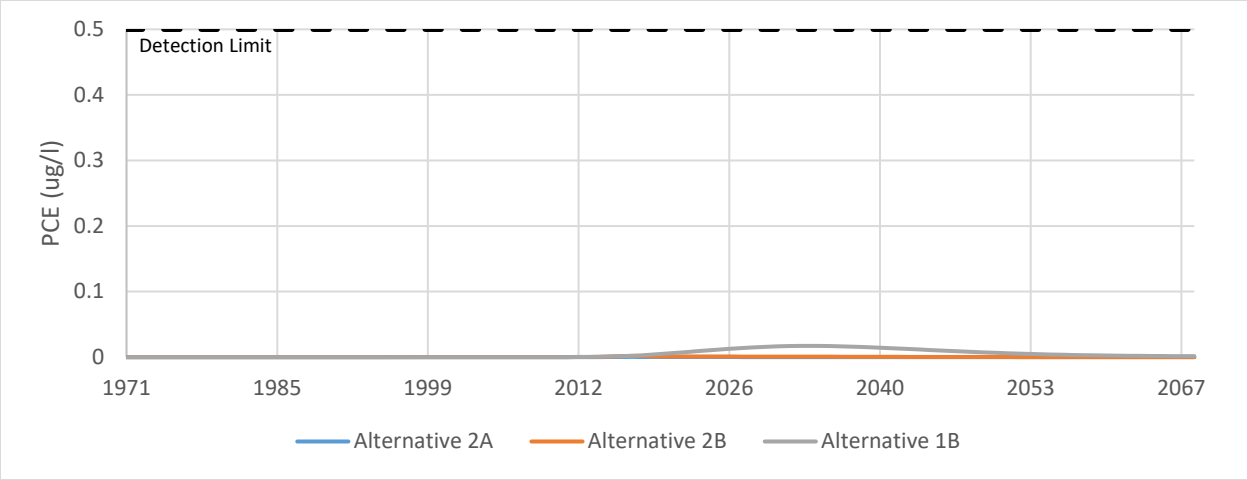

Figure 66. Breakthrough curve for LBWC 1 for Alternatives 2A – Targeted Pumping (blue), 2B – Targeted Pumping (Conservative) (orange), and 1B – Base Treatment (Conservative) (grey).

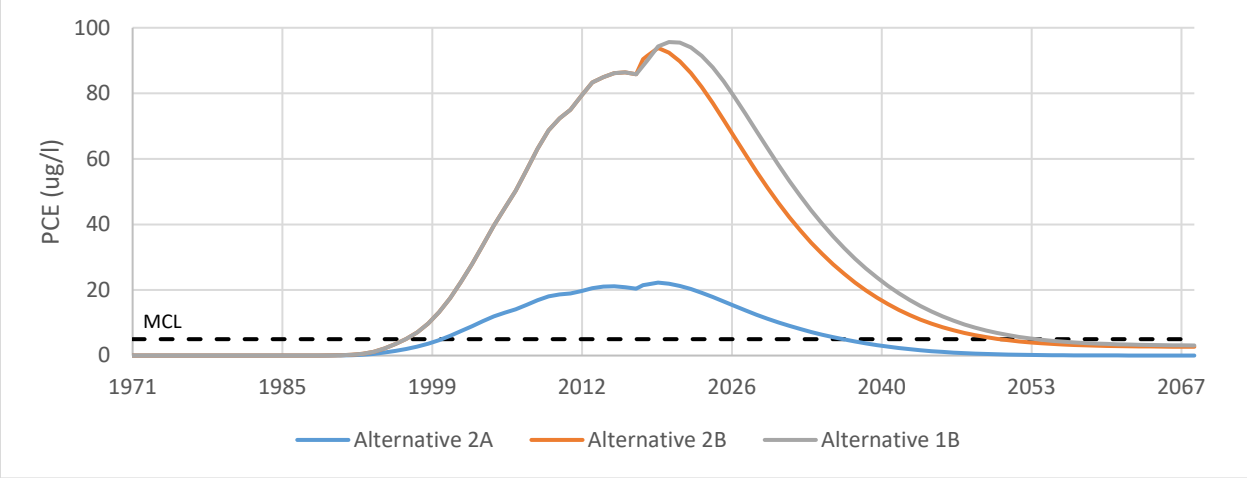

Figure 67. Breakthrough curve for LBWC 5 for Alternatives 2A – Targeted Pumping (blue), 2B – Targeted Pumping (Conservative) (orange), and 1B – Base Treatment (Conservative) (grey).

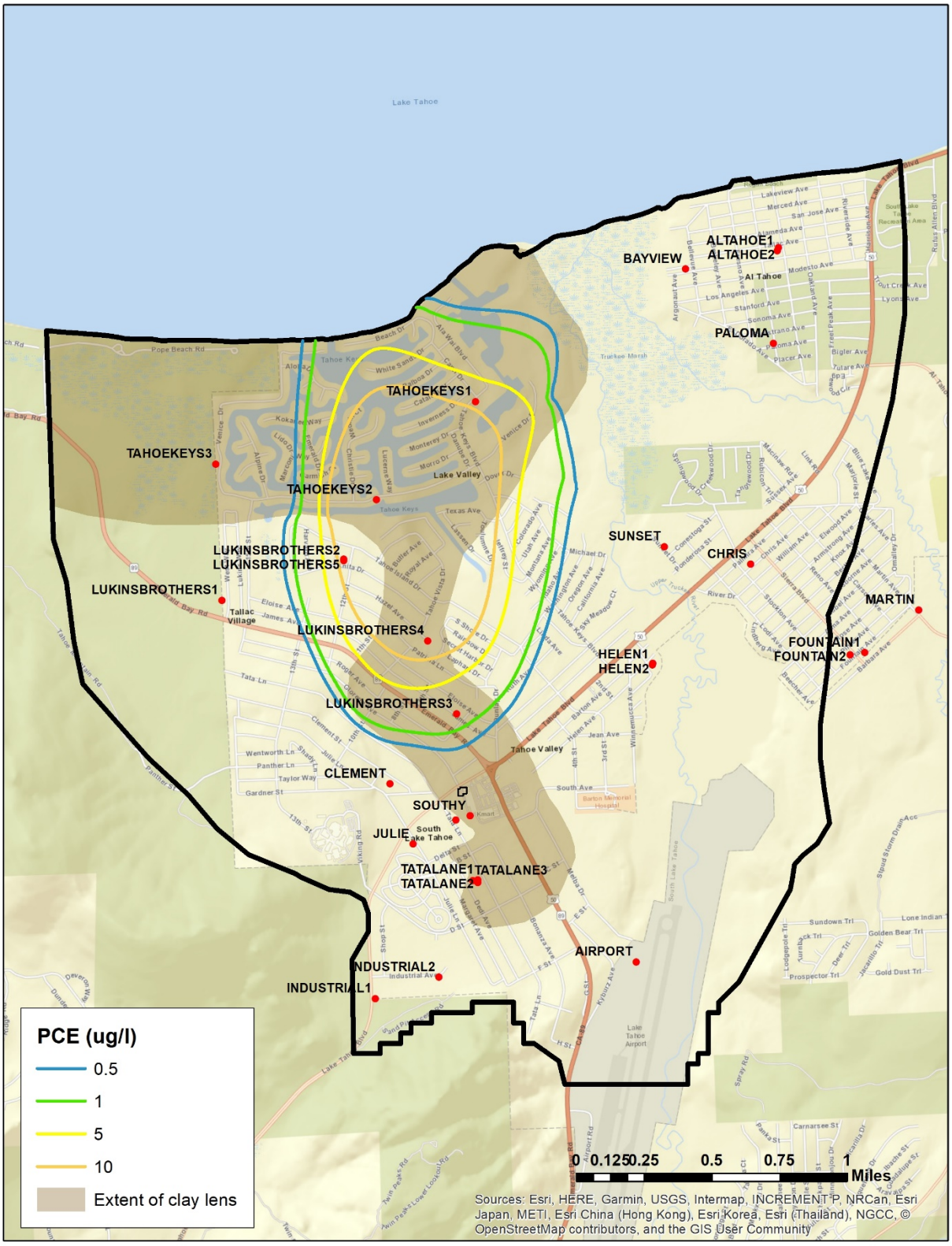

Figure 68. Alternative 3 – Surface Water Conversion. Simulated PCE plume in model layer 1 at the end of the 2033 water year.

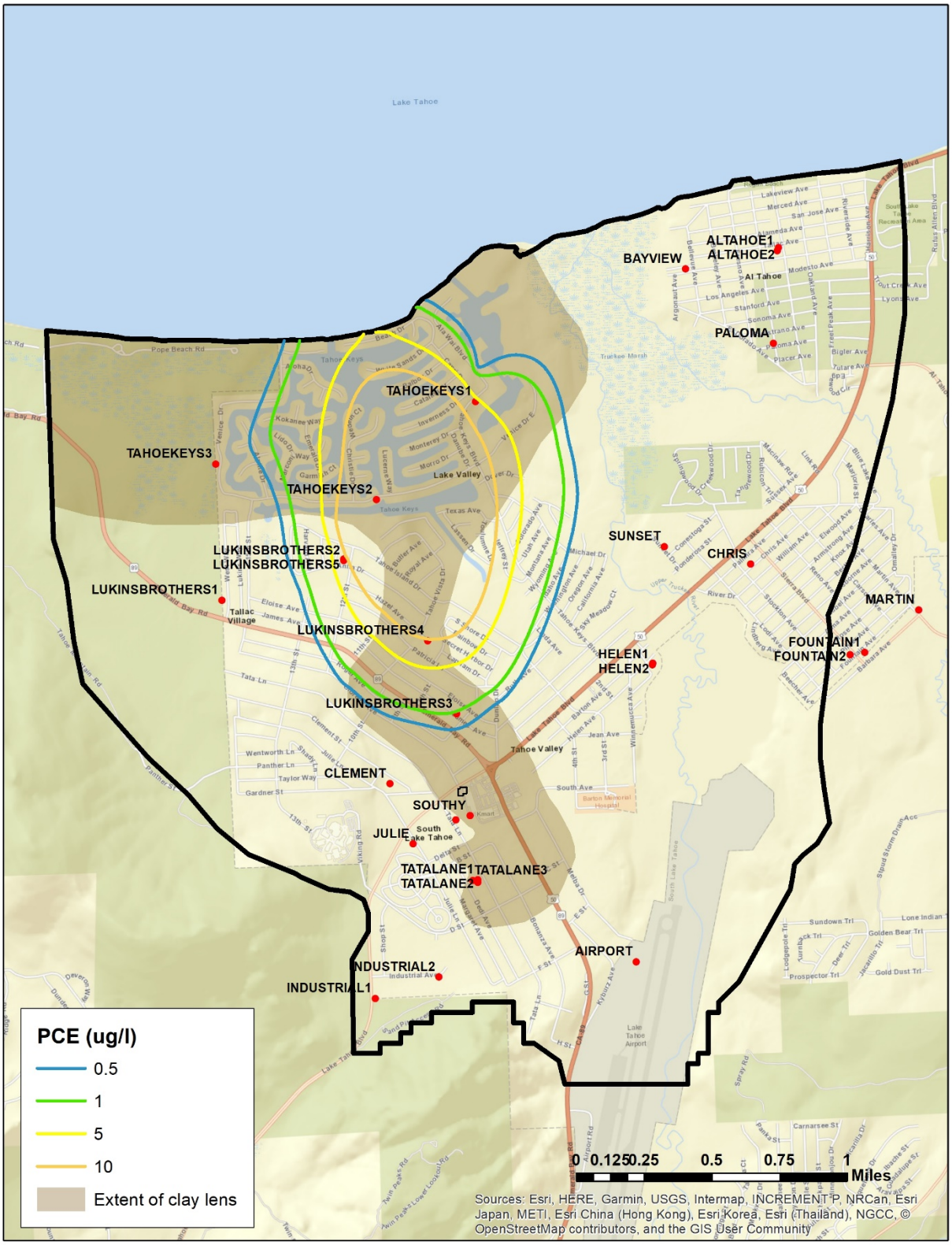

Figure 69. Alternative 3 – Surface Water Conversion. Simulated PCE plume in model layer 2 at the end of the 2033 water year.

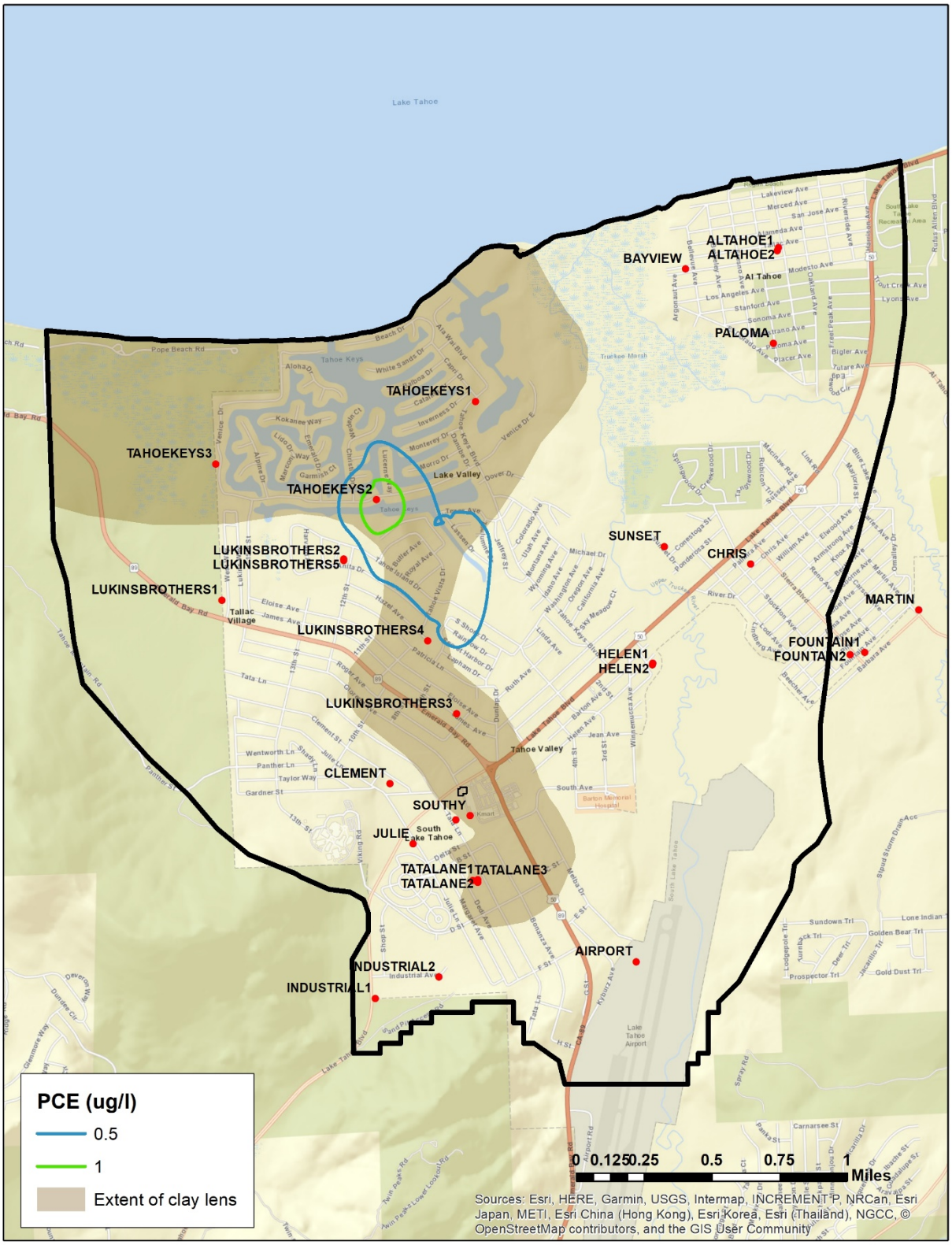

Figure 70. Alternative 3 – Surface Water Conversion. Simulated PCE plume in model layer 3 at the end of the 2033 water year.

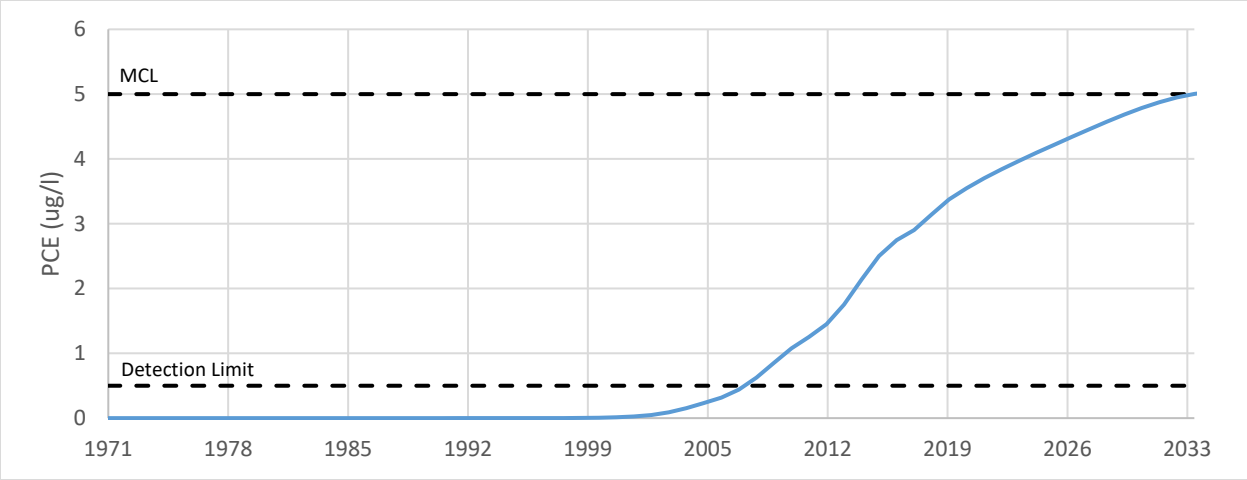

Figure 71. Breakthrough curve for TKWC 1 for Alternative 3A – Surface Water Conversion.

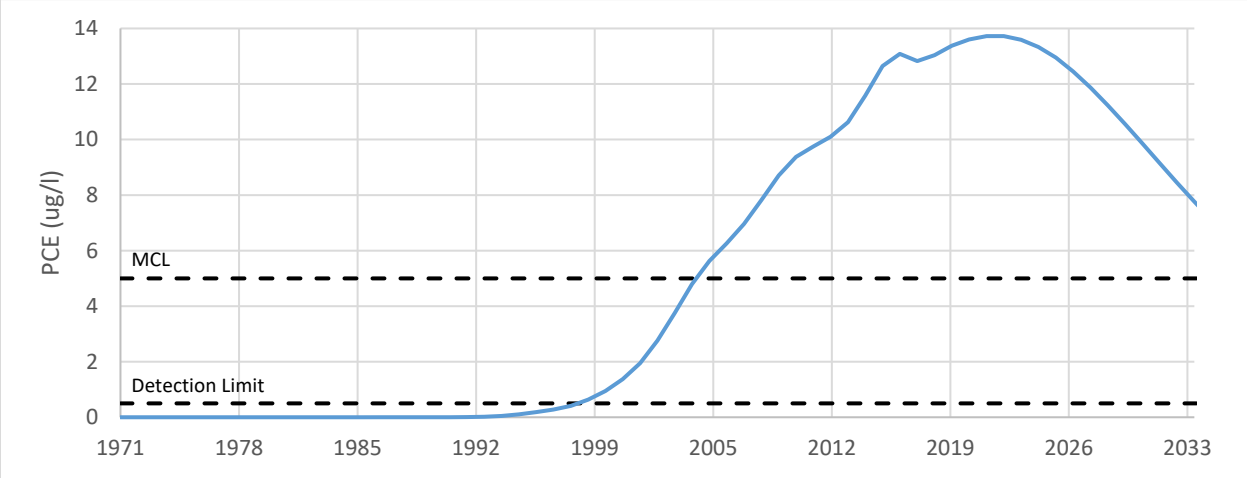

Figure 72. Breakthrough curve for TKWC 2 for Alternative 3A – Surface Water Conversion.

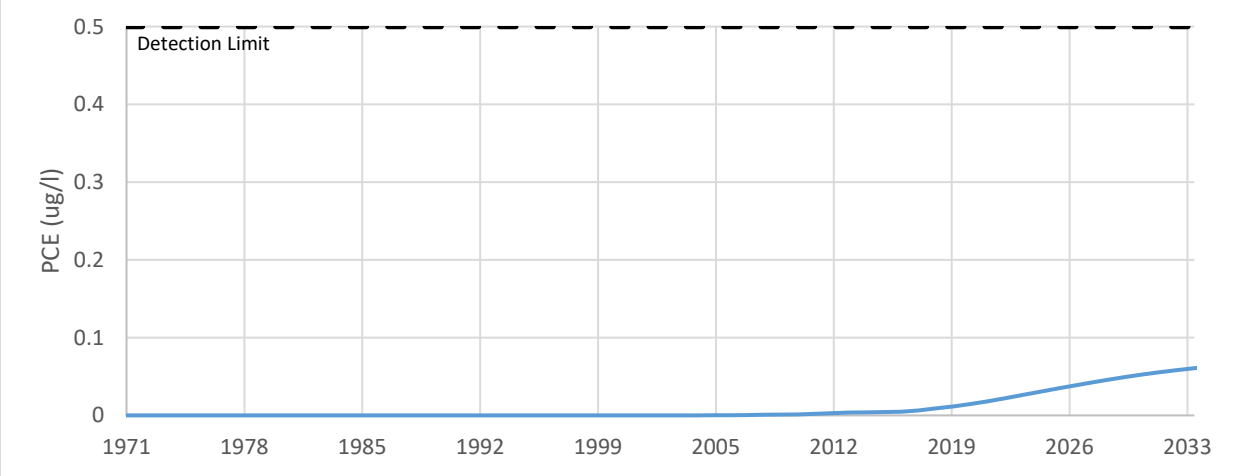

Figure 73. Breakthrough curve for TKWC 3 for Alternative 3A – Surface Water Conversion.

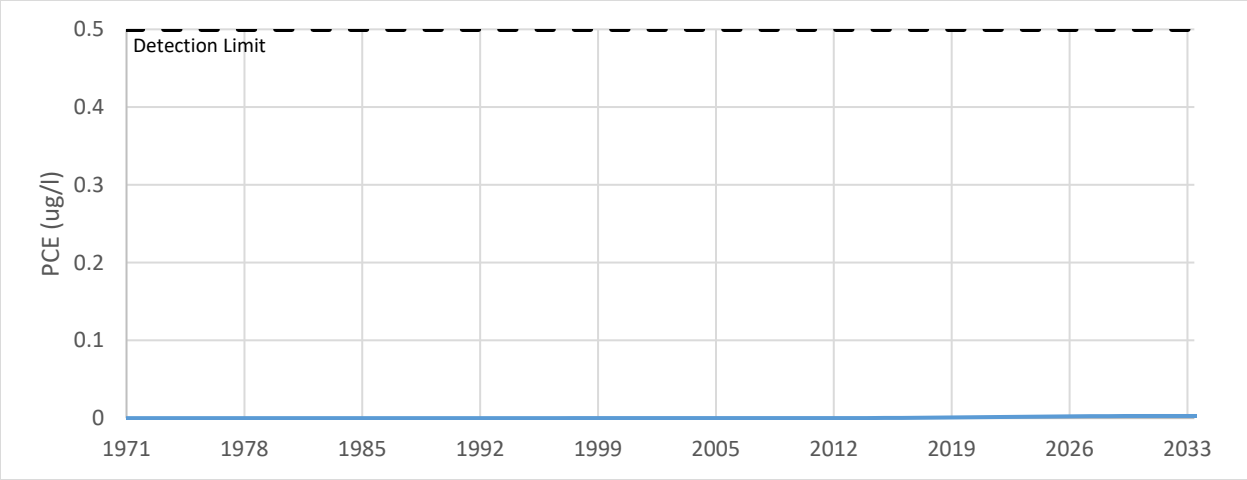

Figure 74. Breakthrough curve for LBWC 1 for Alternative 3A – Surface Water Conversion.

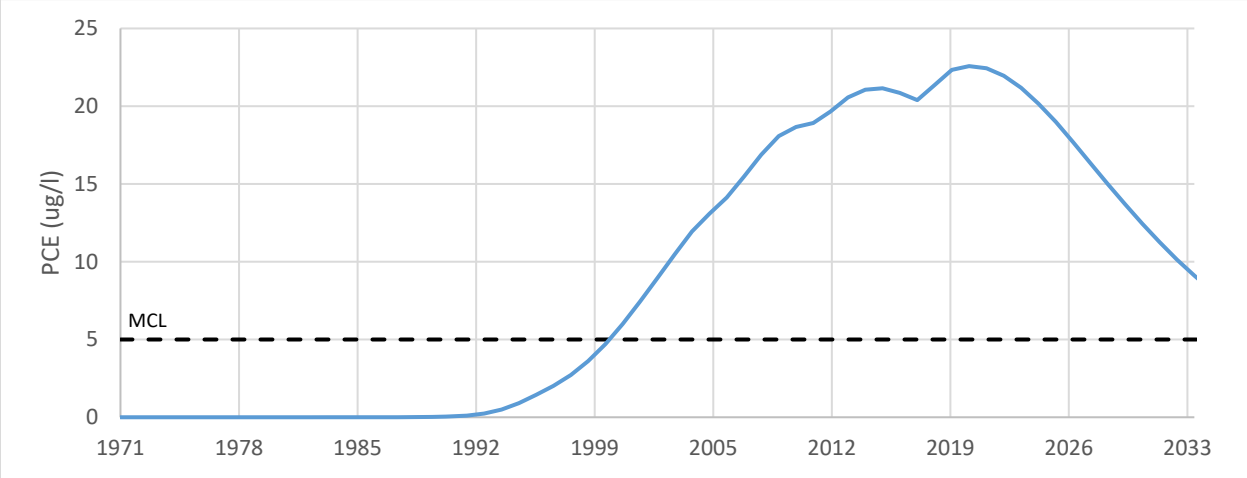

Figure 75. Breakthrough curve for LBWC 5 for Alternative 3A – Surface Water Conversion.

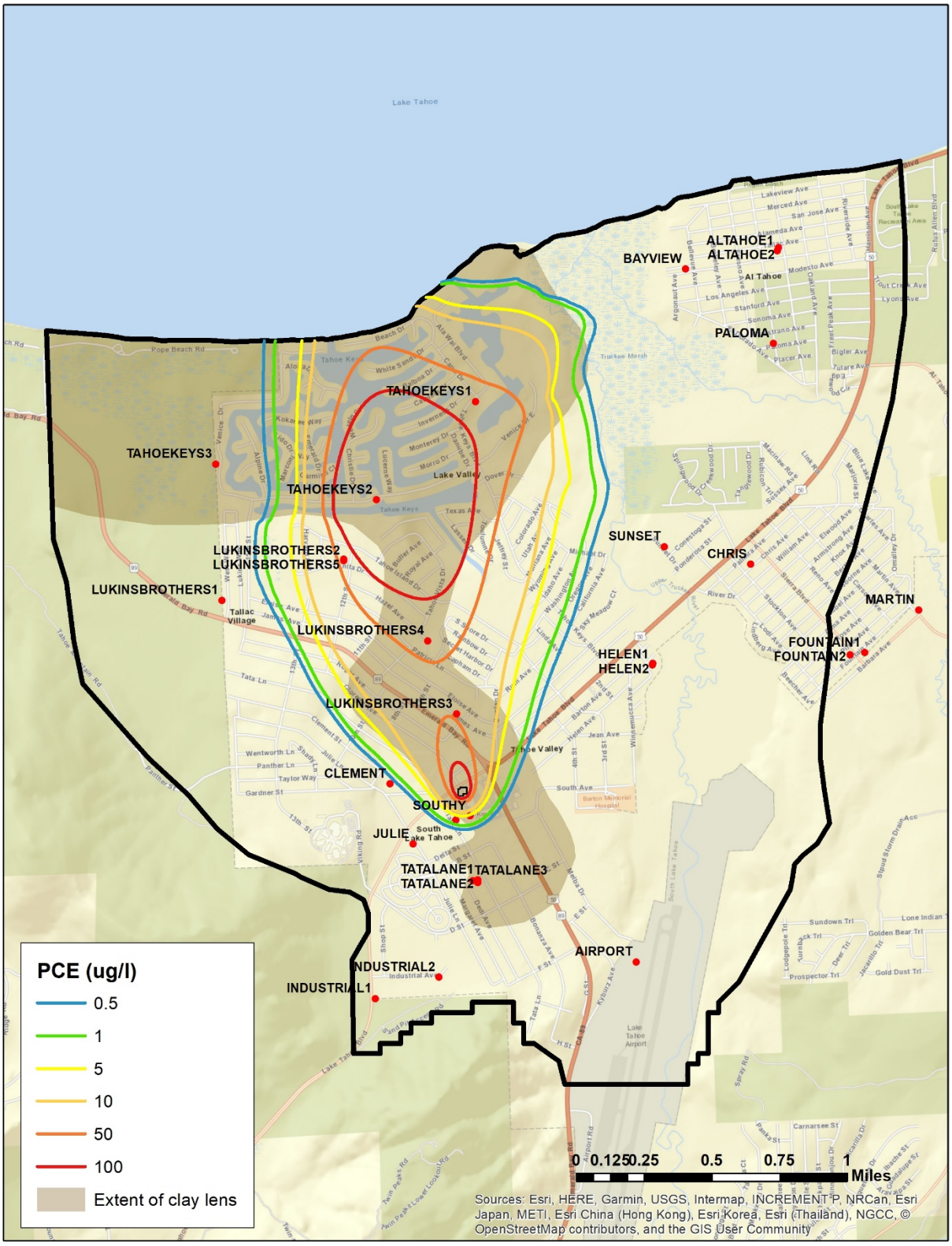

Figure 76. Alternative 3 – Surface Water Conversion (Conservative). Simulated PCE plume in model layer 1 at the end of the 2033 water year.

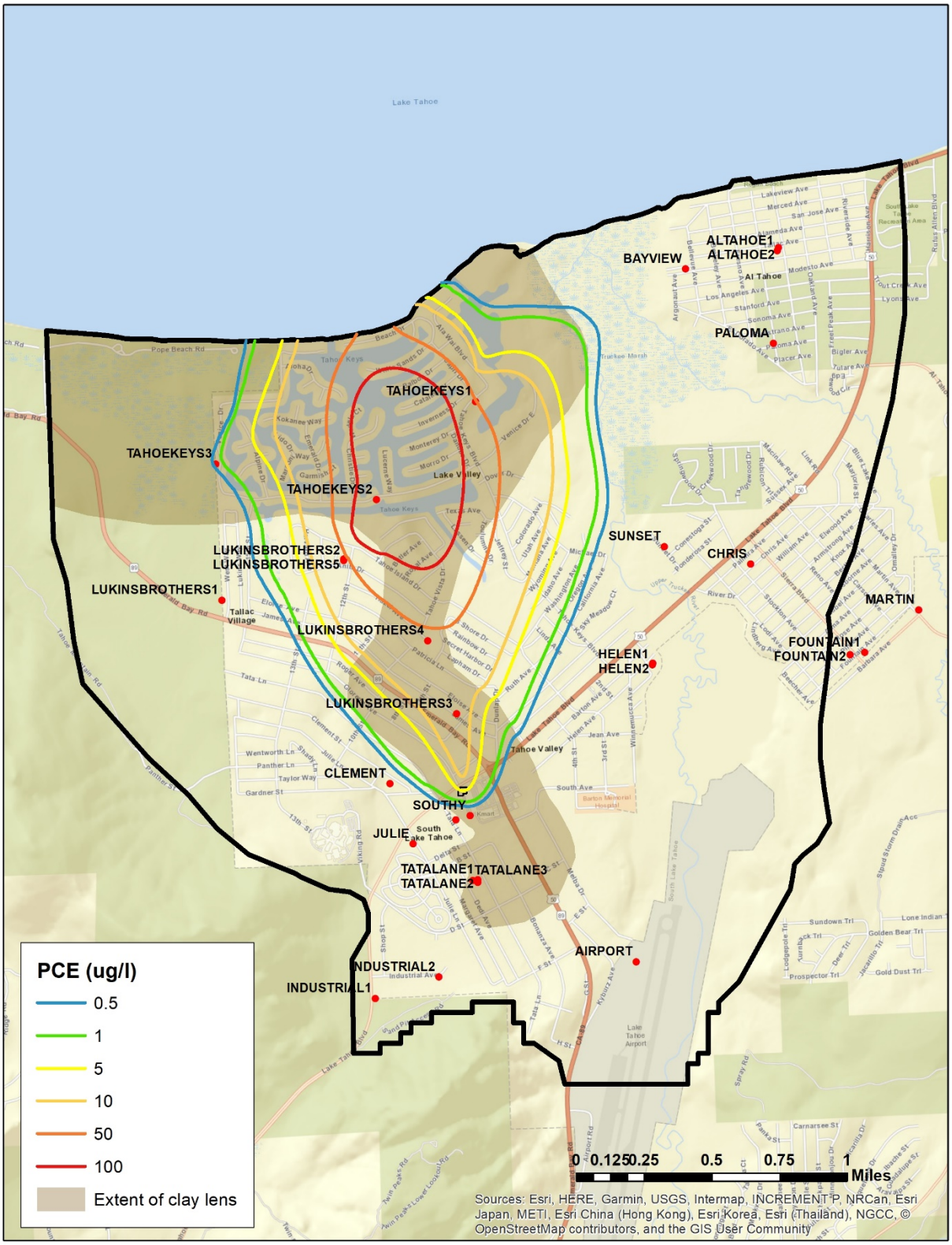

Figure 77. Alternative 3 – Surface Water Conversion (Conservative). Simulated PCE plume in model layer 2 at the end of the 2033 water year.

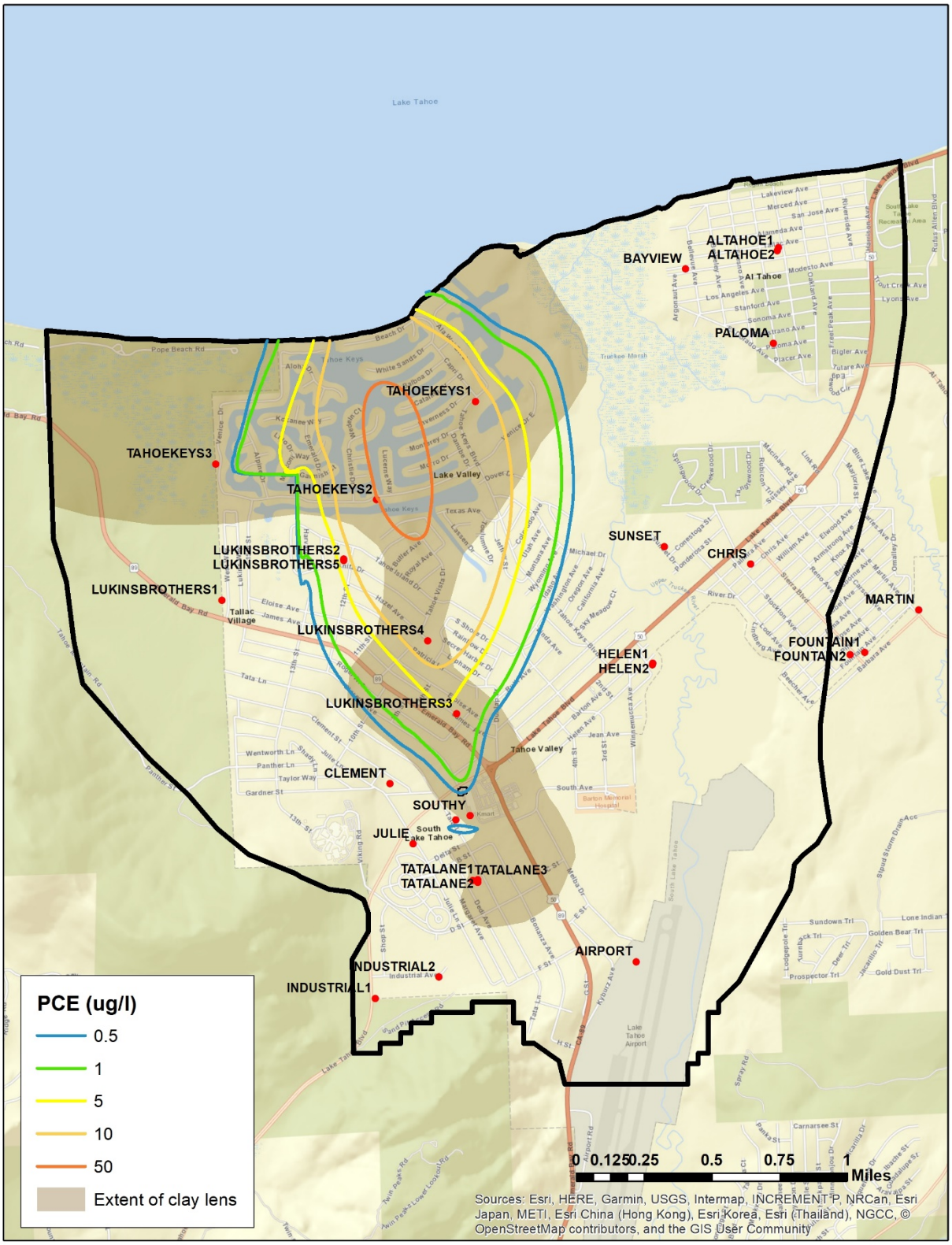

Figure 78. Alternative 3 – Surface Water Conversion (Conservative). Simulated PCE plume in model layer 3 at the end of the 2033 water year.

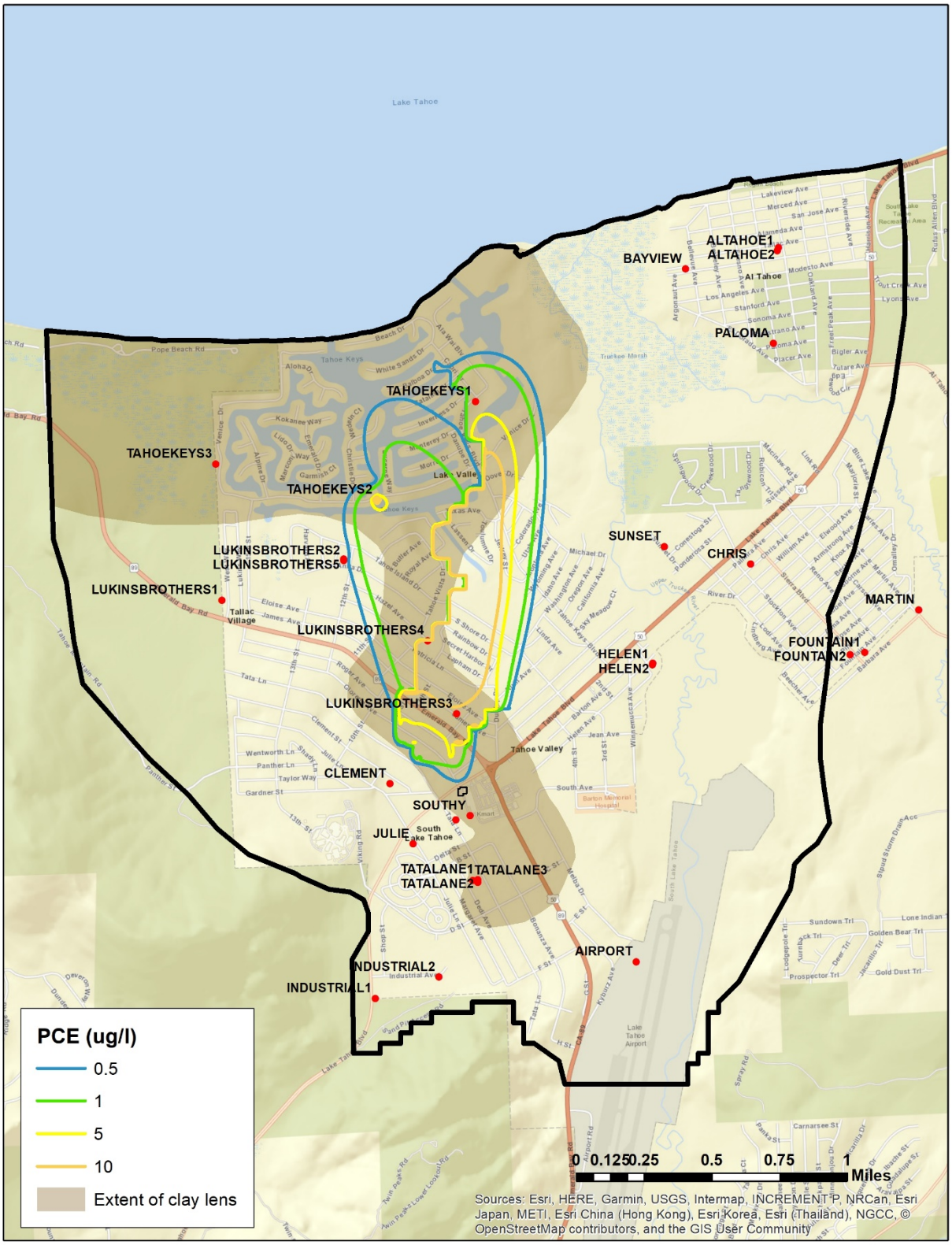

Figure 79. Alternative 3 – Surface Water Conversion (Conservative). Simulated PCE plume in model layer 4 at the end of the 2033 water year.

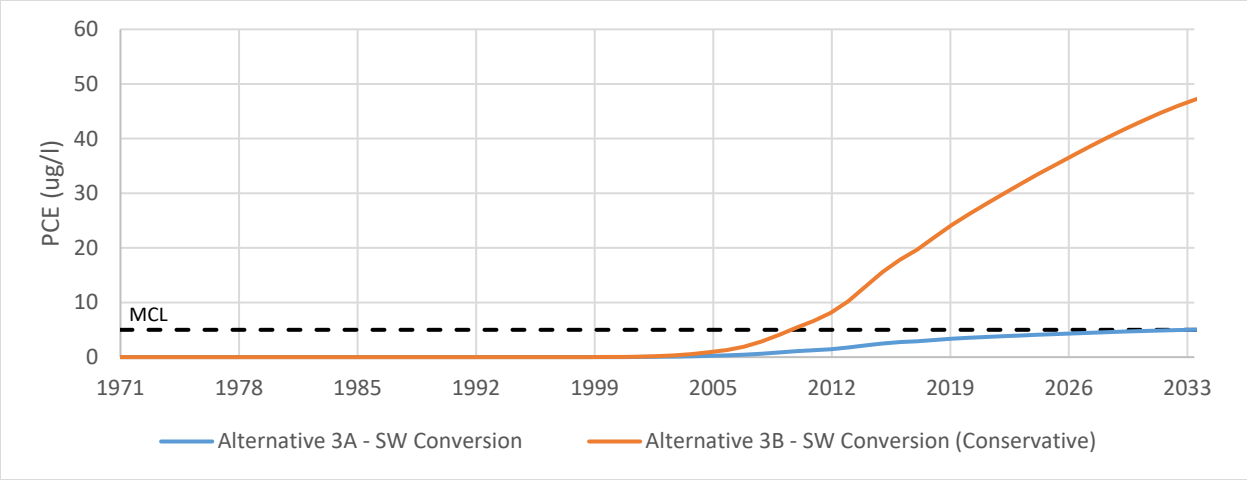

Figure 80. Breakthrough curve for TKWC 1 for Alternatives 3A (blue) and 3B (orange).

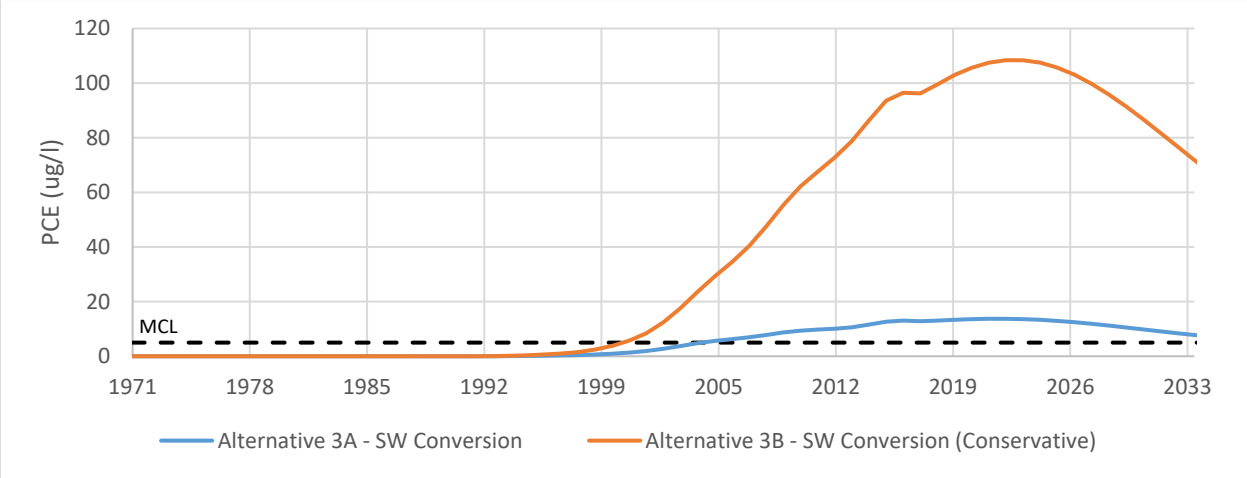

Figure 81. Breakthrough curve for TKWC 2 for Alternatives 3A (blue) and 3B (orange).

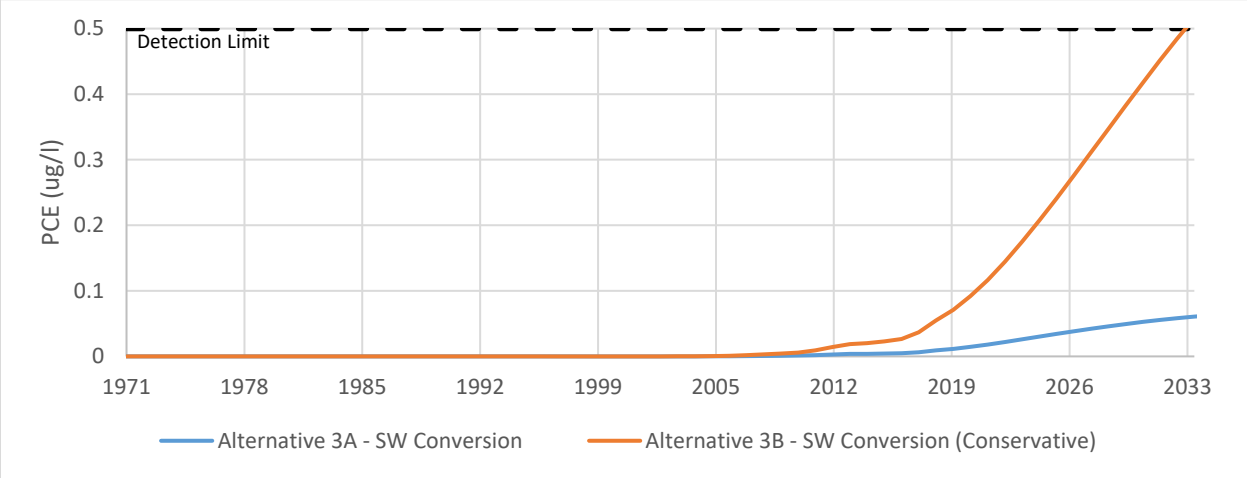

Figure 82. Breakthrough curve for TKWC 3 for Alternatives 3A (blue) and 3B (orange).

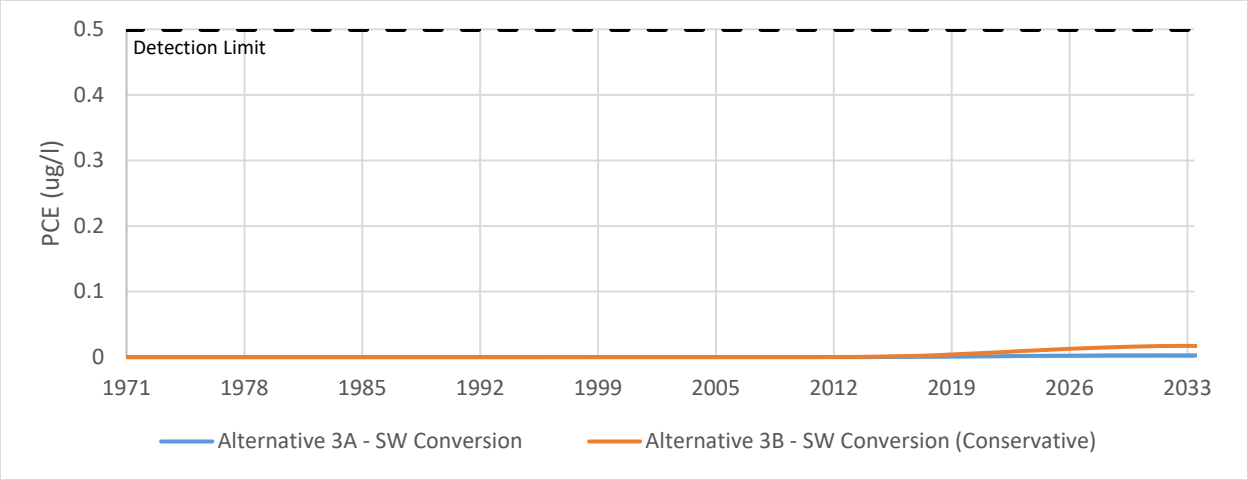

Figure 83. Breakthrough curve for LBWC 1 for Alternatives 3A (blue) and 3B (orange).

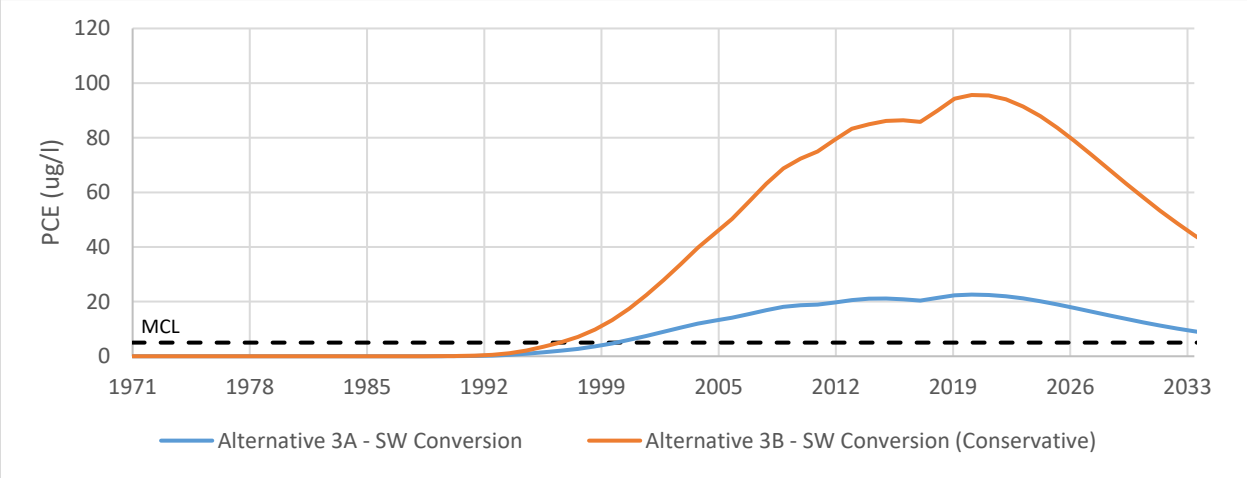

Figure 84. Breakthrough curve for LBWC 5 for Alternatives 3A (blue) and 3B (orange).

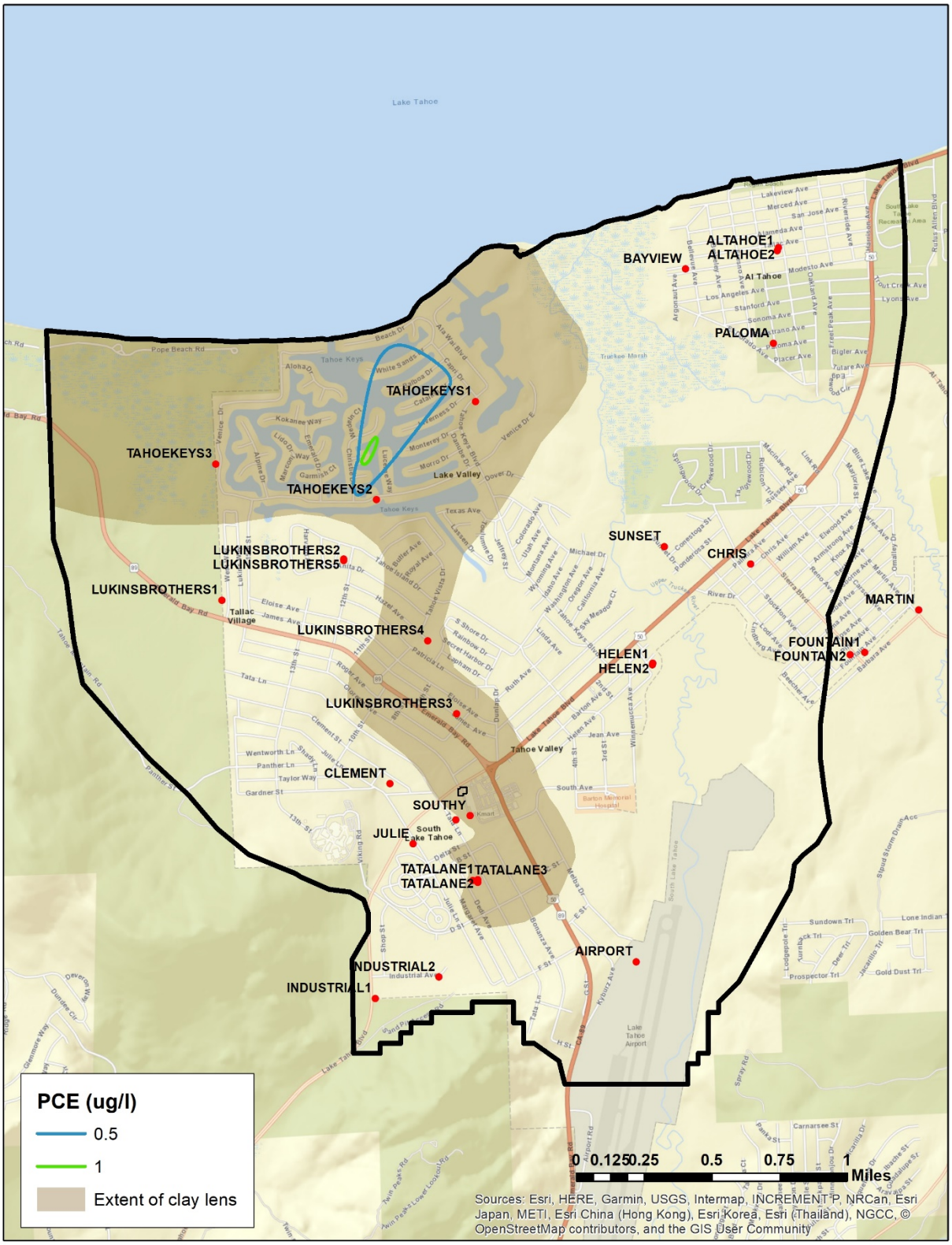

Figure 85. Alternative 4 - 90% of GAC Capacity. Simulated PCE plume in model layer 1 at the end of the 2068 water year. All concentrations are below the MCL for this stress period.

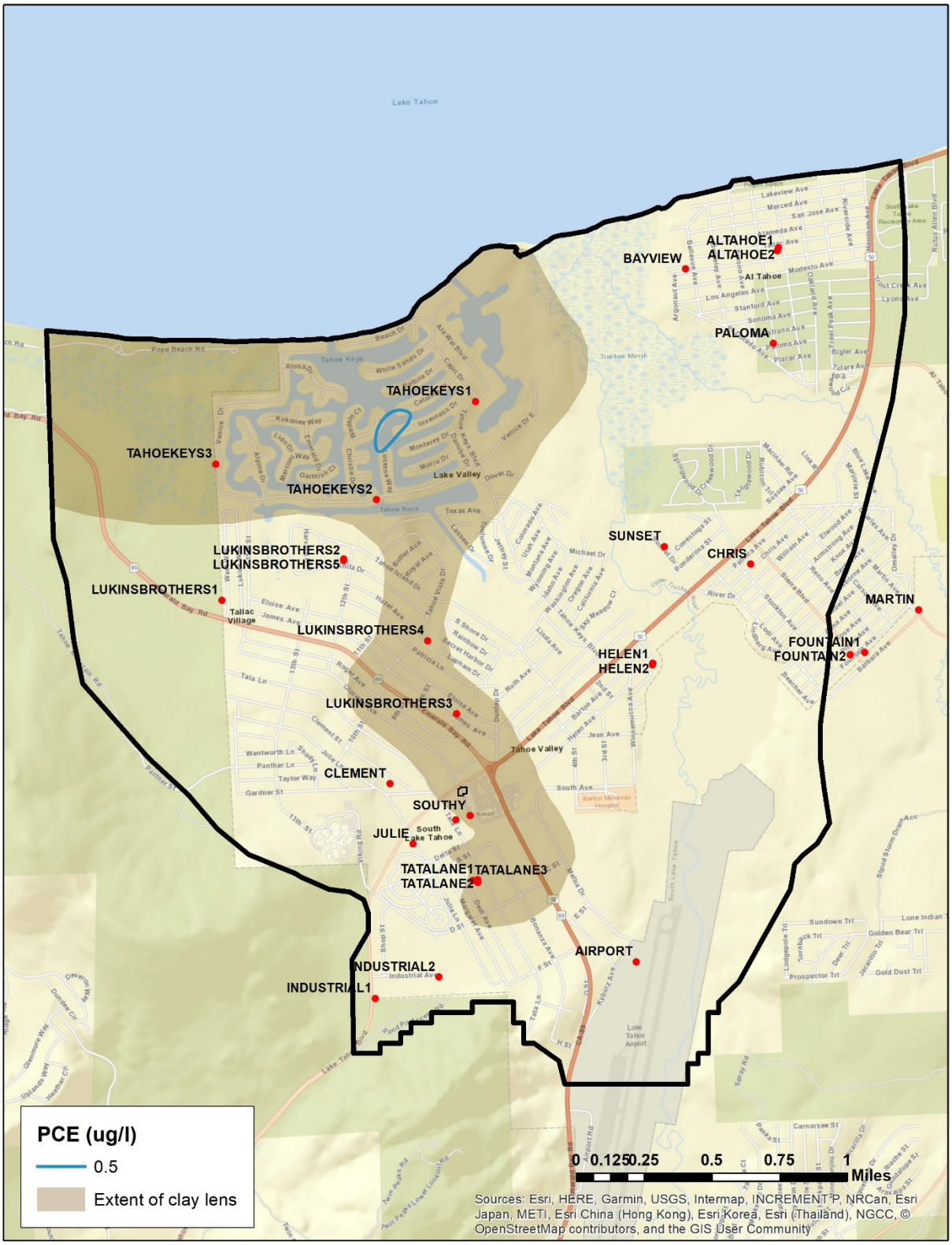

Figure 86. Alternative 4 - 90% of GAC Capacity. Simulated PCE plume in model layer 2 at the end of the 2068 water year. All concentrations are below the MCL for this stress period.

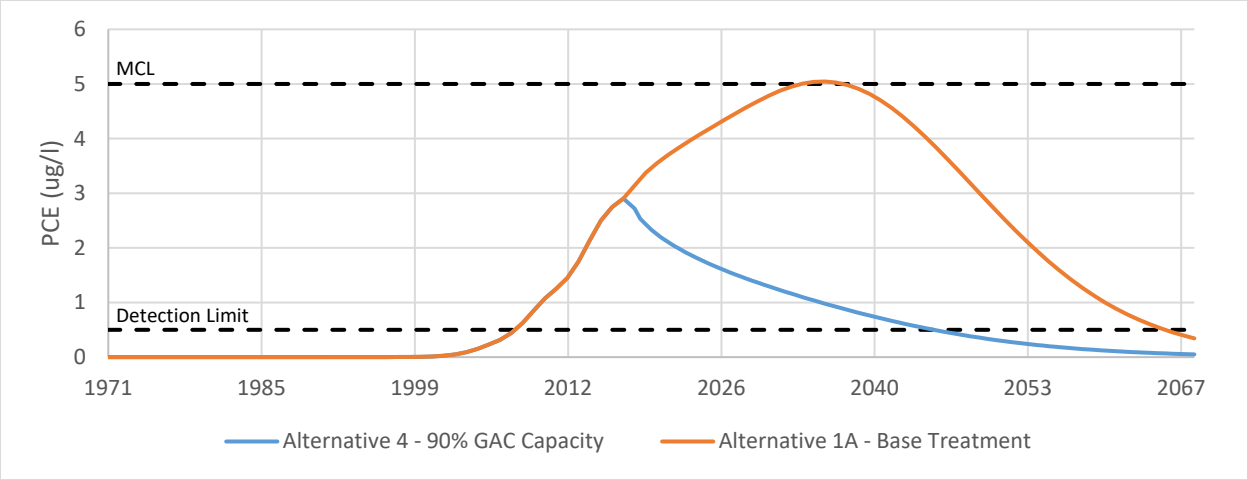

Figure 87. Breakthrough curve for TKWC 1 for Alternatives 4 (blue) and 1A (orange).

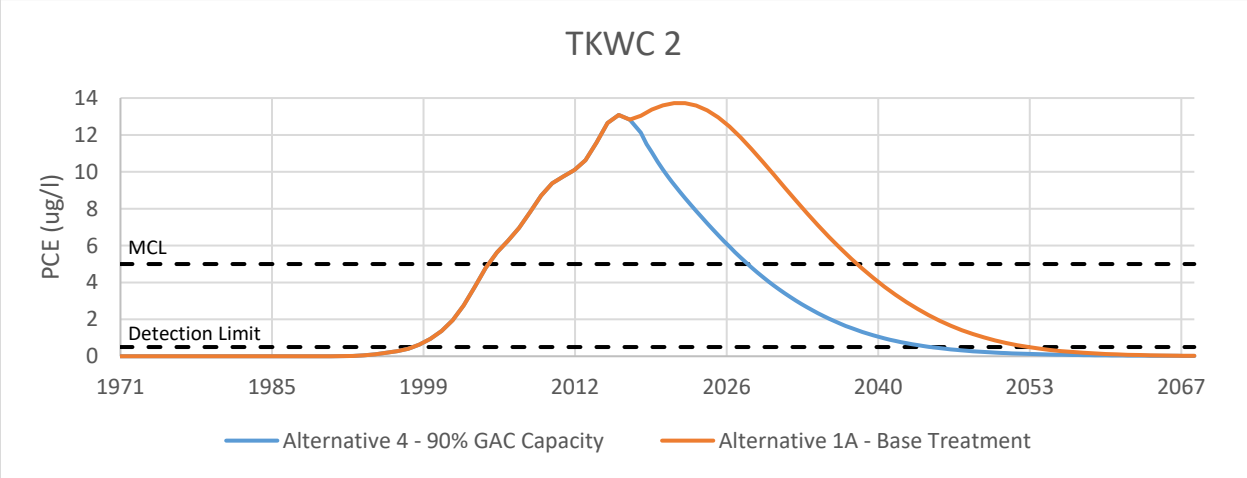

Figure 88. Breakthrough curve for TKWC 2 for Alternatives 4 (blue) and 1A (orange).

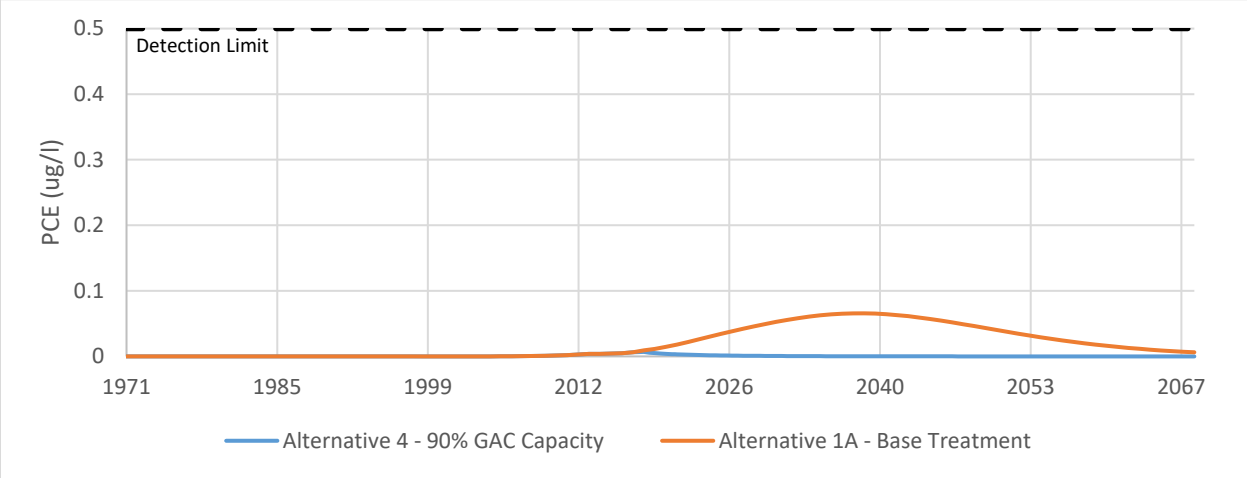

Figure 89. Breakthrough curve for TKWC 3 for Alternatives 4 (blue) and 1A (orange).

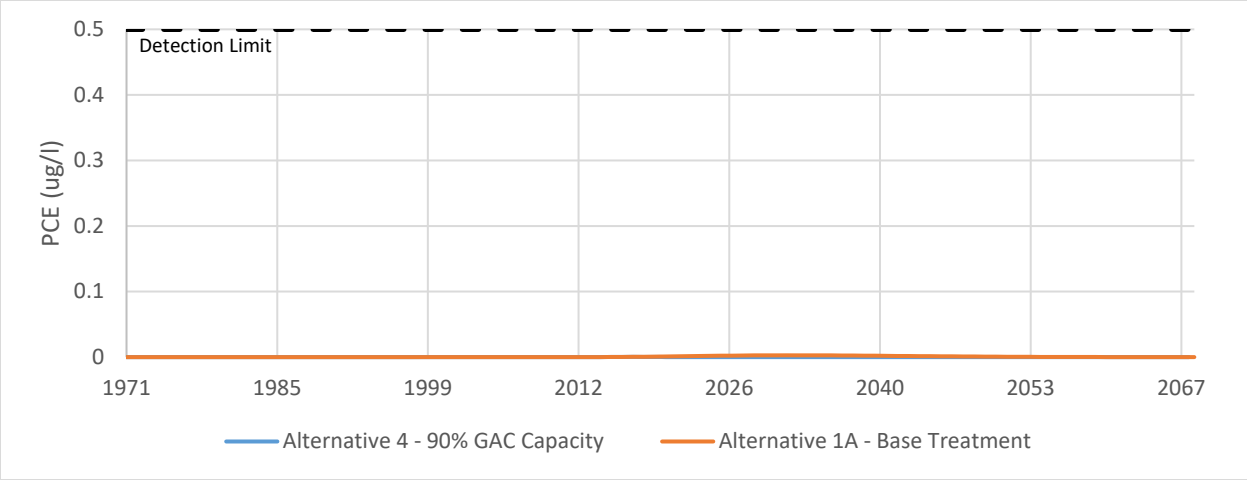

Figure 90. Breakthrough curve for LBWC 1 for Alternatives 4 (blue) and 1A (orange).

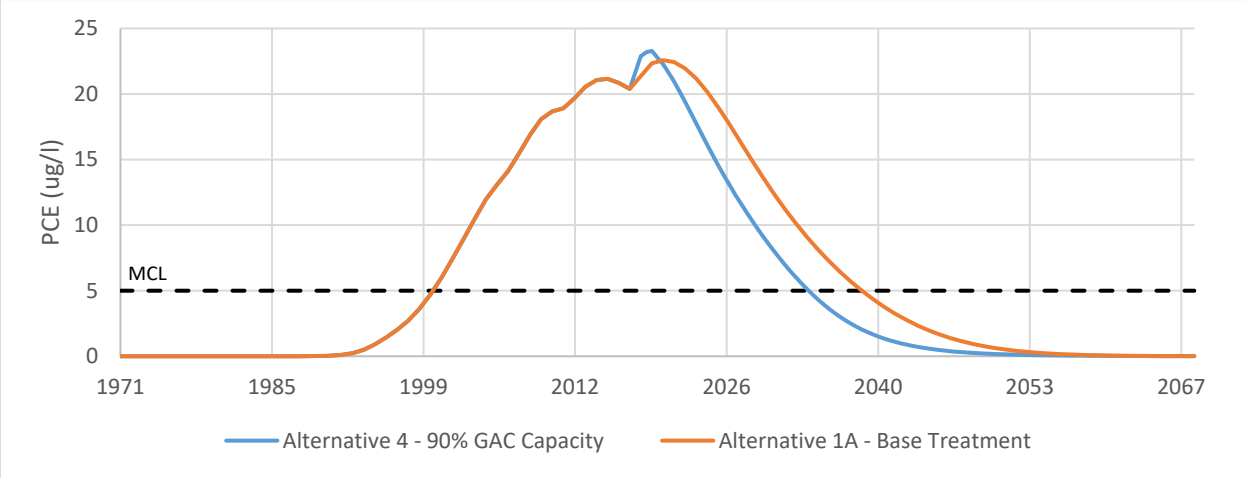

Figure 91. Breakthrough curve for LBWC 5 for Alternatives 4 (blue) and 1A (orange).

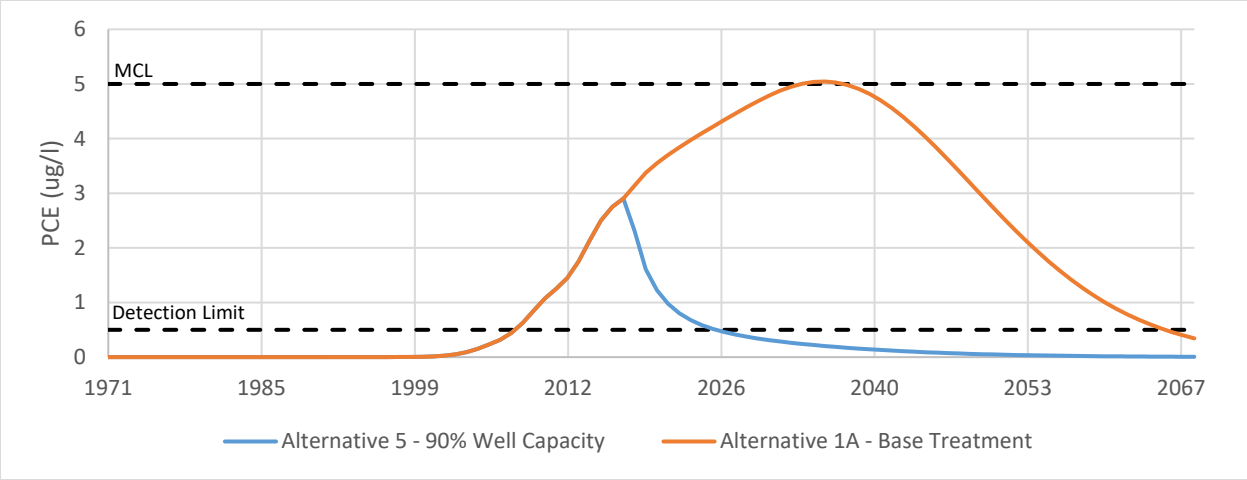

Figure 92. Breakthrough curve for TKWC 1 for Alternatives 5 (blue) and 1A (orange).

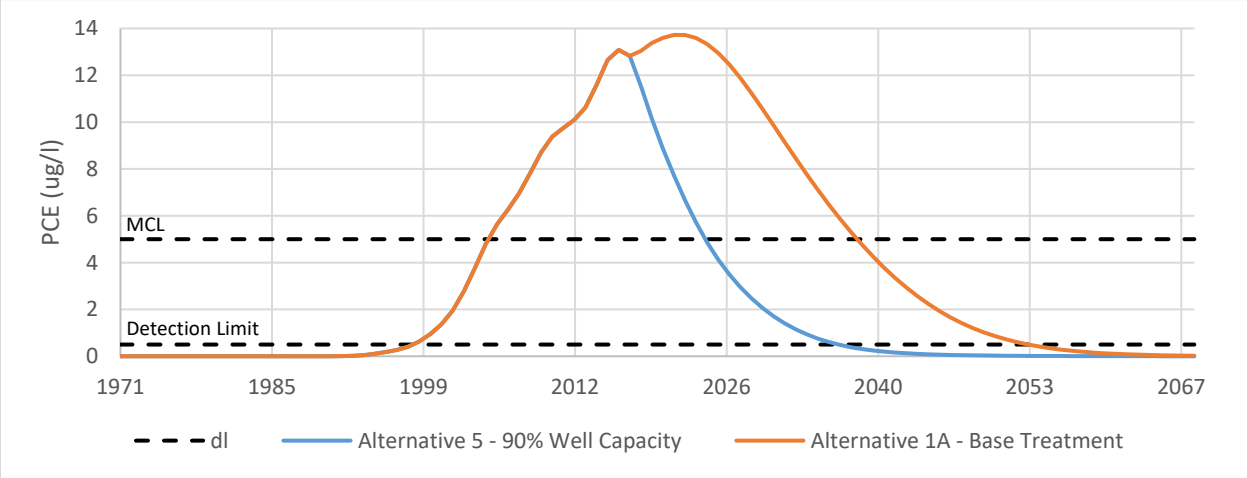

Figure 93. Breakthrough curve for TKWC 2 for Alternatives 5 (blue) and 1A (orange).

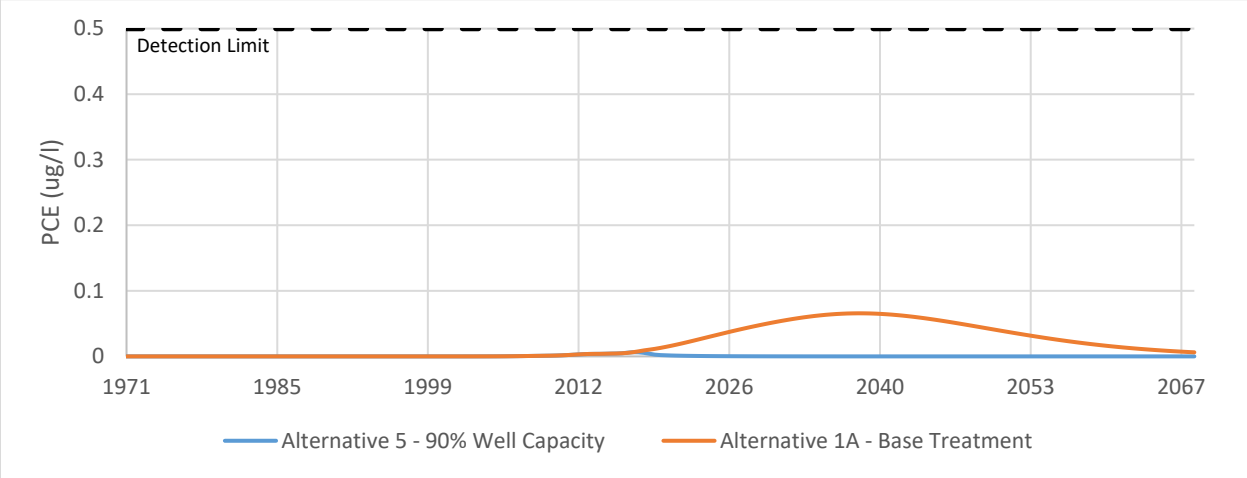

Figure 94. Breakthrough curve for TKWC 3 for Alternatives 5 (blue) and 1A (orange).

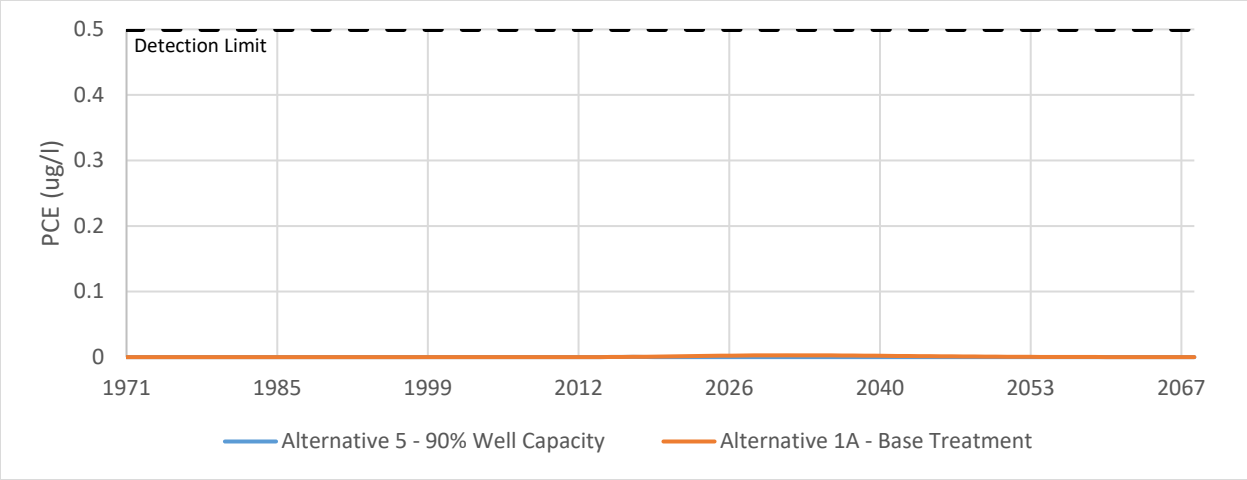

Figure 95. Breakthrough curve for LBWC 1 for Alternatives 5 (blue) and 1A (orange).

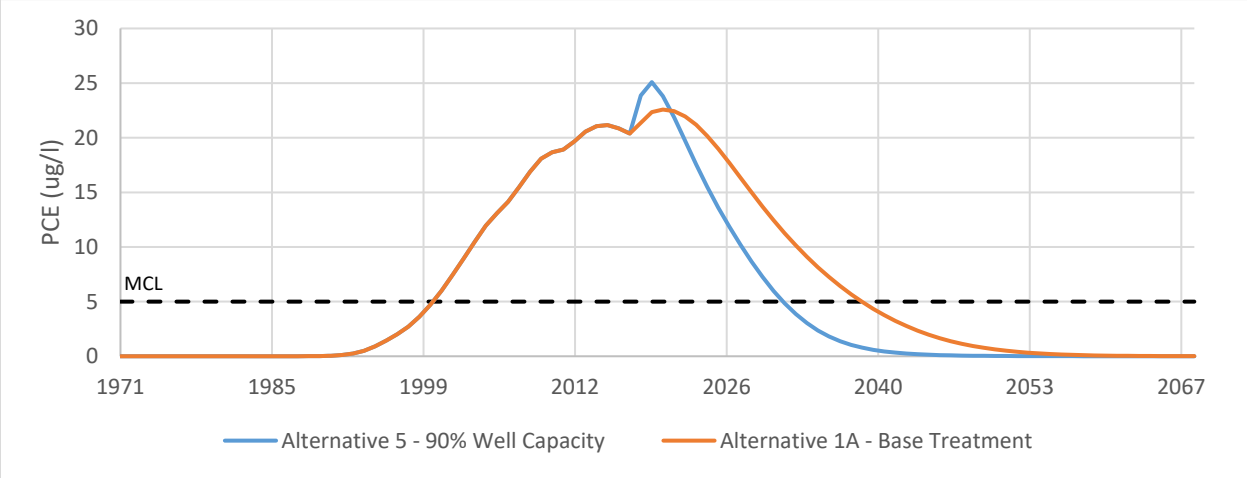

Figure 96. Breakthrough curve for LBWC 5 for Alternatives 5 (blue) and 1A (orange).

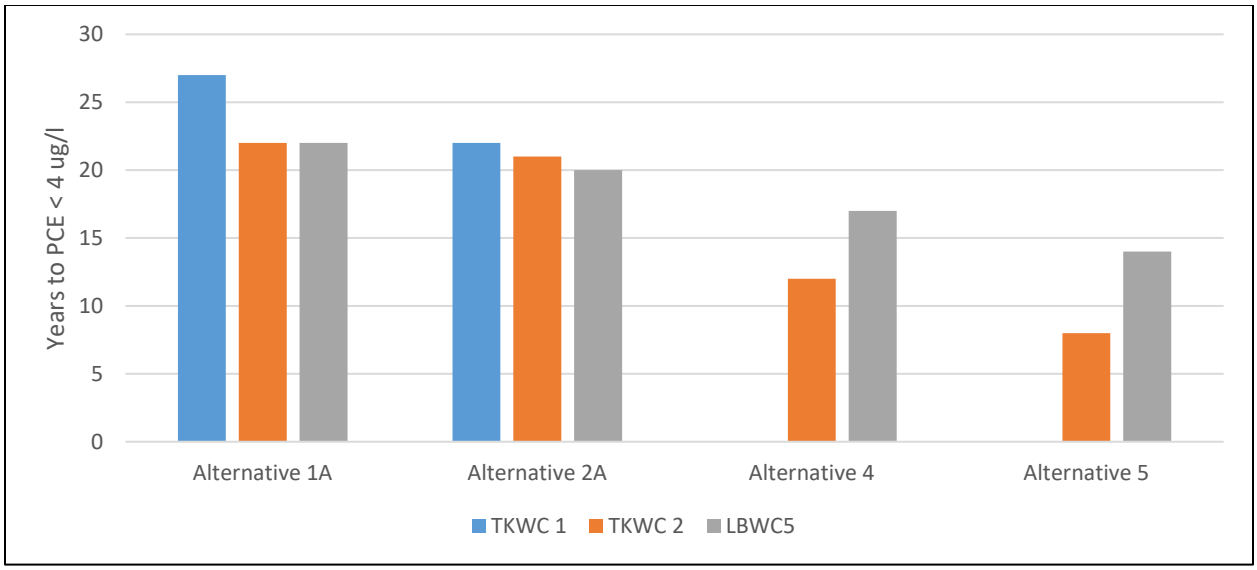

Figure 97. Years after 2018 until simulated PCE concentrations drop below 4 ug/l, by alternative and well. Alternative 3A and 3B simulations are not long enough to show declines below 4 ug/l. Concentrations at TKWC 1 never exceed 4 ug/l in Alternatives 4 and 5.

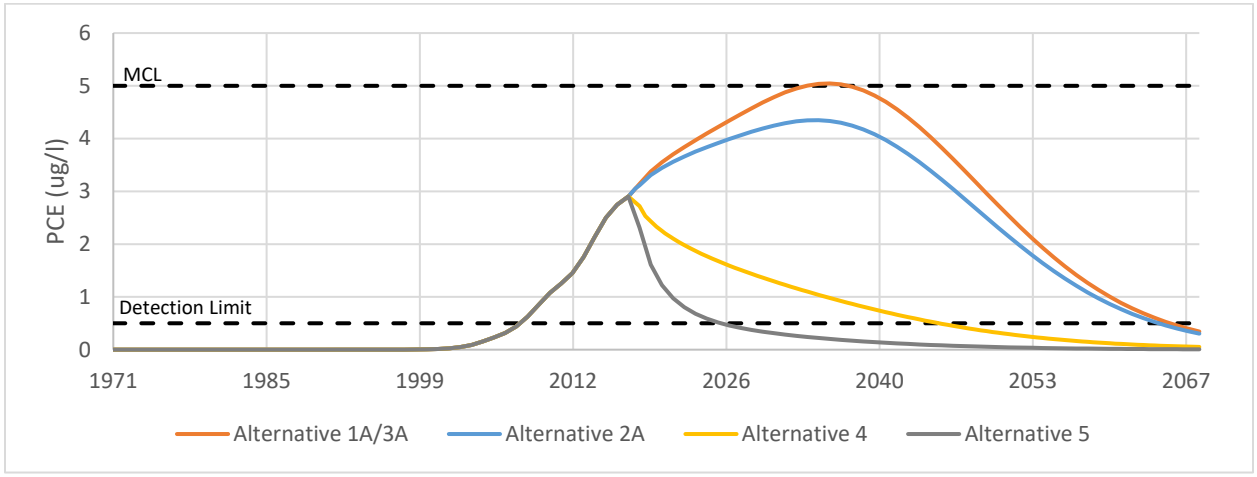

Figure 98. Breakthrough curves for all non-conservative alternatives at TKWC 1. Note Alternative 3A was simulated only through 2033 – results indicated by the 'Alternative 1A/3A' line beyond 2033 are valid only for Alternative 1A.

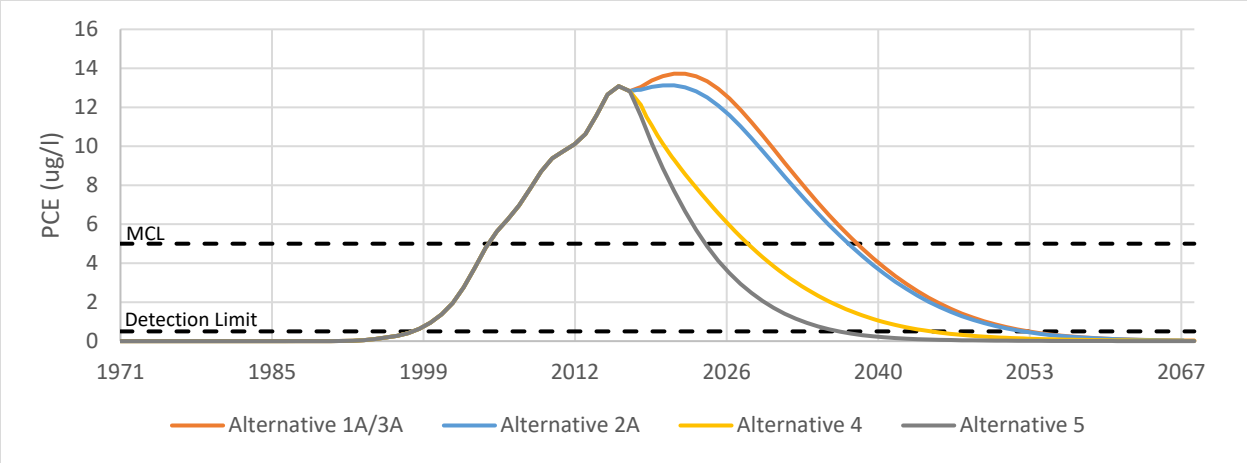

Figure 99. Breakthrough curves for all non-conservative alternatives at TKWC 2. Note Alternative 3A was simulated only through 2033 – results indicated by the 'Alternative 1A/3A' line beyond 2033 are valid only for Alternative 1A.

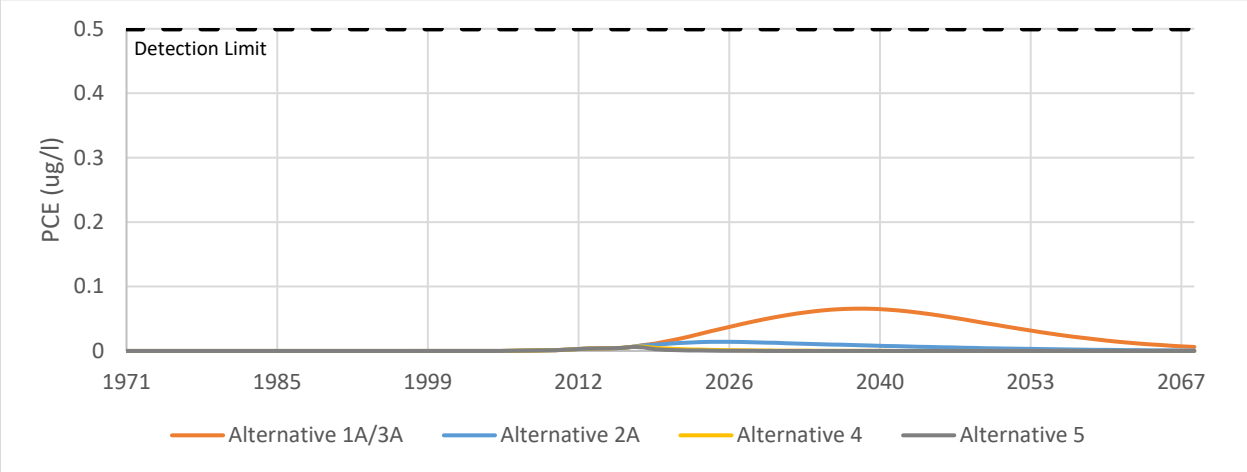

Figure 100. Breakthrough curves for all non-conservative alternatives at TKWC 3. Note Alternative 3A was simulated only through 2033 – results indicated by the 'Alternative 1A/3A' line beyond 2033 are valid only for Alternative 1A.

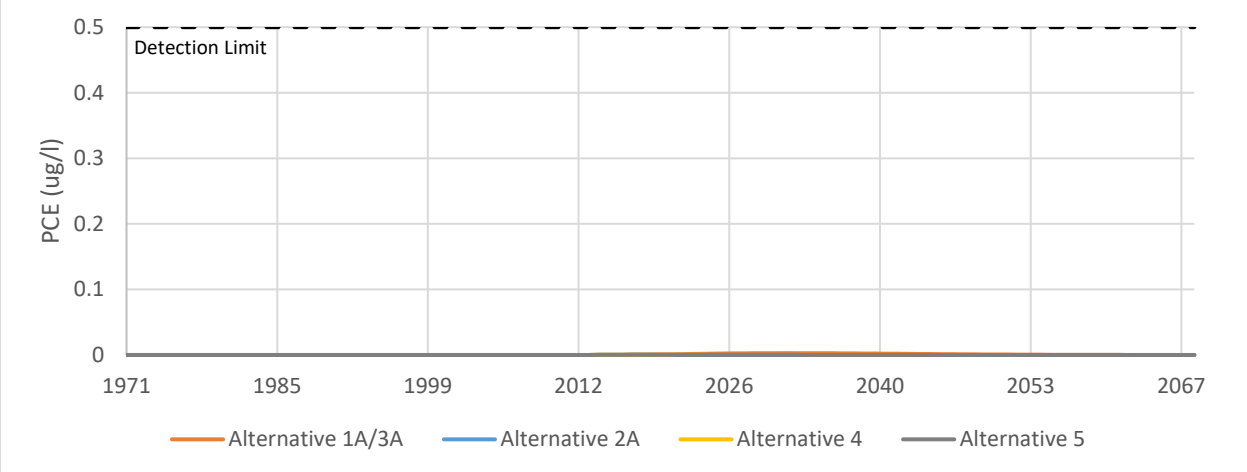

Figure 101. Breakthrough curves for all non-conservative alternatives at LBWC 1. Note Alternative 3A was simulated only through 2033 – results indicated by the 'Alternative 1A/3A' line beyond 2033 are valid only for Alternative 1A.

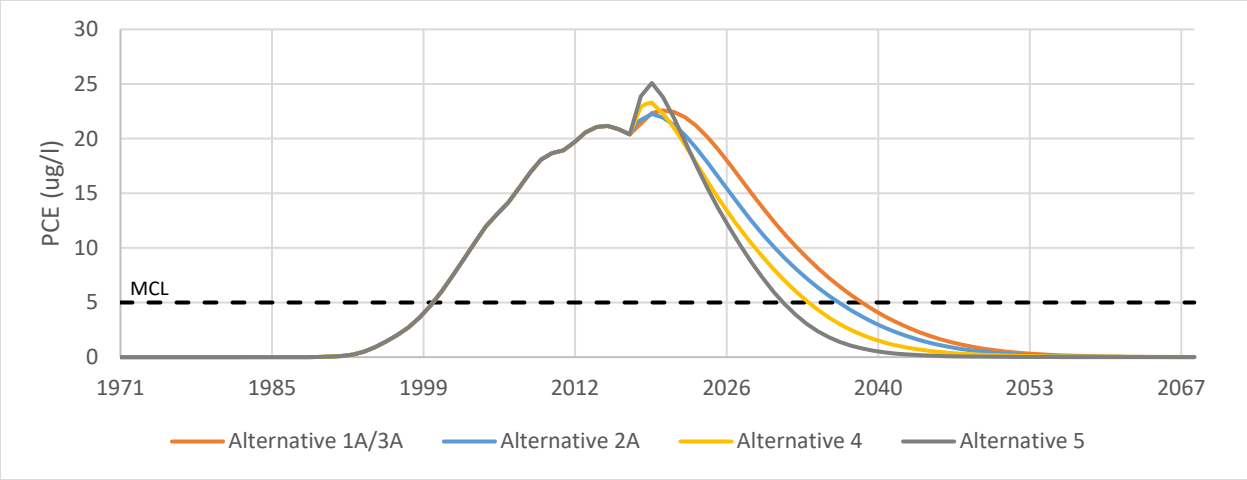

Figure 102. Breakthrough curves for all non-conservative alternatives at LBWC 5. Note Alternative 3A was simulated only through 2033 – results indicated by the 'Alternative 1A/3A' line beyond 2033 are valid only for Alternative 1A.

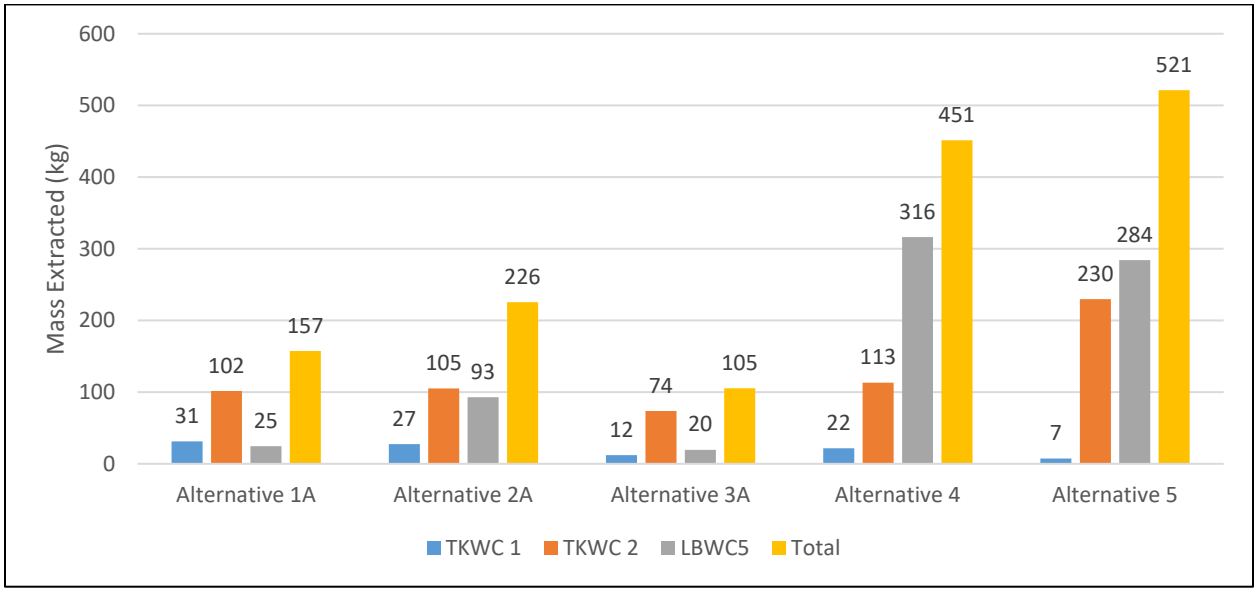

Figure 103. Mass extracted (in kilograms) by alternative and well. Note Alternative 3A simulation was run for only 15 years, while all others are run for 50 years.